

MODELING OF POLYMER MATRIX COMPOSITES USING VBO MODEL AND FINITE ELEMENT METHOD FORMULATIONS

NOVEMBER, 2016

REPUBLIC OF TURKEY YILDIZ TECHNICAL UNIVERSITY GRADUATE SCHOOL OF NATURAL AND APPLIED SCIENCES

MODELING OF POLYMER MATRIX COMPOSITES USING VBO MODEL AND FINITE ELEMENT METHOD FORMULATIONS

ALPEREN ACAR

PH. D. THESIS DEPARTMENT OF MECHANICAL ENGINEERING PROGRAM OF CONSTRUCTION

ADVISER PROF. DR. ÖZGEN ÜMİT ÇOLAK ÇAKIR

İSTANBUL, 2016

REPUBLIC OF TURKEY YILDIZ TECHNICAL UNIVERSITY GRADUATE SCHOOL OF NATURAL AND APPLIED SCIENCES

MODELING OF POLYMER MATRIX COMPOSITES USING VBO MODEL and FINITE ELEMENT METHOD FORMULATIONS

A thesis submitted by Alperen ACAR in partial fulfillment of the requirements for the degree of **DOCTOR OF PHILOSOPHY** is approved by the committee on 28.11.2016 in Department of Mechanical Engineering, Construction Program.

Thesis Advisor	
Prof. Dr. Özgen ÇOLAK ÇAKIR	
Yıldız Technical University	
Approved By the Examining Committee	
Prof. Dr. Özgen ÇOLAK ÇAKIR	
Yıldız Technical University	
Assist. Prof. Dr. Birgül TEMİZTAŞ, Member	
Yıldız Technical University	
Prof. Dr. Fazıl Önder SÖNMEZ, Member	
Boğaziçi University	_
Assoc. Prof. Dr. Şebnem ÖZÜPEK, Member	
Boğaziçi University	_
Assist. Prof. Dr. Vedat TEMİZ, Member	
İstanbul Technical University	



ACKNOWLEDGEMENTS

I dedicate this thesis work to my beloved wife, Ahsen ACAR for her patience and lifelong support.

This thesis work has come into existence with the counseling and guidance of my meritorious advisor Professor Özgen ÇOLAK ÇAKIR. I specially thank her for her great advising and everything she has done for me so far.

During this work, with the 2214-A grant of Scientific and Technological Research Council of Turkey (TUBITAK), a six month visit to Strasbourg University ICUBE Laboratories is effectuated. Support of TUBITAK is highly appreciated.

I gave my gratitude to all of my Professors and colleagues in the team MMB of ICUBE laboratories, University of Strasbourg for their great hospitality and precious aids during my visit to Strasbourg. Valuable contributions of Professor Dr. Said AHZI, Associate Professor Dr. João Pedro DE MAGALHÃES CORREIA and Dr. Crystelle BERNARD from ICUBE laboratories, is particularly appreciated.

I should also thank to Professor Dr. Deniz UZUNSOY and Central Laboratories of Yildiz Technical University for their great contributions on manufacturing and characterization of nanocomposite materials.

I am honored to have had Prof. Dr. Fazıl Önder SÖNMEZ, and Assist. Prof. Dr. Vedat TEMİZ, in my doctoral committee and I thank them for their valuable suggestions.

It is a pleasure to acknowledge my gratitude to all the people involved directly or indirectly in the production of this manuscript.

November, 2016

Alperen ACAR

TABLE OF CONTENTS

Pa	age
LIST OF SYMBOLS	vii
LIST OF ABBREVIATIONS	viii
LIST OF FIGURES	
LIST OF TABLES	
ABSTRACT	
ÖZET	xiv
CHAPTER 1	
INTRODUCTION	1
1.1 Literature Review 1.1.1 Carbon Based Nano Materials 1.1.2 Graphene Fabrication Methods 1.1.3 Properties of Epoxy resins 1.1.4 Production And Characterization Of Nanocomposite Materials 1.1.5 Modeling the Mechanical Behavior of Nanocomposite Materials 1.1.6 Numerical Implementations of Polymer Matrix Composites 1.2 Objective of the Thesis 1.3 Hypothesis	2 4 6 7 14 15 16
CHAPTER 2	
FABRICATION AND CHARACTERIZATION OF GRAPHENE - EPOX	ΚY
COMPOSITES	17
2.1 Fabrication of Graphene Reinforced Epoxy Composites 2.2 Characterization of Graphene Reinforced Epoxy Composites 2.2.1 Characterization of graphene sheets 2.2.2 Tensile Test Results 2.2.3 Dynamic Mechanical Analysis 2.3 Conclusions on Experimental work	18 19 20 24

CHAPTER	3	
MODELIN	G WORK	. 28
3.1	The Viscoplasticity Theory Based on Overstress - An Overview	. 28
	Cooperative – VBO Theory	
	Effective Elasticity Modulus Definition	
3.4	Modifications on visco-plastic part of Cooperative-VBO theory to model	ĺ
	stiffening effect of graphene	. 43
3.5	Simulation Results	. 46
CHAPTER FINITE EL	4 EMENT METHOD PROCEDURE FOR COOPERATIVE VBO MODEI	. 56
	Integration of Constitutive Equations with the Forward Gradient Method	
	Definition of the Jacobian Matrix	
4.3	FEM Integration Scheme Results	. 63
CHAPTER	5	
RESULTS .	AND DISCUSSION	. 70
REFEREN	CES	

CURRICULUM VITAE......76

LIST OF SYMBOLS

$\dot{\gamma}_p$	Plastic strain rate
À	Isotropic stress
D	Total deformation tensor
$\mathbf{d}^{\mathbf{e}}$	Elastic deformation tensor
$\mathbf{d}^{\mathbf{vp}}$	Viscoplastic deformation tens
E	Elasticity Modulus
E_t	Tangent Modulus
G	Equilibrium stress tensor
K	Kinematic stress
K^{eff}	Effective Bulk Modulus
\mathbf{S}	Deviator of Cauchy stress tens
$T_{\rm f}$	Flow Temperature
T_{g}	Glass Transition Temperature
t_i	Internal stress
T_{β}	β Transition Temperature
V	Activation volume
Γ	Overstress invariant
ΔH_{β}	Activation Energy
μ^{eff}	Effective Shear Modulus
ν	Poisson's Ratio
σ	Cauchy Stress Tensor
Ψ	Shape function

LIST OF ABBREVIATIONS

Dynamic Mechanical Analysis **DMA**

Finite Element Method **FEM** GPL **Graphene Platelets**

IUPAC International Union of Pure and Applied Chemistry
NMP N-Methyl-2-pyrrolidone

SEM

Scanning Electron Microscopy
Viscoplasticity Based on Overstress VBO

LIST OF FIGURES

	Page
Figure 1.1	Schematic of Carbon Based Nano materials
Figure 1.2	Schematic illustration of the main graphene production techniques. (a)
8	Micromechanical cleavage. (b) Anodic bonding. (c) Photoexfoliation. (d)
	Liquid phase exfoliation.(e) Growth on SiC. Gold and grey spheres
	represent Si and C atoms, respectively. At elevated T, Si atoms evaporate
	(arrows), leaving a carbon-rich surface that forms graphene sheets. (f)
	Segregation/precipitation from carbon containing metal substrate. (g)
	Chemical vapor deposition. (h) Molecular Beam epitaxy. (i) Chemical
	synthesis using benzene as building block [3]4
Figure 1.3	Schematic showing the preparation procedure for epoxy nanocomposites
rigare 1.5	[7]
Figure 1.4	Comparative images of the dispersion state. From left to right: TEM
Tiguic 1.4	images of 3 wt% thermally exfoliated graphene in TPU by melt and
	solvent processing, and in situ polymerisation [4]140
Figure 2.1	Graphene Fabrication Procedure by pictures
Figure 2.1	Raman spectra of graphene, from Young et al. [31]
Figure 2.3	Raman spectra of graphene sheets
Figure 2.4	Comparision of neat epoxy and %0.1 and %0.5 graphene platelets-epoxy
riguic 2.4	nanocomposite tensile test results. Solvent: asetone
Figure 2.5	Comparision of neat epoxy and %0.1 and graphene platelets -epoxy
rigure 2.3	nanocomposite tensile test results. Solvent: asetone and NMP22
Figure 2.6	Elasticity modulus values for graphene content
Figure 2.7	SEM images of graphene-epoxy nanocomposite
Figure 2.7	Dynamic mechanical properties of epoxy and nanocomposite, Storage
riguic 2.6	Modulus versus Temperature curves
Figure 2.9	Dynamic mechanical properties of epoxy and nanocomposite, Loss
rigure 2.9	Modulus versus Temperature curves
Figure 2.10	
Figure 2.10	Dynamic mechanical properties of epoxy and nanocomposite, tan δ versus
Eigung 2.1	Temperature curves. 26
Figure 3.1	Standard linear solid model (SLS)
Figure 3.2	Rheological representation of VBOP model [37]
Figure 3.3	Evolution of the theree stress-like State Variables of Cooperative-VBO
Eigyma 2.4	model for different temperature values
Figure 3.4	Evolution of the theree stress-like State Variables of Cooperative-VBO
Eigung 2.5	model for different strain rates
Figure 3.5	Micromechanics model for the agglomeration of graphene sheets. [25] 36
Figure 3.6	Modulus versus graphene content for different ξ values
Figure 3.7	Modulus versus Temperature curves for different graphene content 39

Figure 3.8	Modulus versus Strain Rate curves for different graphene content 40
Figure 3.9	Storage Modulus Test – Model Comparison for Neat epoxy41
Figure 3.10	Storage Modulus Test – Model Comparison for) 0.1wt% Graphene-epoxy nanocomposite
Figure 3.11	Storage Modulus Test – Model Comparison for) 0.5wt% Graphene-epoxy
C	nanocomposite
Figure 3.12	Evolution of the three stress-like State Variables of Cooperative-VBO model for Nanocomposites for different graphene fractions
Figure 3.13	Comparison of model responses to compression test data [17] (graphene %wt=0) a) strain rate=0.01 /s b) strain rate=0.1 /s c) strain rate=1/s46
Figure 3.14	Comparison of model responses to compression test data [17] (graphene %wt=0.25) a) strain rate=0.01 /s b) strain rate=0.1 /s c) strain rate=1/s47
Figure 3.15	Comparison of model responses to compression test data [17] (graphene %wt=0.5) a) strain rate=0.01 /s b) strain rate=0.1 /s c) strain rate=1/s48
Figure 3.16	Comparison of model responses to compression test data [17] (graphene %wt=1) a) strain rate=0.01 /s b) strain rate=0.1 /s c) strain rate=1/s49
Figure 3.17	Comparison of model responses to compression test data [17] (strain rate = 0.01/s) a) wt%0 graphene b) wt%0.25 graphene c) wt%0.5 graphene d) wt%1 graphene
Figure 3.18	Comparison of model responses to compression test data [17] (graphene %wt=0.25) a) strain rate=0.01 /s b) strain rate=0.1 /s c) strain rate=1 /s d) strain rate=10/s
Figure 3.19	Comparison of model responses to compression test data [17] (graphene $\%$ wt = 0.5) a) strain rate=0.01 /s b) strain rate=0.1 /s c) strain rate=1 /s d) strain rate=10/s
Figure 3.20	Comparison of model responses to compression test data [17] (graphene %wt=1) a) strain rate=0.01 /s b) strain rate=0.1 /s c) strain rate=1 /s d) strain rate=10 /s
Figure 3.21	Model responses varying with temperature55
Figure 4.1	Flow-Chart of the Forward Gradient Scheme
Figure 4.2	ODE solution – FEM solution comparison for %wt=0, Strain rate = 0.01/s Temperature = 296 K
Figure 4.3	ODE solution – FEM solution comparison for %wt=0, Strain rate = 0.1/s Temperature = 296 K
Figure 4.4	ODE solution – FEM solution comparison for %wt=0, Strain rate = 1/s Temperature = 296 K (Step time (DTIME) = 1e-7)
Figure 4.5	ODE solution – FEM solution comparison for %wt=0.25, Strain rate = 1e-2/s Temperature = 296 K
Figure 4.6	ODE solution – FEM solution comparison for %wt=0.5, Strain rate = 1e-2/s Temperature = 296 K
Figure 4.7	ODE solution – FEM solution comparison for %wt=1, Strain rate = 1e-2/s Temperature = 296 K
Figure 4.8	FEM Scheme results for different step times
Figure 4.9	FEM Scheme results for different number of elements

LIST OF TABLES

	F	Page
Table 2.1	Tensile properties of epoxy and composites with various weight fracti	ions
	of graphene-platelets	23
Table 3.1	Storage modulus model Parameters	
Table 3.2	Parameters for the flow rule, strain softening, calculation of $\Delta H_{\beta}^{\text{eff}}$, V	
	and Tangent modulus E _t	49
Table 3.3	Parameters for the shape function (Ψ) , C function, isotropic stress (A)	and
	tangent modulus (E _t)	50
Table 3.4	Parameters for Effective Elastic Moduli	50

MODELING OF POLYMER MATRIX COMPOSITES USING VBO MODEL and FINITE ELEMET METHOD FORMULATIONS

Alperen ACAR

Department of Mechanical Engineering
Ph. D. Thesis

Adviser: Prof. Dr. Özgen ÇOLAK ÇAKIR

Polymeric materials are widely used in industry and researched in academia due to their low weight and ease on processing. But the mechanical properties of polymers are mostly low, in a comparison to metallic materials. Because of low strength and stiffness the mechanical properties of polymers are needed to be enchanced by composing them with various kinds of reinforcements.

On the other hand, graphene, is a wonder nano-material which has 130 GPa of ultimate strength and 1 TPa of elastisity modulus. This superior properties of graphene makes it a great candidate for a polymer reinforcing agent. But the relevant literture shows us that the technology of polymer matrix graphene nanocomposites has to be improved to exhibit the superior properties of this nano material.

This work has three tresholds, first the production and characterization of grapheneepoxy nanocomposite, second, modeling the total viscoelastic - viscoplastic behavior of the nanocomposite and third part is to implement the proposed model to finite element method for possible future use of the model on structural analysis.

In the composition processes with nanomaterials, the biggest drawback is agglomeration of the nanomaterials. In this work, this problem is tried to overcome using a solvent and a sonication procedure before mixing the nano material with the prepolymer (in this work, epoxy resin). The mechanical characterization of the produced material is done by performing tensile tests and DMA tests. The mechanical properties are enchanced with the addition of graphene.

In this work, Cooperative-VBO model which is developed for modeling temperature dependent mechanical behavior by COLAK, AHZİ and REMOND is modified to represent the behavior of nanocomposites. For modeling the mechanical behavior of nanocomposites, two main modifications are done. First one is redefining stiffnesstemperature model of Mahieux and Reifsdner using a two step Mori-Tanaka scheme. In this scheme, the well dispersed (effective) and agglomerated regions are taken as different phases. Therefore the agglomeration effect of graphene is taken into account. Storage modulus of pure epoxy and graphene-epoxy nanocomposites with different graphene fractions are modeled using the modified model. The model shows good agreement with the experimental results. Second modification is on viscoplastic part, in particular, two scalar material parameters of the plastic strain rate function, activation energy $\Delta H\beta$, and activation volume V are redefined as functions of graphene fraction using Tagayanagi averaging approach. For the post - yield behavior of the nanocomposites, two parameters of the previously used tangent modulus function, E_{T0} and α , are defined as functions of graphene fraction, numerically. Therefore, the total viscoelastic - viscoplastic behavior of graphene nanocomposite materials are defined.

The proposed model is capable of modeling material behavior for different temperature and strain rates as well. Model results are compared to test results to test the accuracy, good match with the experimental data is observed.

In the last part, a computational procedure is defined using forward gradient method, for finite elemnt method implementation. This part leads the further usage of the proposed model for strucural analysis for possible future applications using nanocomposite materials.

This work contributes to the related literature with a unique constitutive equation for modeling of epoxy-graphene nanocomposites. As explained above, the proposed model is capable of modeling the total viscoelastic-viscoplastic, temperature dependent mechanical behavior of such nanocomposites for different graphene fractions. The prediction capabilities of the model is tested through a set of test data, and it is shown that the prediction capabilities of the model are very good. Another unique contribution to the related liteature is the developed computational scheme. With this addition, it is shown that the proposed model can be used for structural analysis on possible future applications.

Key words: Graphene, Nanocomposite, constitutive equation, modeling, VBO

YILDIZ TECHNICAL UNIVERSITY
GRADUATE SCHOOL OF NATURAL AND APPLIED SCIENCES

POLİMER MATRİSLİ KOMPOSİTLERİN VBO MODELİ İLE MODELLENMESİ VE SONLU ELEMANLAR YÖNTEMİ FORMÜLASYONLARI

Alperen ACAR

Makine Mühendisliği Anabilim Dalı

Doktora Tezi

Tez Danışmanı: Prof. Dr. Özgen ÇOLAK ÇAKIR

Polimer malzemeler, hem ağırlık avantajları ve hem de imalat kolaylıkları sebebiyle endüstriyel olarak ve akademik çalışmalarda oldukça yaygın kullanılmaktadırlar. Fakat bu yaygın kullanıma karşın, mekanik özellikleri metalik malzemelere kıyasla çoğunlukla düşük kalmaktadır. Dayanım bakımından karşılaşılan bu yetersizlik bizleri, polimer malzemeleri, çeşitli katkılarla zenginleştirip, dayanımını arttırmaya yöneltmektedir.

Diğer yandan, Grafen, 130 GPa kopma mukavemeti ve 1 TPa civarında ölçülmüş elastisite modülü ile, polimerik malzemelerin dayanımını artırabilecek oldukça güçlü bir takviye malzemesi adayı olmaktadır. Fakat ilgili literatür incelendiğinde, bu olağanüstü özelliklere sahip nano malzemenin teknolojisinin, hem endüstriyel hem de akademik anlamda geliştirilmeye muhtaç olduğu anlaşılmaktadır.

Bu çalışma, üç aşamadan oluşmaktadır. İlk olarak grafen - epoksi nanokompozit malzeme üretilmiş, gerekli görülen mekanik ve morfolojik testlere tabii tutularak üretilen malzeme karakterize edilmiştir. İkinci olarak, malzemenin toplam viskoelastik - viskoplastik davranışını modellenmiş ve son olarak önerilen model için bir hesaplamalı prosedür oluşturularak sonlu elemanlar yöntemi implementasyonu gerçekleştirilmiştir.

Nano malzemerle hazırlanan kompozitlerde karşılaşılan en öneml problem, nano malzemenin topaklanma eğiliminden kaynaklanan, heterojen yapılar olmaktadır. Bu problemin üstesinden gelmek için bu çalışmada grafen öncelikle bir ultrasonik karıştırıcı kullanılarak bir solvent içinde çözdürülmüş, daha sonra epoksi reçine ile karıştırılmıştır. Üretilen malzemenin mekanik karakterizasyonu çekme testleri ve DMA

testleri ile gerçekleştirilmiştir. Grafen katkısı ile mekanik özelliklerin iyileştiği gözlenmiştir.

Nano kompozitin toplam mekanik davranışını modellemek amacıyla, Çolak, Ahzi ve Remond tarafında 2013 yılında geliştirilen Cooperative-VBO modeli modifiye edilmiştir. Model, gerinim hızı tensörünün eklemeli bir formunu kullanmaktadır. Bu sebeple, modelin viskoelastik ve viskoplastik kısımları ayrı ayrı ele alınmıştır. Grafen katkısının viskoelastik davranış üzerindeki etkisini modellemek için iki adımlı bir Mori-Tanaka şeması kullanılmıştır. Bu yaklaşımla, grafenin etkin olarka çözündüğü ve topaklandığı bölgeler ayrı ayrı ele alınmış ve böylece topaklanmanın elastik davranış üzerindeki nonlineer etkisi modellenmiştir. Epoksi ve grafen takviyeli nanokompozit malzemenin DMA testinden elde edilen depolama modulu modifiye edilen model ile modellenmiştir. ve modelin deney sonuçları ile uyumlu cevap verdiği gösterilmiştir.

Viskoplastik kısımda ise, model içindeki iki skalar malzeme parametresi, aktivasyon enerjisi, $\Delta H\beta$, ve aktivasyon hacmi V, Tagayanagi ortalaması yaklaşımı ile grafen oranının fonksiyonu olarak tanımlanmıştır. Akma sonrasında görülen non-lineer davranışın modellenmesi amacıyla da tanjant modülü denklemi içindeki iki parametre, E_{T0} ve α , grafen hacim oranının fonksiyonu şeklinde tanımlanarak tanjant modülü denklemi modifiye edilmiştir. Önerilen model, malzeme üzerindeki grafen katkısını, değişen sıcaklık ve deformasyon hızı ile beraber modelleyebilmektedir. Model cevapları, test sonuçları ile karşılaştırılmış ve oldukça uyumlu oldukları gözlenmiştir.

Son olarak, Forward gradient metodu kullanılarak, hesaplamalı bir prosedür oluşturulmuş, böylece önerilen modelin, sonlu elemanlar yöntemi kullanılarak yapılacak yapısal analizlerde bünye denklemi olarak kullanılması mümkün kılınmıştır.

Çalışma, ilgili literatüre, epoxy nanokompozit malzemesi için kullanılabilecek özgün bir bünye denklemi kazandırmıştır. Önerilen modelin kestirme yetenekleri değişen grafen oranları için test edilmiş ve oldukça uyumlu sonuçlar verdiği gözlemlenmiştir. Çalışmanın ilgili literatüre bir başka katkısı isei model için önerilen hesaplamalı şemadır. Önerilen hesaplamalı çerçeve, bünye denklemini, ileride ihtiyaç duyulması muhtemel yapısal analiz uygulamalarında kullanılmasını mümkün kılmaktadır.

Anahtar Kelimeler: Grafen, Nanokompozit, bünye denklemi, modelleme, VBO

III																							

INTRODUCTION

IUPAC defines polymer as "substance composed of macromolecules". This definition of course covers all types of the macromolecules, but sure lacks of meaning to cover how polymers are inside of life. DNA, which is composed of nucleotides carries our entire genetic heritage is a polymer of course, or the pipe system that brings fresh water to our home is probably made of Polyethylene, also a synthetic polymer consists of ethylene monomers.

Since their discovery in the early 20th century, the technology of synthetic polymers has improved tremendously, and opened their way to all of our homes and almost all industrial applications around the world. The role of academia and academic research of course cannot be ignored in this progress. Actually polymers have created their own field of science, which we are now calling "Polymer Science".

Despite the enormous use in industry and the inevitable interest on academia, polymer materials, or plastic materials, as the name of their form used in industry, has still their own drawbacks. Strength is one of the first disadvantages of polymers coming to mind when an engineer decides to use them on an application. This handicap of polymers has tried to overcome by mixing polymers with reinforcement agents. Some well-known and widely used reinforcement materials are glass or carbon fibers. But the use of those types of conventional reinforcement agents clears away some of the main advantages of polymers, low weight and ease on processing. It also complicates or sometimes removes the possibility, of recycling. In these circumstances, the research on the field of polymers has led to find new unconventional reinforcement agents.

Graphene is a single layer of graphite, or carbon, first isolated and characterized in 2004 in University of Manchester. Andre GEIM and Konstantin NOVOSELOV won the Nobel Prize on physics in 2010 "For groundbreaking experiments regarding the two-

dimensional material graphene." In the past six years, the global market for graphene is reported to have reached \$9 million by 2012 with most sales in the semiconductor, electronics, and battery energy and composites industries.

From the perspective of material strength, graphene is a spectacular material, which has a measured elasticity modulus of 1 TPa and intrinsic strength of 130 GPa [1]. These tremendous properties make graphene a sufficient reinforcement agent for polymer composite materials. However, this great discovery comes with its own challenges of technology. The relevant literature shows us that the technology of graphene and its composites are in need of advancing.

To achieve optimal enhancement in the property of graphene reinforced polymer composites, several key issues such as improvement in dispersion of graphene, alignment of graphene in polymer matrix, surface modifications on graphene platelets for good adhesion/interaction, should be resolved.

On the other hand, understanding the inner mechanics of graphene nanocomposites and modeling the total mechanical behavior is also an important issue in the area of graphene nanocomposites.

1.1 Literature Review

1.1.1 Carbon Based Nano Materials

Nano materials, corresponds to materials which a single unit is sized as 1-1000 nanometers (10^{-9} meters). Among those materials, carbon based ones are an important family due to the superior electrical and mechanical properties.

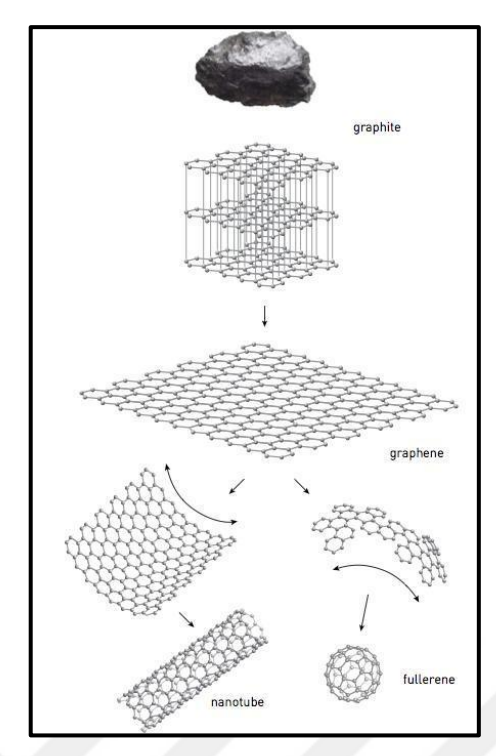


Figure 1.1 Schematic of Carbon Based Nano materials

Graphene, which is considered the basic building block of all graphitic forms (including carbon nanotubes (CNTs), graphite and fullerene), possesses a single layer of carbon atoms in a closely packed honeycomb two-dimensional lattice. Graphene has a large specific surface area (theoretical value 2630 m2 g-1), and both sides of its planar sheets are available for molecule adsorption. The exceptional properties of graphene make it a superior candidate as a good adsorbent in different sample preparation methods [2].

The fullerenes are a class of allotropes of carbon which conceptually are graphene sheets rolled into tubes or spheres. These include the carbon nanotubes (or silicon nanotubes) which are of interest both because of their mechanical strength and also because of their electrical properties. The first fullerene molecule to be discovered, and the family's namesake, buckminsterfullerene (C60), was prepared in 1985 by Richard Smalley, Robert Curl, James Heath, Sean O'Brien, and Harold Kroto at Rice University. The name was homage to Buckminster Fuller, whose geodesic domes it resembles.

Carbon nanotubes (CNTs), discovered in 1991 by Iijima, have diameters from fractions to tens of nanometers and lengths up to several micrometers. CNTs can be considered as a graphene sheet in the shape of a cylinder capped by fullerene-like structures. Single-walled (SWCNTs) and multi-walled (MWCNTs) nanotubes are formed by seamless roll up of single and multi-layers of graphene lamella respectively.

1.1.2 Graphene Fabrication Methods

A rapidly increasing list of graphene production techniques has been developed to enable graphene's use in commercial applications. Isolated 2D crystals cannot be grown via chemical synthesis beyond small sizes even in principle, because the rapid growth of phonon density with increasing lateral size forces 2D crystallites to bend into the third dimension. However, other routes to 2d materials exist.

Fundamental forces place seemingly insurmountable barriers in the way of creating 2D crystals. The nascent 2D crystallites try to minimize their surface energy and inevitably morph into one of the rich variety of stable 3D structures that occur in soot.

But there is a way around the problem. Interactions with 3D structures stabilize 2D crystals during growth. So one can make 2D crystals sandwiched between or placed on top of the atomic planes of a bulk crystal. In that respect, graphene already exists within graphite. One can then hope to fool Nature and extract single-atom-thick crystallites at a low enough temperature that they remain in the quenched state prescribed by the original higher-temperature 3D growth.

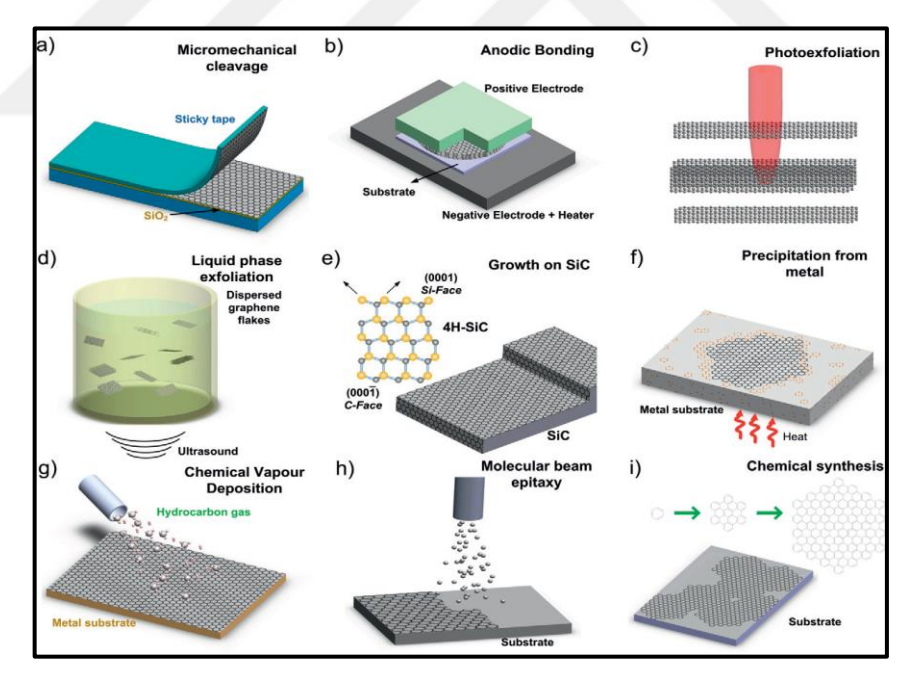


Figure 1.2 Schematic illustration of the main graphene production techniques. (a) Micromechanical cleavage. (b) Anodic bonding. (c) Photoexfoliation. (d) Liquid phase exfoliation.(e) Growth on SiC. Gold and grey spheres represent Si and C atoms, respectively. At elevated T, Si atoms evaporate (arrows), leaving a carbon-rich surface that forms graphene sheets. (f) Segregation/precipitation from carbon containing metal substrate. (g) Chemical vapor deposition. (h) Molecular Beam epitaxy. (i) Chemical synthesis using benzene as building block [3].

Dry exfoliation is the splitting of layered materials (LM) into atomically thin sheets via mechanical, electrostatic, or electromagnetic forces in air, vacuum or inert environments. Micromechanical cleavage (MC), also known as micromechanical exfoliation, has been used for decades by crystal growers and crystallographers. Andre Geim and Konstantin Novoselov initially used adhesive tape to perform the mechanical cleavage. Achieving single layers typically requires multiple exfoliation steps, each producing a slice with fewer layers, until only one remains. After exfoliation the flakes are deposited on a silicon wafer. Crystallites larger than 1 mm and visible to the naked eye can be obtained.

Anodic bonding is widely used in the microelectronics industry to bond Si wafers to glass, to protect them from humidity or contaminations. When employing this technique to produce single layer graphene sheets, graphite is first pressed onto a glass substrate, a high voltage of few kV (0.5 - 2 kV) is applied between the graphite and a metal back contact, and the glass substrate is then heated ($\sim 200 \, ^{\circ}\text{C}$ for $\sim 10 - 20 \, \text{mins}$). If a positive voltage is applied to the top contact, a negative charge accumulates in the glass side facing the positive electrode, causing the decomposition of Na2O impurities in the glass into Na+ and O2 - ions. Na+ moves towards the back contact, while O2 - remains at the graphite-glass interface, establishing a high electric field at the interface. A few layers of graphite, including SLGs, stick to the glass by electrostatic interaction and can then be cleaved off [3].

Laser ablation is the use of a laser beam to remove material from a solid surface. If irradiation results in the detachment of an entire or partial layer, the process is called photo exfoliation.

Graphite can also be exfoliated in liquid environments exploiting ultrasounds to extract individual layers. The liquid-phase exfoliation (LPE) process generally involves three steps: 1) dispersion of graphite in a solvent; 2) exfoliation; 3) "purification". The third step is necessary to separate exfoliated from un-exfoliated flakes, and is usually carried out via ultracentrifugation.

The production of graphite from SiC, was reported by Acheson as early as 1896 for lubricant applications. The growth mechanism has been investigated since the 1960s. Both surfaces (Si(0001)- and C(000-1)- terminated) annealed at high T (>1000 °C) under ultra-high vacuum (UHV) graphitize due to the evaporation of Si.

CVD is a process widely used to deposit or grow thin films, crystalline or amorphous, from solid, liquid or gaseous precursors of many materials. CVD has been the workhorse for depositing many materials used in semiconductor devices for several decades.

Molecular Beam epitaxy or arc discharge can be used to grow single layer graphene of high enough quality to compete with other processes discussed above. Since MBE relies on atomic beams of elements impinging on the substrates, it is difficult to prevent, say carbon, from being deposited on areas where graphene has already grown. Therefore, since MBE is a thermal process, the carbon is expected to be deposited in the amorphous or monocrystalline phase. One might however envisage the use of chemical beam epitaxy (CBE) to grow graphene in a catalytic mode, taking advantage of the CBE ability to grow or deposit multiple materials, such as dielectrics or layered materials, on the top of graphene, to form hetero structures.

1.1.3 Properties of Epoxy resins

Epoxy is a term used to denote both the basic components and the cured end products of epoxy resins, as well as a colloquial name for the epoxide functional group. Epoxy resins, also known as polyepoxides, are a class of reactive pre-polymers and polymers which contain epoxide groups. Epoxy resins may be reacted (cross-linked) either with themselves through catalytic homo-polymerization, or with a wide range of co-reactants including poly-functional amines, acids (and acid anhydrides), phenols, alcohols and thiols. These co-reactants are often referred to as hardeners or curatives, and the cross-linking reaction is commonly referred to as curing. Reaction of polyepoxides with themselves or with poly-functional hardeners forms a thermosetting polymer, often with high mechanical properties, temperature and chemical resistance. Epoxy has a wide range of applications, including metal coatings, use in electronics / electrical components/LED, high tension electrical insulators, fiber-reinforced plastic materials and structural adhesives.

Epoxy resins are low molecular weight pre-polymers or higher molecular weight polymers which normally contain at least two epoxide groups. The epoxide group is also sometimes referred to as a glycidyl or oxirane group.

A wide range of epoxy resins are produced industrially. The raw materials for epoxy resin production are today largely petroleum derived; although some plant derived

sources are now becoming commercially available (e.g. plant derived glycerol used to make epichlorohydrin).

Epoxy resins are polymeric or semi-polymeric materials, and as such rarely exist as pure substances, since variable chain length results from the polymerization reaction used to produce them. High purity grades can be produced for certain applications, e.g. using a distillation purification process. One downside of high purity liquid grades is their tendency to form crystalline solids due to their highly regular structure, which require melting to enable processing.

An important criterion for epoxy resins is the epoxide content. This is commonly expressed as the epoxy equivalent weight, which is the number of epoxide equivalents in 1 kg of resin (Eq./kg), or as the equivalent weight, which is the weight in grams of resin containing 1 mole equivalent of epoxide (g/mol). One measure may be simply converted to another:

Equivalent weight (g/mole) = 1000 / epoxide number (Eq./kg)

The equivalent weight or epoxide number is used to calculate the amount of co-reactant (hardener) to use when curing epoxy resins. Epoxies are typically cured with stoichiometric or near-stoichiometric quantities of curative to achieve maximum physical properties.

As with other classes of thermoset polymer materials, blending different grades of epoxy resin, as well as use of additives, plasticizers or fillers is common to achieve the desired processing and/or final properties, or to reduce cost. Use of blending, additives and fillers is often referred to as formulating.

1.1.4 Production And Characterization Of Nanocomposite Materials

In all Nano-composite fabrication procedures, the dispersion of Nano filler is the most significant step [4]. A well dispersed composite structure ensures a maximized interface area between matrix and filler. Such that, from a molecular point of view, a successful load transformation from matrix to filler will be achieved.

Unfortunately, it is a known fact that all nano fillers including graphene has a strong trend of agglomeration. Therefore, largest efforts in the area of developing fabrication procedures for nanocomposites concentrated on achieving a homogenous and well dispersed composite structure.

Procedures developed in order to achieve good dispersion could be classified under three main strategies [4];

- 1- Solvent Processing
- 2- in situ polymerization
- 3- Melt Processing.

1.1.4.1 Solvent Processing

This method actually consists in three steps;

- 1. Dispersion of graphene sheets or platelets in a proper solvent by various mixing techniques like mixers or more exquisite methods such as ultra sonication,
- 2. Addition of the matrix material,
- 3. Removal of the solvent by evaporation or distillation.

Several composites has been fabricated and reported in the related literature using such procedures [5,6], [7]. Ramanathan et al. [5] has investigated elasticity modulus E, glass transition temperature Tg, ultimate strength and thermal degradation on composites of PMMA reinforced by single walled carbon nanotubes, exfoliated graphene and functionalized graphene sheets. The intention of functionalization in this manner is using a surface agent to enhance the interface bond forces between Nano reinforcement and matrix material. Ramanathan et al. reported that in a comparison of three different Nano fillers, the most significant improvement is determined on composites that include FGS (functionalized graphene sheets) as the reinforcement material.

Because of the simple operations on this technique, it is expected that the composites will be prepared using such procedures. However, like almost every engineering method, this method comes with its own unfair able features. The caution of this method is that the solvents, especially organic solvents used in fabrication polymer matrix composites, adsorbed on the graphitic galleries of graphene in a permanent way [8]. The work of Barroso et al. [8] analyses the existence of both polar and non-polar solvents using ¹³C NMR and elemental techniques. They found that the all tried solvents penetrated and modified the graphitic layers of graphene and even after very meticulous removal and drying protocols, traces of solvent material remained adsorbed on the

material. Existence of a solvent in the structure of finished composite surely reduces the reliability of the composite material.

1.1.4.2 In situ Polymerization

This strategy starts with a step of mixing graphene platelets or chemically modified graphene sheets with the monomers, in our case pre polymers such as epoxy resin. And this step follows the polymerization reaction proceeds by adjusting parameters such as temperature and time.

Works of fabrication by in situ polymerization technique could be found in literature for both thermoplastics and epoxy matrix composites [7,9,10], [11], [12], [13]

Prolong et al. [9] compared several methods for dispersion of Nano filler in the epoxy matrix. High shear mixing, calendaring and a combination of two methods are compared. The structure of nanocomposite is determined by X-ray diffraction and scanning electron microscopy techniques. And the thermo – mechanical behavior of material is measured by DSC, DMTA and TGA techniques. The work has reported that the most effective technique to disperse the Nano filler in the matrix material is calendaring.

Work of Rafiee et al. [7] has compared the mechanical properties of epoxy nanocomposites reinforced by graphene platelets, single walled carbon nanotubes and multi walled carbon Nano tubes. The procedure of fabricating nanocomposite in this work is as follows; first, graphene platelets (GPL) is dispersed in acetone by ultrasonication for 1.5 hour. Then the epoxy resin is added to the mixture and sonicated for another 1.5 h. Next the acetone is evaporated on a magnetic stir plate for 3 hours at 70 °C. The evaporation procedure continues in a vacuum chamber for 12 hour at 70 °C. After the cooling of this mixture, a curing agent is added, and mixed in a shear mixer for 4 minutes at 200 rpm. Finally the mixture is placed in a vacuum chamber to degas the epoxy for approximately 30 minutes. The curing is made on silicone molds at room temperature on 90 psi for 24 hours followed by a post cure of 4 hour at 90 °C. The schematic given in the work to explain the procedure is given in Figure 1.

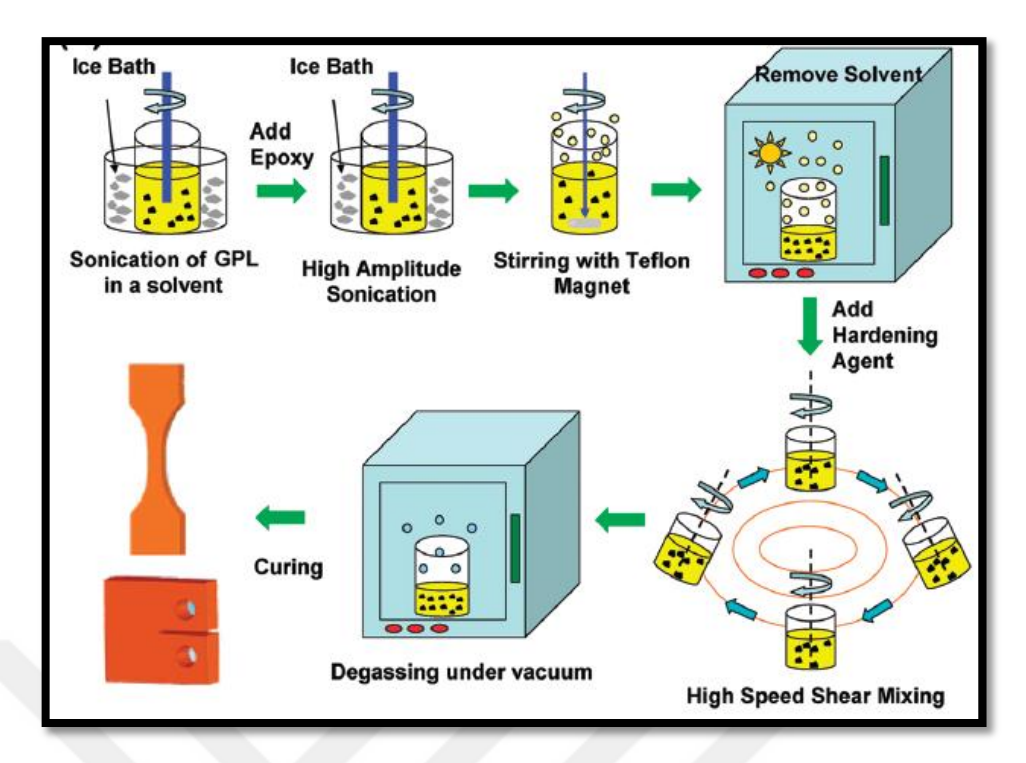


Figure 1.3 Schematic showing the preparation procedure for epoxy nanocomposites [7].

The work also reports that the most significant improvement is obtained by graphene platelets. The elasticity modulus is increased by 31% compared to the pure epoxy and 3% for single walled nanotubes.

Therefore, for the fabrication of epoxy/graphene composites, work of Rafiee [7] et al. gives a good start point.

Kulia et al. [11] used the method of emulsion polymerization of methyl methacrylate monomer in graphite oxide for the purpose of producing PMMA/graphene nanocomposites. Also a number of experimental methods were applied on the produced materials by Kulia et al. [11]. Raman spectrometry and FTIR analyses were performed to show the existence of graphene in the material. DMA and DSC analyses were conducted to determine the thermal transitions of the produced material. Storage modulus and Tg values were found to be greater than neat PMMA.

Another work was performed by Layek et al. [12]using atom transfer radical polymerization (ATRP) with functionalized graphene (MG) and PMMA used as a filler with PVDF matrix. The morphology of the material was determined using atomic force microscopy (AFM). Also in this work, FTIR analysis and WAXS, DSC, TGA and DMA analyses were performed to determine the thermal and mechanical behavior of

the polymer. Tg was decreased while the mechanical properties were improved compared to plain PVDF material.

Potts et al. [13] also performed an experimental work to produce and determine thermomechanical properties of modified graphene oxide and reduced graphene oxide/PMMA nanocomposites. Injection molded (composite material prepared by insitu polymerization) samples were subjected to tensile testing. Results have showed that for both composites, modulus is increased.

The work of Wang et al. [10] gives a simple and facile approach for preparation of PMMA/graphene composites using free radical polymerization technique.

The procedure on the work of Wang et. Al is as follows; a graphene/NMP (N-Methyl-2-pyrrolidone) solution is added to a three neck flask, sonicated in a low power sonic bath for 2 hours. Then under N₂ flow protection and magnetic stirring, 0.05 gr of AIBN (Azobisisobutyronitrile) is added. The mixture is heated at 80 °C. After reacting for 48 hours, the resultant solution is precipitated in 300 ml of methanol. The precipitate was collected and dissolved in 100 ml of THF (tetrahydrofuran). The solution was centrifuged at a speed of 10,000 rpm for 0.5 h, and then collected the solid at the bottom. This procedure was repeated for several times (at least five times) until no obvious sediments were observed when the supernatant was added into methanol. Finally, the product was dried under vacuum at 40 °C for 24 h.

On the sequel part of their work, Wang et al. [10] is characterized the final composite material by SEM, FTIR, TGA and tensile tests. They report that the resulting PMMA/GPMMA composite films enhances in mechanical properties, such as elasticity modulus and tensile strength increases by 151% and 115% compared to pure PMMA.

To sum up, the advantages of *in situ* polymerization technique are; it provides a strong interaction between incorporated particles and the polymer matrix. And this strong interaction enhances the stress transfer, and as a result the mechanical properties. This technique also enables and outstanding and homogenous dispersion of Nano filler in the polymer matrix, this also ensures the enhanced mechanical properties.

But the technique itself does not let the researcher only to focus and analyze the effect of Nano filler in the polymer matrix morphology and final mechanical or thermal properties, but also in the polymerization reaction (or curing reaction for the case of epoxy).

1.1.4.3 Melt Processing

Between the three main techniques compared, melt processing is the most commercially attractive technique. This technique is also more versatile and environmentally friendly [4].

The technique consists of direct addition of the Nano filler into the polymer melt using a twin screw extruder. Twin screw is used for improving the dispersion in the composite structure.

Though the usage of twin screw, the works in the related literature still reports a lower degree of dispersion [4]. Also the low bulk density of graphene makes extruder feeding a troublesome task.

Valles et al. [14] have prepared graphene oxide and base washed graphene oxide / PMMA nanocomposites by melt mixing using a twin screw extruder. The loading rates are between 0.5 and 10% by weight. The nanocomposites have been compared through dynamic mechanical thermal (DMTA) analysis, TGA and tensile tests. It is reported that the base washed graphene oxide serves better as a reinforcement in nanocomposite materials.

1.1.4.4 Comparison of Different Techniques and Review of the related literature

The work of Tang et al. [15] aims to discover the effect of dispersion state on mechanical behavior of Reduced graphene oxide (RGO) epoxy nanocomposites. In their work, it is clearly stated that highly dispersed RGO resulted in higher strength and fracture toughness of epoxy resin than the poorly dispersed RGO, but for both tensile and flexural moduli no significant differences was observed for different levels of dispersion. Glass transition temperature and electrical conductivity are also investigated in this work, and the well dispersed RGO fillers are found to be much more effective to increase Tg and electrical conductivity of epoxy resin.

Prolongo et al. [9] combined two main strategies to achieve a homogenous composite structure, three mill calendaring and sonication. Their work continued with mechanical, thermal and electrical characterization tests. It is reported that the graphene content in the epoxy matrix leaded to an increase in elasticity modulus. But due to a weak interface, strength and elongation at break are reduced. Moghadam et al. [16] proposed a functionalization method to improve the interface between graphene and epoxy. Their

method includes a silane coupling agent bonded to graphene platelets through an oxidation and functionalization process. The elasticity modulus and fracture toughness of nanocomposites of functionalized GNPs were enhanced 15% and 82%, respectively.

Shadlou et al. [17] investigated the mechanical behavior of graphene-epoxy nanocomposites for different strain rates by both tensile and compression tests. They reported that the composite material behaves more brittle with an increasing value of strain rate, as expected. The work also includes the SEM images of the crack surfaces and comparison of some widely used mechanical models to predict the yield stress of nanocomposites. Yue et al. [18] investigated the synergetic effects when two different forms of carbon, graphene and carbon nanotubes (CNTs) are used together as the reinforcing agent in an epoxy matrix dispersed by ultra-sonication, with different GPL – CNT ratios. The most effective CNT - GNP ratio is found to be 8:2 respectively. It is verified by optical microscopy, UV–Vis spectra technique and TEM technique that the addition of GNP to the epoxy – CNT system, both the dispersion state and stability of CNTs in epoxy is improved.

In another work of Prolongo et al. [19], the influence of thickness and lateral size of graphene flakes in an epoxy matrix is investigated. In this work, SEM and Raman spectroscopy techniques are used to determine size and thickness of GPLs. Three different graphene Nano-platelets, with different thickness and flake sizes, were added to epoxy matrix through a high shear mixing process to ensure a homogenous composite structure. It is stated that the rise of the weight of graphene flakes, causes to a decantation mechanism and this ends up with a less homogenous structure. The decrease of nanoparticle filler size raises the stacking ratio. An increase of lateral dimensions of GPLs, increases the thermal stability and therefore the degradation temperature. Work of Rafiee et al. [20] has compared the mechanical properties of epoxy nanocomposites reinforced by graphene platelets, single walled carbon nanotubes and multi walled carbon nanotubes. The work reports that the most significant improvement is obtained by graphene platelets. The elasticity modulus is increased by 31% compared to the pure epoxy and 3% for single walled nanotubes.

From a modest study of the related literature, it could be seen that, in situ polymerization method ensures fabricating a well dispersed nano filler and strongly bonded interface. Such a structure will surely result as significant improvement on mechanical properties of the composite material. Figure 1.4 shows TEM images of

graphene/TPU (Thermoplastic Polyurethane) nanocomposites. The images clearly reveal the dispersion state of the samples: melt processing samples present highly orientated thick stacks, while both solvent and in situ polymerization samples show homogeneously distributed thin sheets.

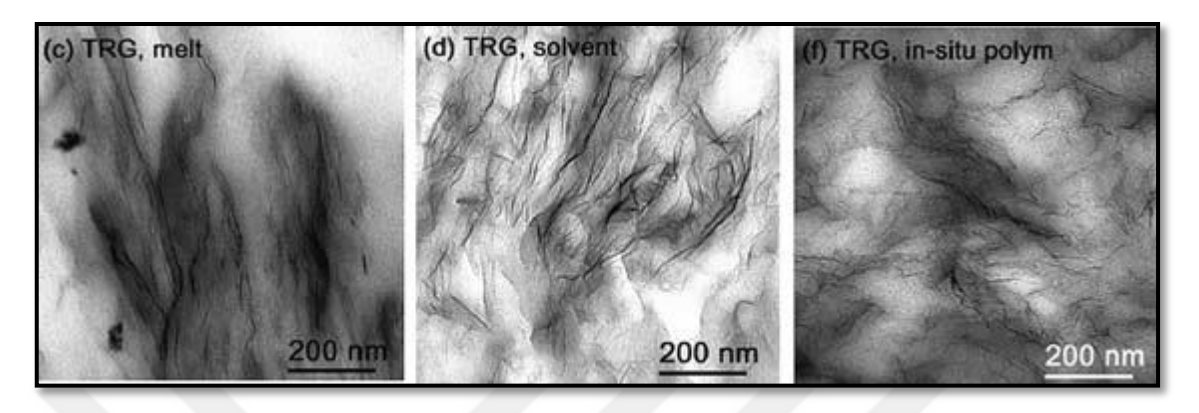


Figure 1.4 Comparative images of the dispersion state. From left to right: TEM images of 3 wt.-% thermally exfoliated graphene in TPU by melt and solvent processing, and in situ polymerization [4]

Therefore, if the complexity of the procedure (the polymerization reaction) could be neglected by an attentive and methodical study, this method should be used for the fabrication of nanocomposites.

1.1.5 Modeling the Mechanical Behavior of Nanocomposite Materials

Graphene has its own challenges for advancing in its technology. Creating a composite structure and characterizing the effect of composition on mechanical behavior is one of the challenges on state of the art graphene technology. The relevant literature reports that the stiffening effect of graphene is highly affected by agglomeration of graphene flakes. In other words, only a small fraction of graphene content is used to enhance the modulus value of the composite structure.

Xu et al. [21] proposed a hyper elastic constitutive equation using density functional theory of quantum mechanics for modeling mechanical behavior of graphene. In the model, the energy depends on the principal invariants of the right Cauchy–Green tensor and the strains in both zigzag and armchair directions. The use of both strains gives the model the ability to account for anisotropic behavior of graphene sheets. Proposed model is compared to Nano indentation tests from literature.

Parashar et al. [22] has investigated the fracture characteristics of graphene nanocomposites using a 3d representative volume element approach with finite elemnt

method. Van der Waals bonds between the polymer and graphene phases are modeled using truss elements. With their theoretical study, they reported that a good dispersion state ensures an enhancement in fracture toughness.

A multiscale Monte Carlo Finite Element Method is used by Spanos et al. [23] to determine mechanical behavior of polymer matrix - carbon nanotube composites. The proposed model takes account for the non-uniform dispersion state of the nano-fillers. They used the proposed FEM model to calculate the elasticity modulus and Poisson's ratio of the nanocomposites. They compared the model results to tensile test results from literature.

Montazeri and Tabar [24] is used molecular dynamics and finite elements method to determine elastics constants of nanocomposites. They reported the numerical results they produced are not very compatible with existing experimental results. They also reported that at low fractions, graphene performed better than carbon nanotubes as a reinforcing agent.

The work of Ji et al. [25] proposes an elasticity modulus definition which considers the agglomeration effect of graphene using Mori-Tanaka micromechanics method. In their work, graphene as a reinforcement agent also compared to carbon nanotubes, and shown the advantages of graphene. Major handicaps on reinforcing mechanism of graphene is also studied numerically in their work.

In brief, experimental work from literature reports that the existence of graphene in a polymer matrix has a stiffening effect on overall mechanical behavior. But this effect is highly affected by agglomeration tendency of graphene sheets and polymer-graphene interphase effects. Therefore, an elaborative work to define this effect—both theoretically and numerically- is needed.

1.1.6 Numerical Implementations of Polymer Matrix Composites

The progress on computer technology and efficient finite element techniques increased the demands for more realistic and accurate constitutive models. But the proposed models should be put in a numerical scheme for proper usage on accurate structural analysis.

Khani et al. [26] investigated the elastic properties of coiled carbon nanotube reinforced nano composites. In this work, a representative volume element approach, which

consists of three phases, filler, interphase and matrix, is used. The results show that the elastic moduli of randomly and unidirectional dispersed nanomaterial decrease when the coil tube or the coil diameter increases. In addition, reinforcement ratio increases by increasing the number of coils. A constitutive model for fiber reinforced polymer plies is proposed and implemented to an implicit FEM scheme by Flatscher et al. [27]. The implementation is made as a material routine for an implicit FEM package. With the implementation, the constitutive model is readily applicable in non-linear FEM analyses of laminated composite components. An isotropic, finite deformation version of VBO theory is implemented to finite element method by Gomaa et al. [28], [29]. Computational procedures are derived for the one-step forward gradient and the backward Euler methods.

1.2 Objective of the Thesis

This work is aimed to determine and model the mechanical behavior of Graphene-Epoxy nanocomposites. In this manner, the specimens are produced and subjected to necessary mechanical and morphological tests. With the test results, the Cooperative VBO theory is extended to model the nonlinear stiffening effect of graphene. The proposed model is implemented to Finite element method for further usage of structural analysis.

1.3 Hypothesis

In order to model the stiffening effect of graphene in a polymer matrix, the agglomeration behavior of graphene should not be neglected. Therefore, to model the total viscoelastic – viscoplastic behavior of graphene nanocomposites, a non-linear, temperature and rate dependent model which covers the agglomeration effects is needed.

FABRICATION AND CHARACTERIZATION OF GRAPHENE – EPOXY COMPOSITES

From a modest study of the related literature, it could be seen that, in situ polymerization method ensures fabricating a well dispersed nano filler and strongly bonded interface. Such a structure will surely result as significant improvement on mechanical properties of the composite material. On the other hand, working with prepolymers such as epoxy resin obligates us to make the dispersion before polymerization reaction.

2.1 Fabrication of Graphene Reinforced Epoxy Composites

Graphene nano-platelets is supplied by OOO HOLDING ZOLOTAYA FORMULA, from Russia. Epoxy resin is based on System 2000 epoxy resin by Fibregrast Inc. USA and System 2120 epoxy hardener is used as curing agent. This type of hardener is chosen due to delayed hardening time of 120 minutes. Such a long hardening time allows us to operate mixing and degassing operations freely. The mixing ratio of epoxy resin and hardener is 70:30 respectively, by weight, as recommended by producer. All the reagent are used as received. Two different types of solvents, acetone and *N*-Methyl-2-pyrrolidone (NMP) are used to see the effect of different solvents on the material.

Graphene epoxy composites are prepared following the procedure below;

1- Graphene platelets (GPL) are dispersed in acetone by ultra-sonication for 1.5 hour. (An ultrasonic probe sonicator is used.)

- 2- Epoxy resin is added to the mixture and sonicated for another 1.5 h. (System 2000 Epoxy Resin by Fibregrast Inc. USA)
- 3- Acetone is evaporated on a magnetic stir plate for 3 hours at 70 °C.
- 4- The evaporation procedure continues in a vacuum chamber for 12 hour at 70 °C.
- 5- After the cooling of this mixture, a curing agent is added, and mixed in a vacuum mixer for 10 minutes.
- 6- The mixture is placed in a vacuum chamber to degas the epoxy for approximately 30 minutes. (vacuum oven is used as the vacuum chamber)
- 7- The curing is made on custom build soft silicone molds at room temperature on 60 °C for 24 hours followed by a post cure of 4 hour at 90 °C.



Figure 2.1 Graphene Fabrication Procedure by pictures

2.2 Characterization of Graphene Reinforced Epoxy Composites

The characterization of graphene platelets (GPL) and composites consisted of the analysis of their morphological features and the determination of their thermomechanical and mechanical properties. The morphology of GPL and composites is investigated by Scanning Electron Microscopy (SEM). Tensile tests were performed using dumbbell shaped samples following the ASTM D638-10 [30], in MTS with a

crosshead speed of 2 mm/min. For each material, five specimens are tested and the averages of them are taken.

Raman spectra for graphene was obtained using Renishaw-In Via Raman microscope with an argon green laser light (wavelength 532 nm, laser power 100 %, scanning time 100 s).

Thermo-mechanical behavior is studied by Dynamic Mechanical Thermal Analysis (DMA) in three point bending mode. The experiments were carried out at 1 Hz frequency, scanning from 35 to 200 0 C using heating rate of 5^{0} C/min. The dimensions of samples were 35x13.5x3.2 mm. The maximum of tan δ vs. temperature plots was used to determine α -relaxation associated to the glass transition temperature.

2.2.1 Characterization of graphene sheets

Raman Spectroscopy has been used to characterize the number of layers in graphene. Graphene samples with different numbers of layers show significant differences in their Raman spectra. In a single layer graphene, G' (or 2D) Raman band is twice the intensity of the G band while in two layer material, the G band is stronger than 2D band. In addition, the 2D band is shifted to higher wave-number. D bands are found in the samples of imperfect or damaged graphene [31]. Figure 2 exhibiting different Raman spectra of graphene is replotted from [31].

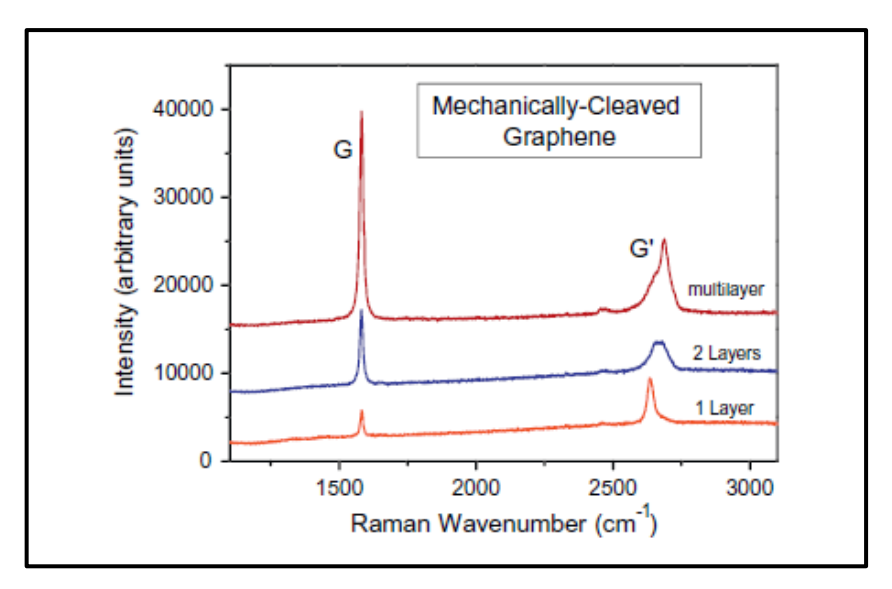


Figure 2.2 Raman spectra of graphene, from Young et al. [31]

A Raman spectrum of used graphene shows three dominant peaks as shown in Figure 2.3. The G band at 1588 cm⁻¹ and 2D band at 2633 cm⁻¹ shows the general characteristics of graphene. The peak at 1339 cm⁻¹ is associated with structural defects.

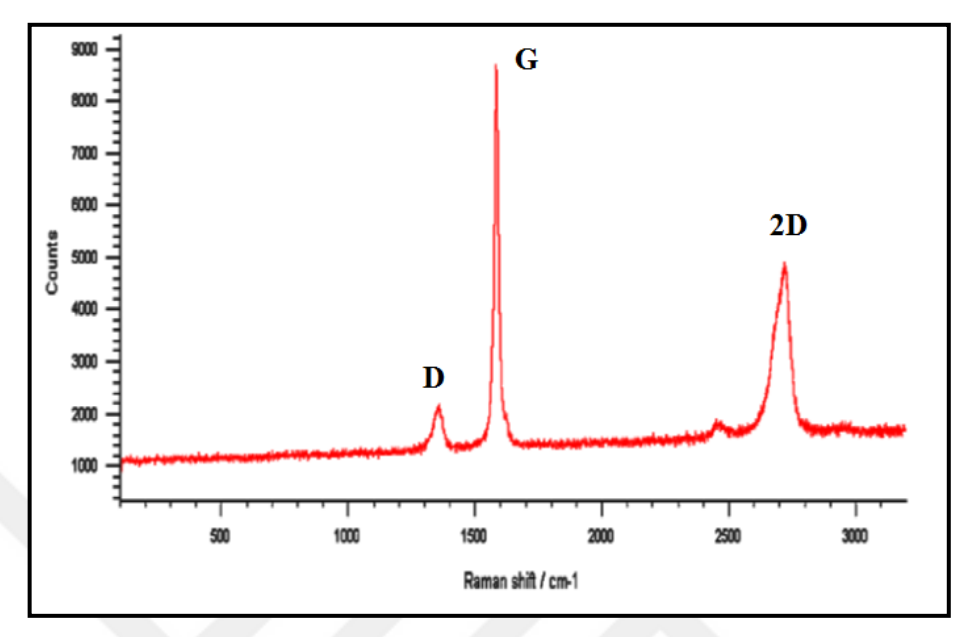


Figure 2.3 Raman spectra of graphene sheets

Intensity ratio of I_G/I_D exhibits defect quantity. A high ratio indicates a small disorder arising from structural defects as observed in the graphene used in this work.

2.2.2 Tensile Test Results

Samples are subjected to tensile test according to ASTM D638-10 [30] with a rate of 5 mm/min . The graphene platelets are used as the reinforcement agent in epoxy matrix in two different ratios (0.1% and 0.5%) and in two different solvent (acetone and *N*-Methyl-2-pyrrolidone (NMP)). Comparison of neat epoxy and %0.1 and %0.5 graphene platelets-epoxy nanocomposite tensile test results when acetone is used as solvent is depicted in Figure 2.4.

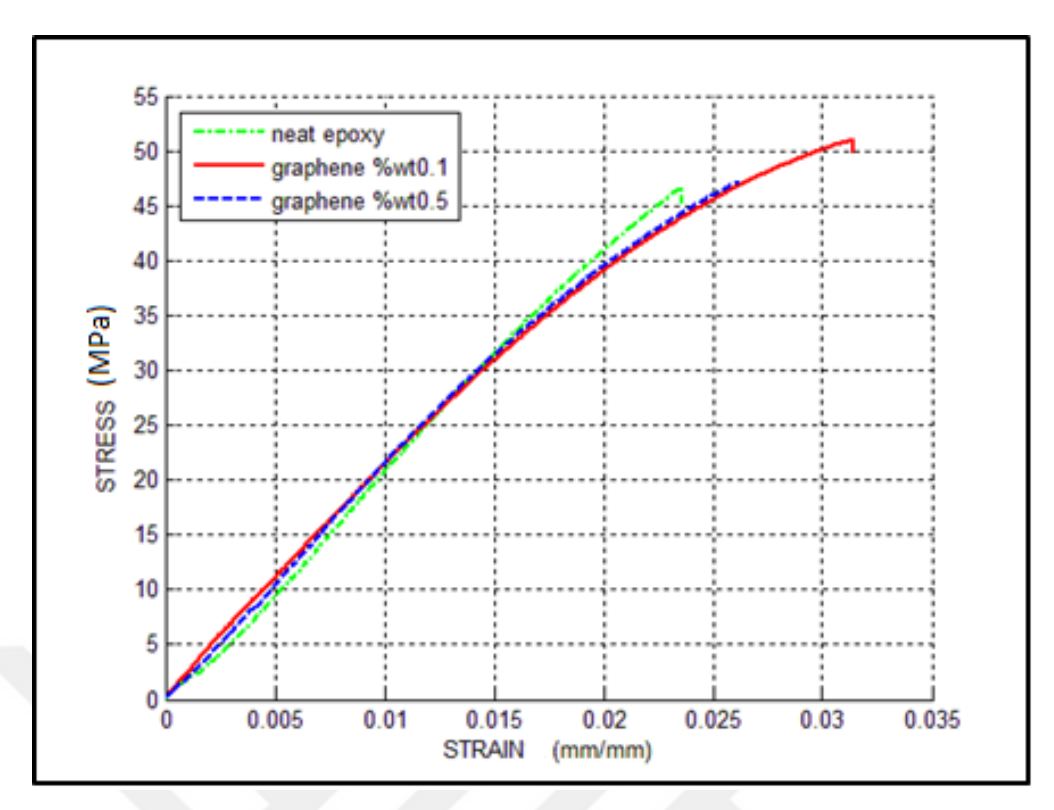


Figure 2.4 Comparison of neat epoxy and %0.1 and %0.5 graphene platelets-epoxy nanocomposite tensile test results. Solvent: acetone

As seen from Fig. 2.5, epoxy resin and its composite all exhibit brittle behavior. A small improvement of the ductility and toughness was observed upon the addition of graphene-platelets, probably due to energy dissipation at the interface between particles and matrix. Addition of graphene platelets enhances the strength without leading a decrease in the strain to failure. The tensile strength and strain to failure of nanocomposites of GPL reinforced epoxy nano-composite were enhanced 9.31% and 34.78%, respectively while small improvement is observed in the elasticity modulus. The reason obtaining these results is a weak interfacial bond between the GPL and epoxy.

To achieve optimal enhancement in the property of graphene/polymer composites, several key issues should be resolved: Improved dispersion of graphene, alignment of graphene in polymer, surface modification of graphene for good adhesion/interaction. To observe the effect of solvent on the dispersion of graphene on epoxy, in addition to acetone, NMP is used as solvent in nano-composite manufacturing. Tensile tests results are depicted in Figure 2.5. Tensile properties of epoxy and composites with various weight fractions of graphene-platelets is given in Table 2.1

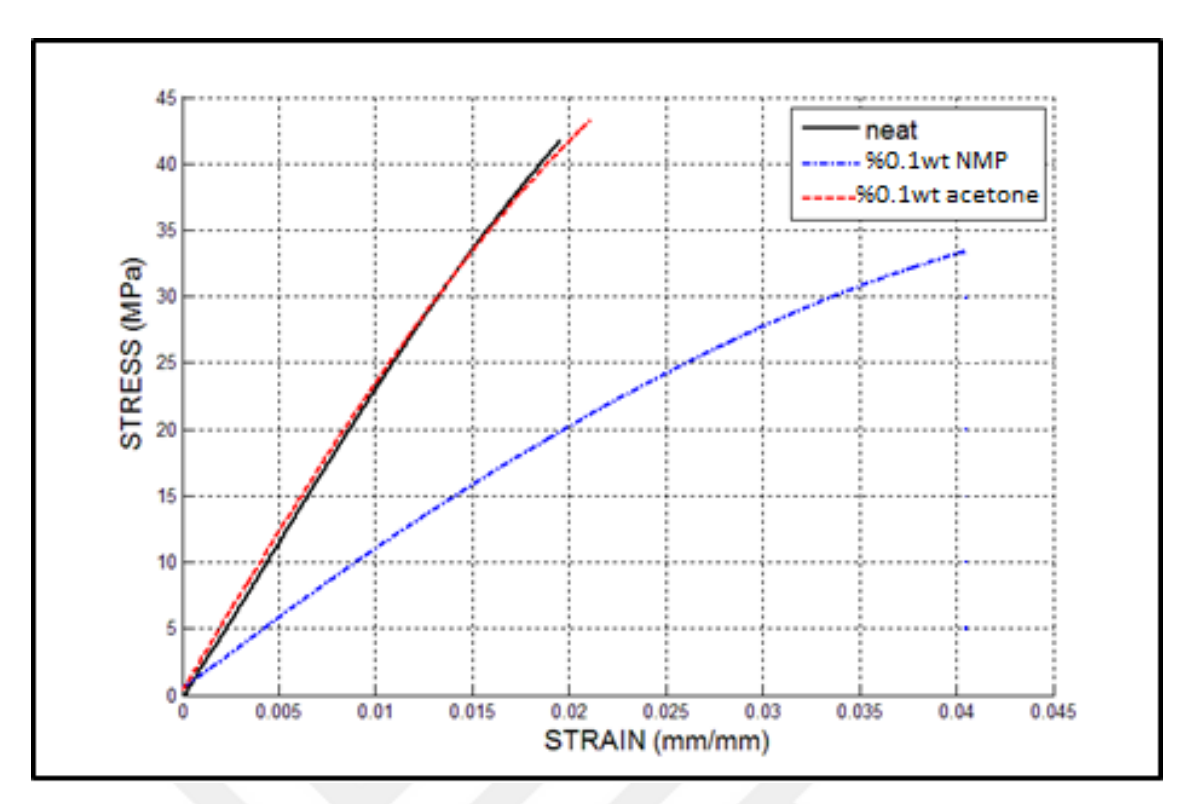


Figure 2.5 Comparison of neat epoxy and %0.1 and graphene platelets -epoxy nanocomposite tensile test results. Solvent: acetone and NMP

Evaporation of solvent is an important issue in nano-composite manufacturing. For the case of acetone, solvent is evaporated on a magnetic stir plate for 3 hours at 70 °C. Due to the evaporation problems of NMP, the evaporation time is raised to 6 hours at 90 °C. The evaporation procedure continues in a vacuum chamber for 12 hour at 70 °C for acetone and 90 °C for NMP. Even though, duration on magnetic stir plate and vacuum chamber is increased, the deteriorated mechanical properties (Figure 2.5) have shown that there is residual of NMP solvent in the structure. This residual solvent caused the weakening of the material.

Table 2.1 Tensile properties of epoxy and composites with various weight fractions of graphene-platelets.

	Pure Epoxy	0.1% Graphene Composite (Acetone)	0.5% Graphene Composite (Acetone)	0.1% Graphene Composite (NMP)
Elasticity Modulus (MPa)	2286	2361	2278	1061
Tensile Strength (MPa)	46.68	51.03	47.17	33.35
Strain to failure (mm/mm)	0.023	0.031	0.026	0.040

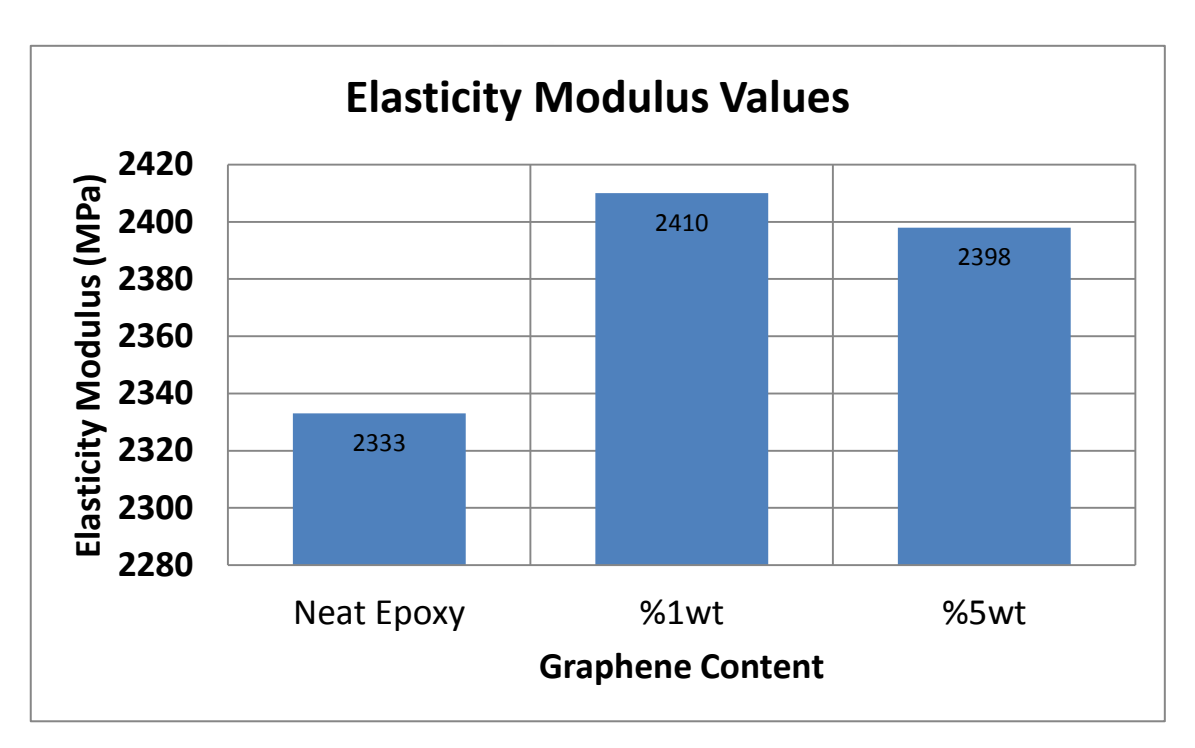
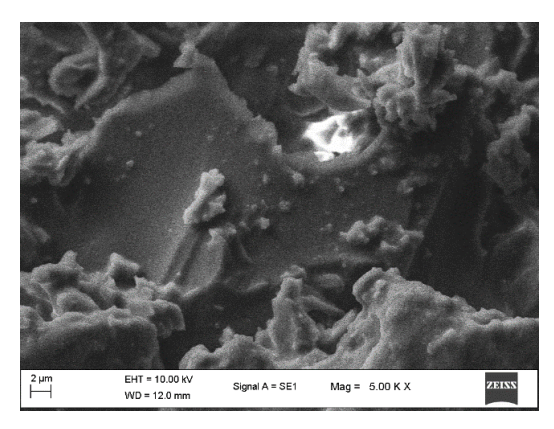


Figure 2.6 Elasticity modulus values for graphene content.

Since a small improvement of the elasticity modulus, tensile strength and ductility was observed upon the addition of graphene-platelets, the dispersion of graphene sheets in epoxy resin is investigated using SEM and results are given in Figure 2.7.



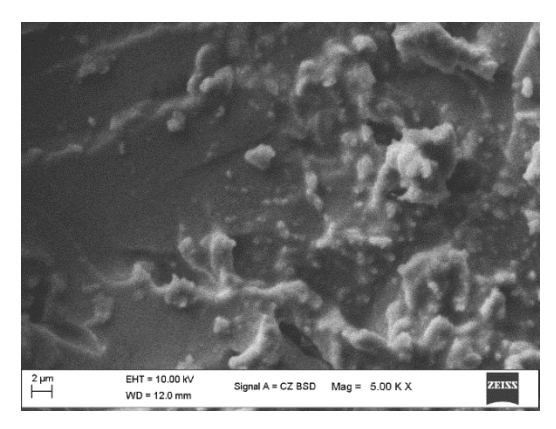


Figure 2.7 SEM images of graphene-epoxy nanocomposite

The SEM images present that graphene flakes embedded in the epoxy matrix. Agglomeration of graphene flakes was observed in the images. Due to the graphene's planar shape, it tends to aggregate much more compared to other nanofillers. The agglomeration decreases the interfacial contact area of the graphene with matrix material, and as a result, the expected boosted the mechanical properties can not be observed.

2.2.3 Dynamic Mechanical Analysis

Dynamic mechanical analysis (abbreviated DMA, also known as dynamic mechanical spectroscopy) is a technique used to study and characterize materials. It is most useful for studying the viscoelastic behavior of polymers. A sinusoidal stress is applied and the strain in the material is measured, allowing one to determine the complex modulus. The temperature of the sample or the frequency of the stress are often varied, leading to variations in the complex modulus; this approach can be used to locate the glass transition temperature of the material, as well as to identify transitions corresponding to other molecular motions. The viscoelastic property of a polymer is studied by dynamic mechanical analysis where a sinusoidal force (stress σ) is applied to a material and the resulting displacement (strain) is measured. For a perfectly elastic solid, the resulting strain and the stress will be perfectly in phase. For a purely viscous fluid, there will be a 90 degree phase lag of strain with respect to stress. Viscoelastic polymers have the characteristics in between where some phase lag will occur during DMA tests.

Figure 2.7-2.9 shows storage modulus, loss modulus and tan δ plot for neat epoxy and graphene reinforced epoxy nano-composites with acetone used as solvent. On the glassy region, for neat epoxy resins, storage modulus is measured as 5594 MPa. As expected, with the addition of 0.1% and 0.5% by weight, storage modulus increases to 6702 MPa

and 8145 MPa, respectively. This can be surely explained with the stiffening effect of GPLs.

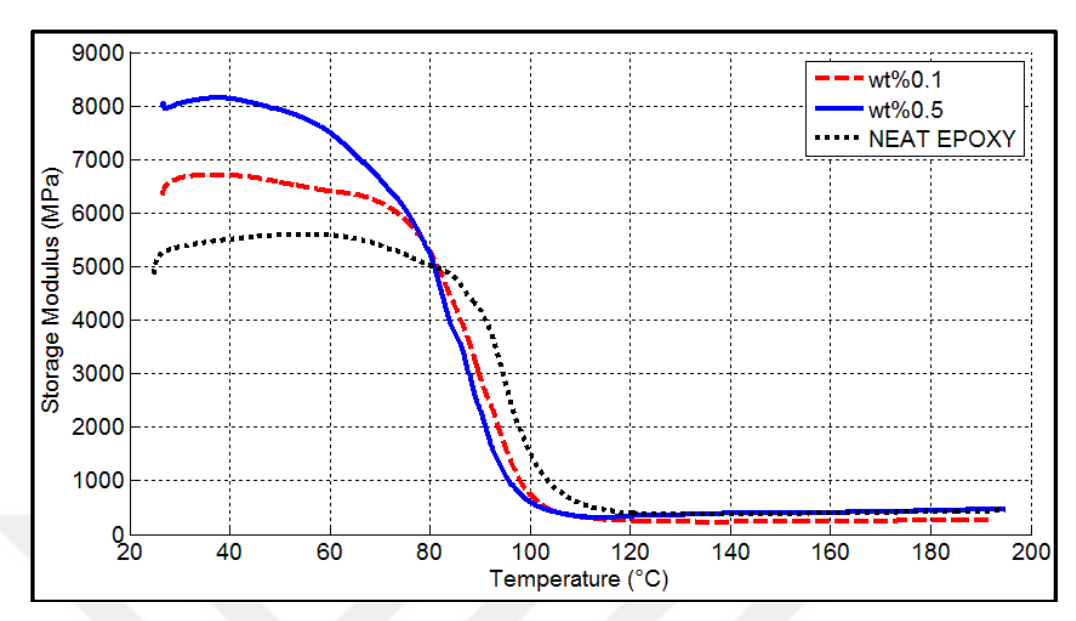


Figure 2.8 Dynamic mechanical properties of epoxy and nanocomposite, Storage Modulus versus Temperature curves.

Despite the minimal change of elasticity modulus values shown on the tensile test results, storage modulus of nanocomposite materials has increased dramatically from 5600 MPa to 6700MPa for wt%0.1 composite and 8000 MPa for wt%0.5 MPa.

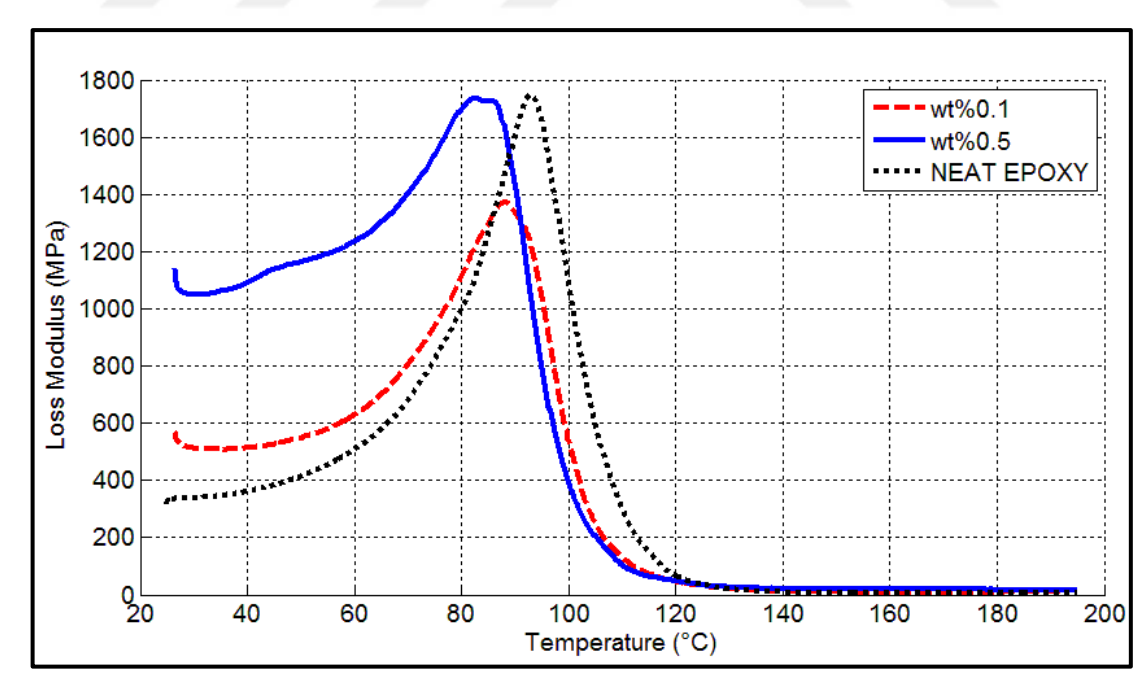


Figure 2.9 Dynamic mechanical properties of epoxy and nanocomposite, Loss Modulus versus Temperature curves.

The loss modulus is a measure of energy dissipation, though as a modulus it is hardness or stiffness of a material. In the region of the glass transition molecular segmental

motions are activated, however motions occur with difficulty, described as molecular friction that dissipates much of the force.

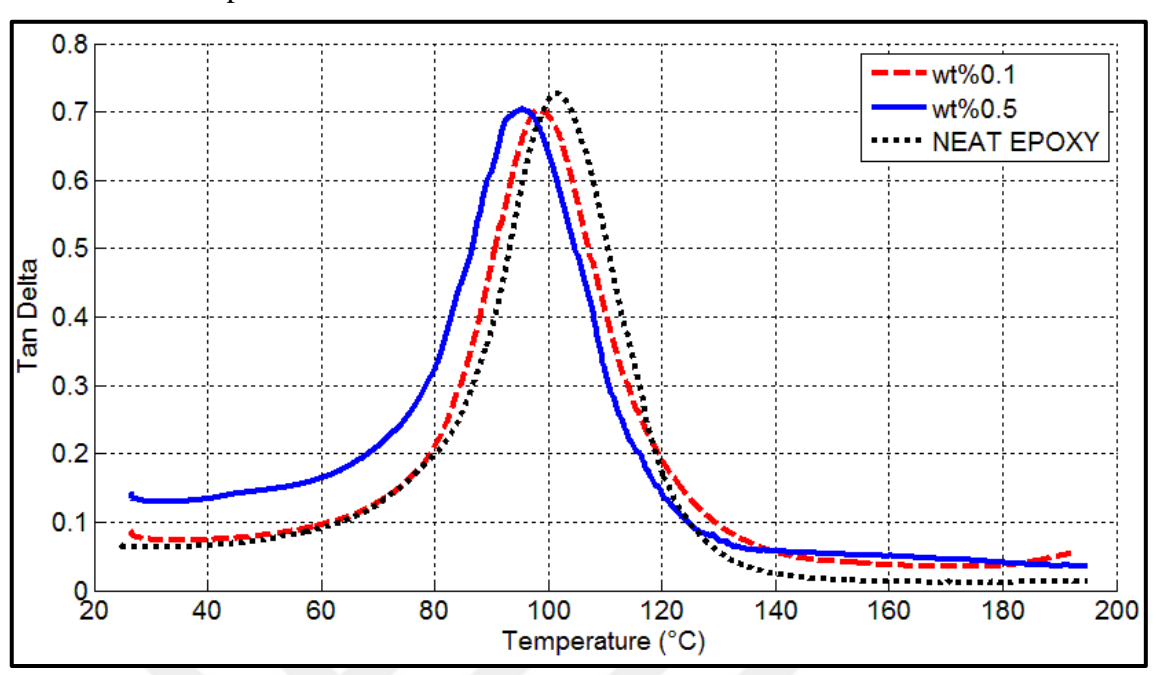


Figure 2.10 Dynamic mechanical properties of epoxy and nanocomposite, $\tan \delta$ versus Temperature curves.

The peak of tan δ curve is considered as glass transition temperature (Tg) of polymers. Increase or no change of Tg was observed in previous works. Prolongo et al.[19] Suggested that the addition of graphene Nano platelets (GNPs) into epoxy has no significant effect on the glass transition temperature of the matrix. In another study by Naebe et al. [32] stated that the addition of thermally reduced graphene and functionalized graphene into epoxy matrix result in the rise of Tg of polymers [32]. In our work, neat epoxy resin shows a Tg of 101°C. With the addition of 0.1 and 0.5 wt. % graphene Nano platelets, Tg reduces to 98 °C and 95 °C respectively.

2.3 Conclusions on Experimental work

In nano composite systems, the dispersion of the reinforcing phases is still an important issue.

- 1. The effect of process parameters on graphene synthesis should be investigated.
- 2. Addition of graphene platelets enhances the modulus and strength without leading reduction in the strain to failure.
- 3. Tg is stayed almost constant with the addition of graphene. A slight decrease on Tg is expected due to some work on the relevant literature, but it should be

- reminded that the GPL used in this work are not functionalized, which leads to a weak interface between epoxy and GPL.
- 4. An improvement of the ductility and toughness was observed upon the addition of graphene-platelets.
- 5. When NMP is used as solvent, the solvent cannot be removed entirely. The residual of the solvent decreases the properties of the material.

MODELING WORK

This part is aimed to extend the Cooperative-VBO theory of Çolak, Ahzi and Remond [33] for modeling of graphene-polymer nanocomposites.

It is obvious from the experimental work that the existence of graphene in a polymer matrix has a stiffening effect on overall mechanical behavior. But the nonlinear nature of this stiffening effect, caused by agglomeration tendency of graphene sheets and polymer-graphene interphase effects, coerces us to an elaborative work of modeling.

Cooperative-VBO approach for finite deformation theory proposes an additive form of the strain rate tensor. In simpler words, total deformation is obtained by addition of an elastic contribution and a viscoplastic contribution. Elastic deformation of the material is substantially controlled by a well-known parameter, the elasticity modulus. And relatively more complicated visco-plastic deformation is controlled by plastic shear strain rate function of Cooperative model [34], [35] used as the flow function of VBO theory [36], [37].

3.1 The Viscoplasticity Theory Based on Overstress - An Overview

There are two classes of continuum theories. One of them is classical plasticity theories in which all time effects, such as rate sensitivity, creep, relaxation and strain recovery are excluded. The second class of continuum theories contains viscoplasticity theories which assume that inelastic deformation is rate dependent even at low homologous temperatures.

The viscoplasticity models represented by unified state variable theories do not permit the separation of creep and plasticity. One of the unified state variable theories is Viscoplasticity Theory based on Overstress (VBO) developed by Krempl and his coworkers for metallic materials, [38] [39]. State variables in the model are defined as

macroscopic averages of events associated with microstructure changes and cannot be directly measured or controlled.

VBO model is based on standard linear solid (SLS) model. SLS's rheological representation is given in Fig. 3.1.

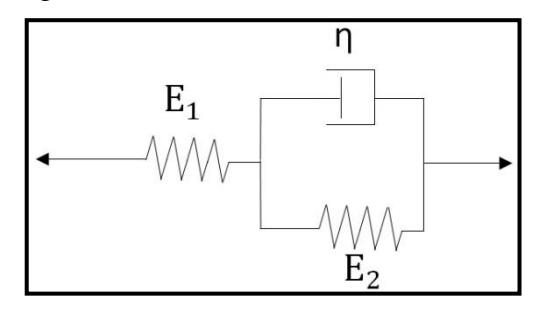


Figure 3.1 Standard linear solid model (SLS).

Governing equation for SLS model is given in Eq. 3.1.

$$\sigma(E_1 + E_2) + \eta \frac{d\sigma}{dt} = E_1 E_2 \varepsilon + E_1 \frac{d\varepsilon}{dt}$$
(3.1)

When Eq. 1 is written in overstress form, Eq. 2 is obtained.

$$\dot{\varepsilon} = \frac{\dot{\sigma}}{E_1} + \frac{\sigma - aE_2\varepsilon}{a\eta} \tag{3.2}$$

Where E1, and E2 are stiffness's of springs and η is viscosity function. (

In equation 3.2, $(\sigma\text{-}aE2\epsilon)$ is called "overstress". The overstress concept is used to develop VBO theory. It is initially developed for modeling the mechanical behavior of metallic materials. However, due to the similarities observed in the polymeric and metallic materials' behavior, VBO is modified to capture mechanical behavior of polymers as well [40] [37] [36].

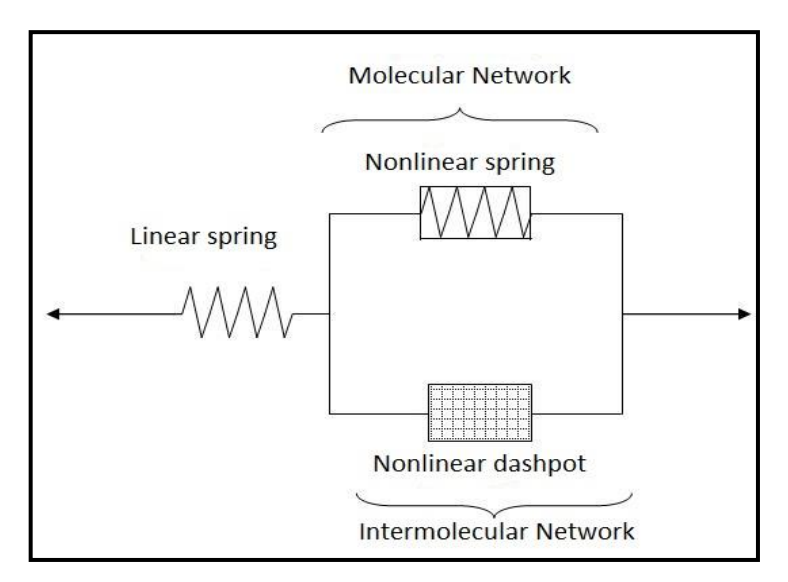


Figure 3.2 Rheological representation of VBOP model [37].

The deviator of flow law of VBO for small strain, incompressibility and isotropy is given by

$$\dot{\mathbf{e}} = \dot{\mathbf{e}}^{\text{el}} + \dot{\mathbf{e}}^{\text{vp}} = \frac{1+\nu}{\text{CE}}\dot{\mathbf{s}} + \frac{3}{2}F \left[\frac{\Gamma}{D}\right] \left(\frac{\mathbf{s} - \mathbf{g}}{\Gamma}\right)$$
(3.3)

Where s and g are respectively the deviators of the Cauchy stress tensor σ and the equilibrium stress, G which is the stress that the material can sustain at rest. E is Young's modulus and v is the elastic Poisson's ratio. $\dot{\mathbf{e}}^{el}$ and $\dot{\mathbf{e}}^{in}$ Are deviators of elastic and inelastic strain rates, respectively. One main difference between VBO and VBOP, is the parameter C, given by

$$C = 1 - \lambda (|G - K|/A)^{\alpha}$$
(3.4)

Where λ and α are model parameters. For metals, C is usually set to "1" for representing linear unloading behavior. Γ is the overstress invariant with the dimension of stress defined by

$$\Gamma^2 = \frac{3}{2}(\mathbf{s} - \mathbf{g}) : (\mathbf{s} - \mathbf{g})$$
(3.5)

F[] is the positive, increasing flow function with the dimension of 1/time and F[0]=0. The flow function F[] is set as a power law equation. It is responsible for modeling nonlinear rate sensitivity and is given by

$$F[] = B \left(\frac{\Gamma}{D}\right)^{m} \tag{3.6}$$

With B as a universal constant having the dimension of 1/time. D is the drag stress, which can be considered as another state variable with a growth law. However, in this study it is a constant.

One of the tensor valued state variables is the equilibrium stress. The equilibrium stress is similar but not quite the same as the back stress in rate-independent plasticity models. In plasticity models the back stress is considered as repository for kinematic hardening, whereas in VBOP the repository for kinematic hardening is the kinematic stress. The equilibrium stress is the stress that must be overcome to generate inelastic deformation. The growth law for the deviator of equilibrium stress, g, which is the rate-independent contribution to hardening, is;

$$\dot{\mathbf{g}} = \mathbf{\psi} \frac{\dot{\mathbf{s}}}{E} + \mathbf{\psi} \mathbf{F} \left[\frac{\Gamma}{D} \right] \left(\frac{\mathbf{s} - \mathbf{g}}{\Gamma} - \frac{\mathbf{g} - \mathbf{k}}{A} \right) + \left(1 - \frac{\mathbf{\psi}}{E} \right) \dot{\mathbf{k}}$$
(3.7)

Where ψ is shape function bounded by Et/ $<\psi<$ E. It affects the transition from the quasi elastic to the inelastic region. The isotropic stress A is a scalar state variable for modeling rate independent cyclic hardening (or softening) behavior. Its effect is similar to the isotropic hardening in rate-independent plasticity.

The evolution of the shape function is given in Eq. 3.8.

$$\psi = \psi_1 + \left(\frac{\mathbf{C}_2 - \psi_1}{\exp(\mathbf{C}_3 \left| \boldsymbol{\varepsilon}^{\mathbf{i} \mathbf{n}} \right|)}\right), \quad \psi_1 = \mathbf{C}_1 \left(1 + \mathbf{C}_4 \left(\frac{|\mathbf{G}|}{\mathbf{A} + |\mathbf{K}| + \xi \Gamma^{\zeta}}\right)\right)$$
(3.8)

Where, C1, C2, C3, C4, ξ and ζ are material parameters determined using transition regions from elastic to viscoplastic responses of the stress-strain curves.

3.2 Cooperative – VBO Theory

In the year 2013, with the collaboration of Çolak Ahzi and Remond [33], Cooperative theory developed by Richeton et al. [35] [34][41] is unified with VBO theory of Krempl.[38,39,42].

Cooperative model considers yield phenomenon as the jump of macromolecules from one equilibrium position to another. Under a significant stress level, the distortion on the molecule will be enough to overcome the activation barrier of the deformation reaction, jumps to a hole (like the dislocation theory in metals). And the permanent molecular movement which we define as plastic strain, begins.

This model uses a form of the famous Arrhenius equation known as the Eyring equation in order to take into account the deformation rate and temperature effects. The Eyring equation (occasionally also known as Eyring–Polanyi equation) is an equation used in chemical kinetics to describe the variance of the rate of a chemical reaction with temperature. It was developed almost simultaneously in 1935 by Henry Eyring, Meredith Gwynne Evans and Michael Polanyi. This equation follows from the transition state theory (aka, activated-complex theory) and is trivially equivalent to the empirical Arrhenius equations which are both readily derived from statistical thermodynamics in the kinetic theory of gases.

The plastic strain rate function used by Cooperative theory is given below,

$$\dot{\gamma}_{p} = \dot{\gamma}_{0} \exp\left(-\frac{\Delta H_{\beta}}{RT}\right) \sinh^{n}\left(\frac{(\tau - ti)V}{2kT}\right)$$
(3.9)

Here $\dot{\gamma}_p$ is the shear strain rate, $\dot{\gamma}_0$ is a material parameter, pre-exponential strain rate,

 ΔH_{β} is the activation energy, R is the universal gas constant, k is Boltzmann constant, T is the absolute temperature (in Kelvin) τ is the yield shear stress and V is the activation volume. Here ti is the internal stress given by;

$$\dot{t_i} = h \left(1 - \frac{t_i}{\tau_{ps}} \right) \dot{\gamma}^p \tag{3.10}$$

And τ_{ps} is the stress referring to the preferred structure state of the material which is used as a scalar in this work.

VBO theory fundamentally uses the same principle, but it does not do this such a molecular perspective. In VBO, as explained below, equilibrium stress is defined as the stress level that should be surpassed to generate plastic deformation. And as seen in Eq 3.7, it consists of three parts as, elastic contribution, flow law and kinematic effects. The concept Cooperative theory proposed is used as the flow function in VBO theory, which generates a multiscale, viscoplastic theory entitled as, Cooperative – VBO theory. In cooperative VBO theory, the total deformation is defined as;

$$\mathbf{d} = \mathbf{d}^{\mathbf{e}} + \mathbf{d}^{\mathbf{vp}} = \frac{1+\nu}{CE} \dot{\mathbf{s}} + \frac{3}{2} \gamma^{p} \frac{\mathbf{s} - \mathbf{g}}{\Gamma}$$
(3.11)

With the plastic strain rate function defined as;

$$\gamma^{p} = \gamma^{0} \exp\left(-\frac{\Delta H_{\beta}}{R \cdot T}\right) \sinh\left(\frac{(\Gamma - ti)V}{2kT}\right)$$
(3.12)

It is easily noticed that the only difference from eq. 3.9 is that the effective equivalent shear (τ) is replaced by the overstress invariant of VBO theory defined as;

$$\Gamma^2 = \frac{3}{2} (\mathbf{s} - \mathbf{g}) : (\mathbf{s} - \mathbf{g}) \tag{3.13}$$

And the new form of equilibrium stress, g is defined as;

$$\dot{\mathbf{g}} = \psi \frac{\dot{\mathbf{s}}}{E} + \overline{\Psi} \gamma^{p} \left(\frac{\mathbf{s} - \mathbf{g}}{\Gamma} - \frac{\mathbf{g} - \mathbf{k}}{A} \right) + \left(1 - \frac{\psi}{E} \right) \dot{\mathbf{k}}$$
(3.14)

And kinematic stress which covers the tension / compression asymmetry of the mechanical behavior known as Bauschinger effect is defined as;

$$\dot{\mathbf{k}} = \overline{E}_T \gamma^p \frac{\mathbf{s} \cdot \mathbf{g}}{\Gamma} \tag{3.15}$$

Here \bar{E}_t is defined as;

$$\bar{E}_t = \frac{E_t}{1 - \frac{E_t}{E}} \tag{3.16}$$

Actually, a deep consideration on both theories shows us that the two notions, overstress and effective equivalent shear stress indicates to the same physical phenomenon, the difference between the actual stress state and the equilibrium stress.

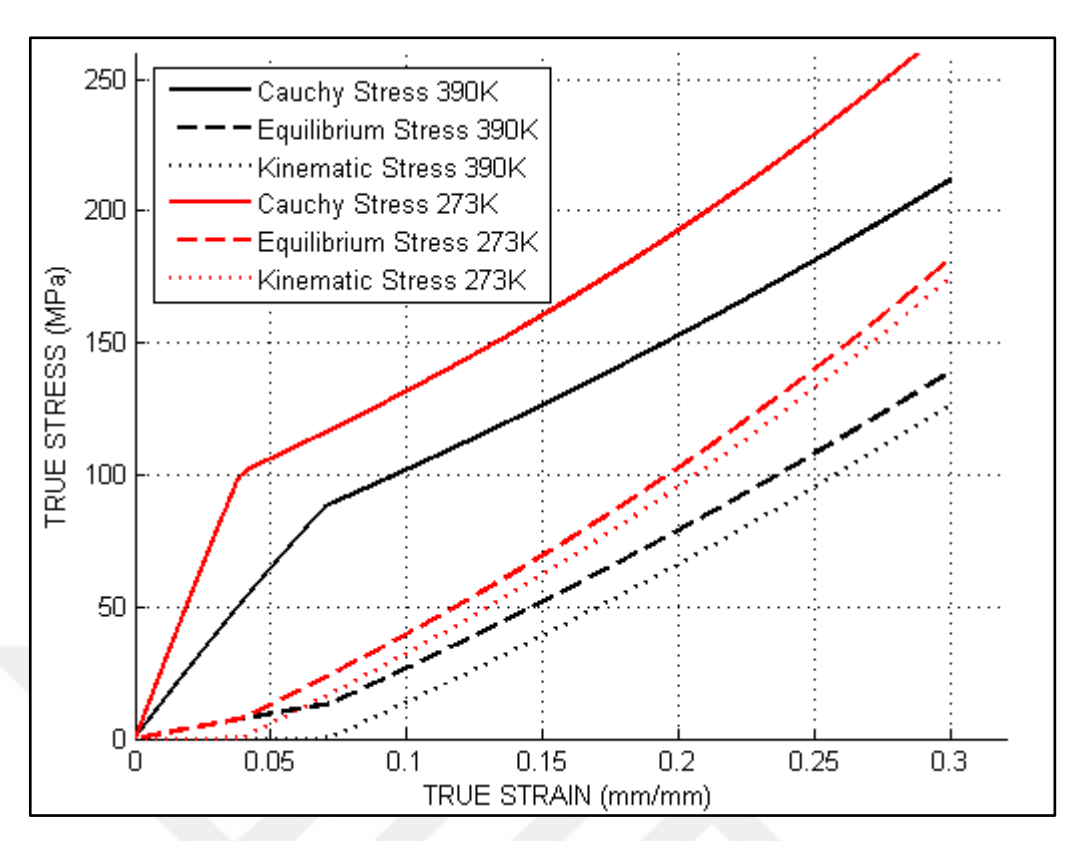


Figure 3.3 Evolution of the three stress-like State Variables of Cooperative-VBO model for different temperature values

Therefore Cooperative – VBO theory gives us a concept which comprises the advantages of continuum methods and the deep understanding which is served by molecular theories. Due to those advantages, Cooperative VBO theory is chosen to model the mechanical behavior of polymer matrix graphene nanocomposites.

As seen from figures 3.3-3.4, two stress like state variables, as a result Cauchy stress is changing with changing temperature and strain rate. Their variation trend seems proper with common knowledge.

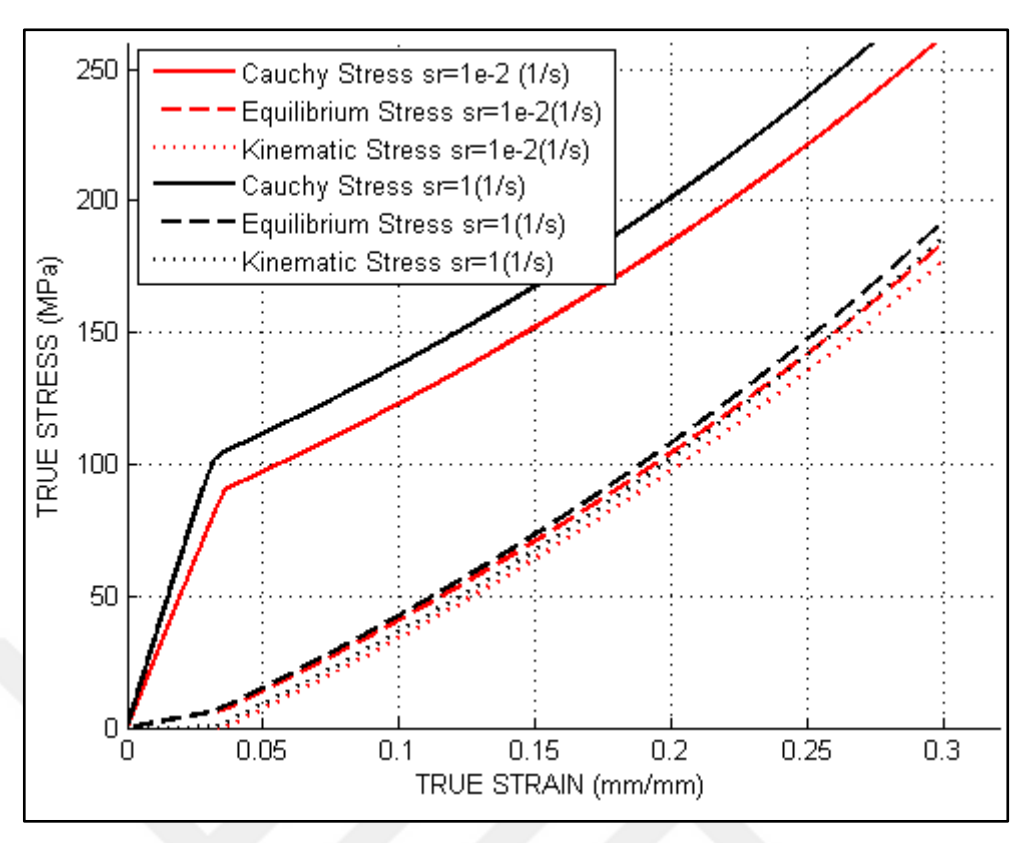


Figure 3.4 Evolution of the theree stress-like State Variables of Cooperative-VBO model for different strain rates

3.3 Effective Elasticity Modulus Definition

It is a well-known fact that the mechanical behavior of polymeric materials significantly changes with changing temperature and strain rate. Richeton et al. [41] used the elasticity modulus equation which defines the elasticity modulus as the Weibull statistics of bond breakage proposed by Mahieux and Reifsnider [43,44] and extended this theory to include rate effects. This definition of elasticity modulus is employed by some constitutive theories successfully [33,41].

On the other hand, the nonlinear stiffening effect of graphene composition in a polymer matrix is widely investigated in literature both experimentally and theoretically [17,25,45–47]. The relevant literature reports that the stiffening effect of graphene is highly affected by agglomeration of graphene flakes. In other words, only a small fraction of graphene could be used to enhance the mechanical behavior of the composite structure.

The work of Ji et al. [25] proposes an effective elasticity modulus definition which takes into account the agglomeration effect of graphene using Mori-Tanaka micromechanics method.

In our work, the bond breakage theory used and improved by Richeton et al. [41] and Çolak et al [33] is extended to cover the effect of graphene content by redefining the three constant modulus values " E_i " (the modulus values on the onset of three transition temperatures) which are used as scalars in Richeton's work. In order to redefine modulus values as a function of graphene fraction, the Mori Tanaka scheme developed by Ji et al. [25] is used.

Mori Tanaka expressions, α_r , β_r , δ_r and η_r are defined as;

$$\alpha_r = \frac{3k_m + 2n_r - 2l_r}{3n_r} \tag{3.17}$$

$$\beta_r = \frac{4\mu_m + 7n_r + 2l_r}{15n_r} + \frac{2\mu_m}{5p_r} \tag{3.18}$$

$$\delta_r = \frac{3k_m(n_r + 2l_r) + 4(k_r n_r - l_r^2)}{3n_r} \tag{3.19}$$

$$\eta_r = \frac{2}{15} \left(k_r + 6m_r 8\mu_m - \frac{l_r^2 + 2\mu_m l_r}{n_r} \right) \tag{3.20}$$

Where subscript r stands for the reinforcement (graphene in our case), and subscript m stands for the polymer matrix. k, m, n, l, p are parameters of the Hill's moduli [46], μ is shear modulus.

The reinforcing phase in composite is apt to agglomerate causing a non-uniform distribution which ends up with weakening of mechanical properties [45] as explained above. Therefore the Mori-Tanaka micromechanics scheme is applied one more time, but this time with an "agglomerated phase" and an "effective matrix phase" in order to model the agglomeration effect on elasticity modulus.

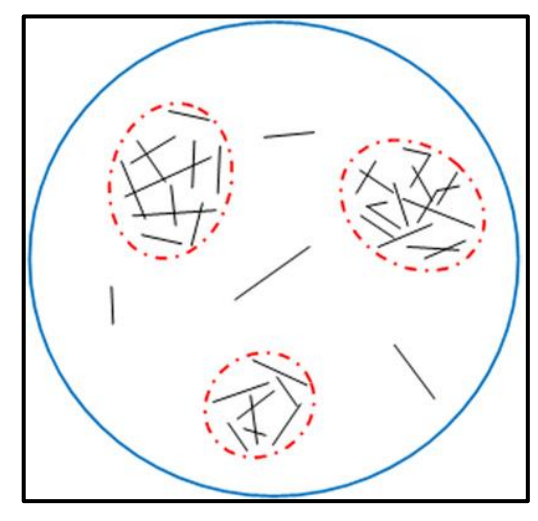


Figure 3.5 Micromechanics model for the agglomeration of graphene sheets. [25]

Naturally, the volume fractions of those two phases are needed to be defined. They are defined by two parameters as;

$$\xi = \frac{V_{agglomer}}{V} \tag{3.21}$$

$$\zeta = \frac{V_r^{agglomer}}{V_r} \tag{3.22}$$

After this definition of the two separate phases, the Bulk and shear modulus of agglomerated and out (effective matrix) phases are calculated separately as;

$$\kappa_{agglomer} = \kappa_m + \frac{(\delta_r - 3\kappa_m \alpha_r)c_r \zeta}{3(\xi - c_r \zeta + c_r \zeta \alpha_r)}$$
(3.23)

$$\kappa_{out} = \kappa_m + \frac{c_r(\delta_r - 3\kappa_m \alpha_r)(1 - \zeta)}{3[1 - \xi - c_r(1 - \zeta) + c_r(1 - \zeta)\alpha_r]}$$
(3.24)

$$\mu_{agglomer} = \mu_m + \frac{c_r \zeta(\eta_r - 2\mu_m \beta_r)}{2(\xi - c_r \zeta + c_r \zeta \beta_r)}$$
(3.25)

$$\mu_{out} = \mu_m + \frac{c_r(1-\zeta)(\eta_r - 2\mu_m \beta_r)}{2[1-\xi - c_r(1-\zeta) + c_r(1-\zeta)\beta_r]}$$
(3.26)

And the expressions for the effective bulk modulus and shear modulus due to the Mori Tanaka scheme yields to;

$$\kappa^{eff} = \kappa_{out} \left[1 + \frac{\xi(\left(\frac{\kappa_{agglomer}}{\kappa_{out}}\right) - 1)}{1 + \alpha(1 - \xi)(\left(\frac{\kappa_{agglomer}}{\kappa_{out}}\right) - 1)} \right]$$
(3.27)

$$\mu^{eff} = \mu_{out} \left[1 + \frac{\xi(\left(\frac{\mu_{agglomer}}{\mu_{out}}\right) - 1)}{1 + \beta(1 - \xi)\left(\frac{\mu_{agglomer}}{\mu_{out}}\right) - 1\right)} \right]$$
(3.28)

Where,

$$\alpha = 3\kappa_{out}/(3\kappa_{out} + 4\mu_{out}) \tag{3.29}$$

$$\beta = 6(\kappa_{out} + 2\mu_{out})/5(3\kappa_{out} + 4\mu_{out})$$
(3.30)

And now effective elastic moduli can easily be calculated as;

$$E_i^{eff} = \frac{9\kappa^{eff}\mu^{eff}}{3\kappa^{eff} + \mu^{eff}}$$
 (3.31)

As seen from equations (3.21-3.22), ζ =1 indicates that all the graphene in the composite structure is agglomerated in the subsections which we call "agglomerated phase". In this case, an increase at ξ enlarges the volume fraction of agglomeration phase, which yields to a more uniform microstructure. As a result, efficient modulus value will increase with

increasing ξ . Figure 3.6 shows this case. And it should be noticed that the curves reaches to an limit value, which physically means that the increasing graphene content does not affect linearly the value of efficient modulus but at some point it reaches to a limit. This also seems consistent with the agglomeration theory we used above.

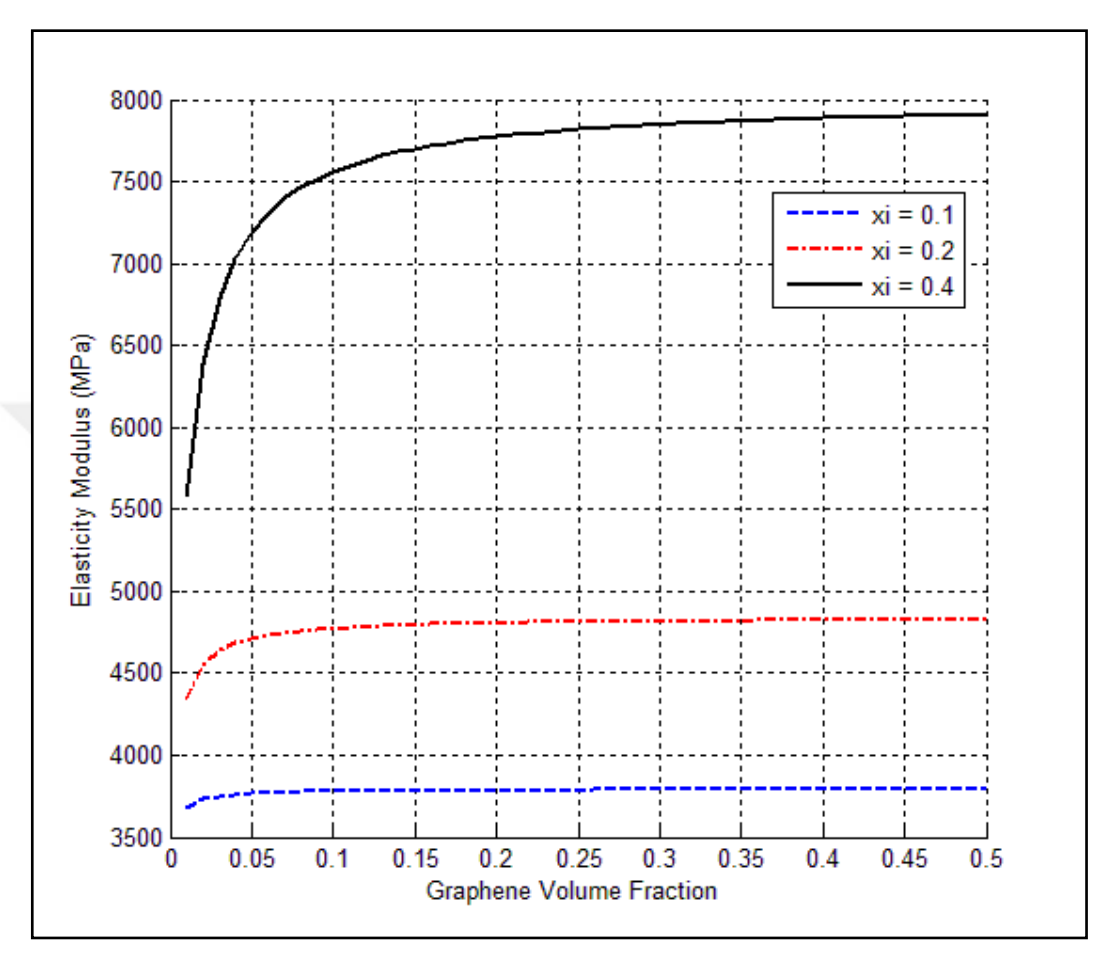


Figure 3.6 Modulus versus graphene content for different ξ values

To show the temperature and strain rate dependency of elasticity modulus, the figures below are plotted. Figure 3.7 shows modulus value decreases with increasing temperature as expected. And the three transitions can still be modeled through Richeton's theory.

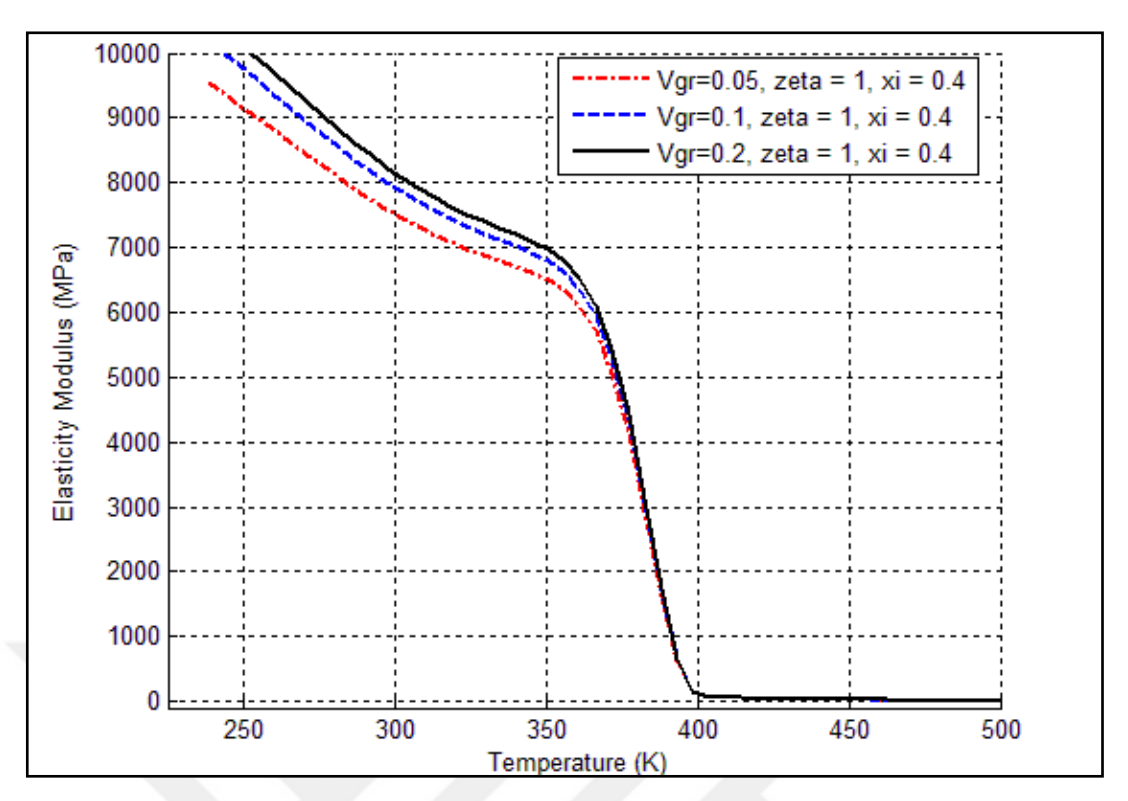


Figure 3.7 Modulus versus Temperature curves for different graphene content

As explained below, the effective moduli definition given in Eq 3.31 is used as a parameter in the temperature and strain rate dependent elasticity modulus equation as the reference modulus value E_i [33,41].

$$E_i = E_i^{eff} \left(1 + s. \log \left(\frac{\dot{\varepsilon}}{\dot{\varepsilon}^{ref}} \right) \right) \tag{3.32}$$

Dynamic Mechanical Analysis (DMA) reveals that amorphous polymers undergo three main transitions which are beta relaxation, glass transition and flow. They are characterized by the associated transition temperatures, T_{β} , T_g , T_f . The three transition temperatures are defined as

$$\frac{1}{T_{\beta}} = \frac{1}{T_{\beta}^{ref}} + \frac{k}{\Delta H_{\beta}} ln\left(\frac{\dot{\varepsilon}}{\dot{\varepsilon}^{ref}}\right) \tag{3.33}$$

$$T_g = T_g^{ref} + \frac{-c_2^g log(\frac{\dot{\varepsilon}}{\dot{\varepsilon}^{ref}})}{c_1^g + log(\frac{\dot{\varepsilon}}{\dot{\varepsilon}^{ref}})}$$
(3.34)

$$T_f = T_f^{ref} \left[1 + 0.01 log \left(\frac{\dot{\varepsilon}}{\dot{\varepsilon}^{ref}} \right) \right]$$
 (3.35)

 T_{β} , T_{g} , T_{f} are transition temperatures at a reference strain rate ($\dot{\varepsilon}^{ref}$), used as parameters in the equations. c_{1}^{g} and c_{2}^{g} are the Williams–Landel–Ferry (WLF) parameters, Richeton et al. [41].

And finally the graphene fraction, temperature and rate dependent elasticity modulus is calculated as;

$$E(\theta, \dot{\varepsilon}) = (E_1(\dot{\varepsilon}) - E_2(\dot{\varepsilon})exp\left[\left(\frac{\theta}{T_{\beta}(\dot{\varepsilon})}\right)^{m_1}\right] + (E_2(\dot{\varepsilon}) - E_3(\dot{\varepsilon})exp\left[\left(\frac{\theta}{T_g(\dot{\varepsilon})}\right)^{m_2}\right] + E_3(\dot{\varepsilon})exp\left[\left(\frac{\theta}{T_f(\dot{\varepsilon})}\right)^{m_3}\right]$$
(3.36)

Figure 3.8 shows Elasticity modulus versus strain rate curves for different volume fractions of graphene. As seen from the figure, rate dependency can be modeled through Richeton's theory similar to temperature dependency.

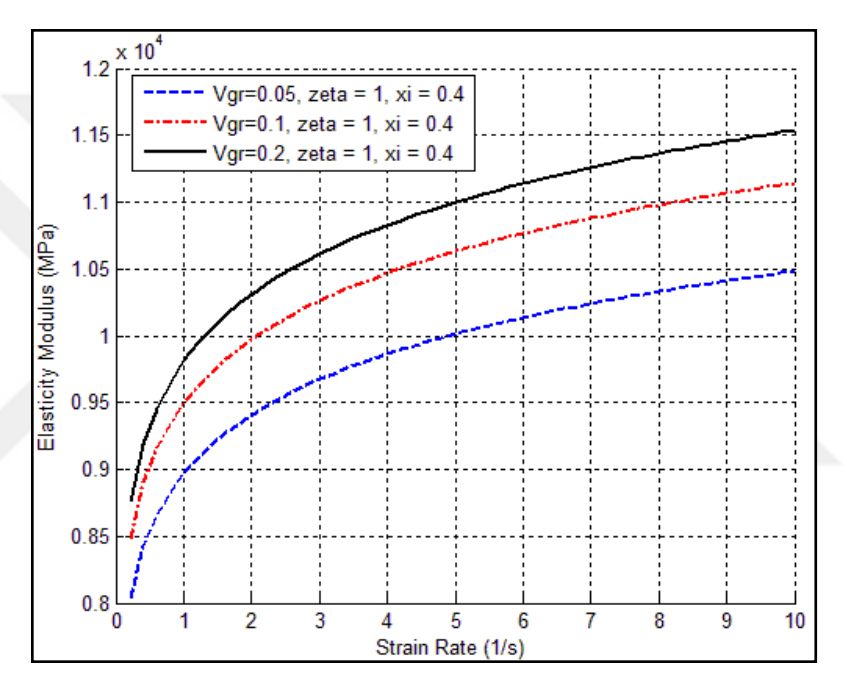


Figure 3.8 Modulus versus Strain Rate curves for different graphene content

In order to test the accuracy of the proposed model, the storage modulus which is related to stiffness of the material is modeled and the simulation results are compared to experimental data from Acar et al. [45]. The parameters of modified model are given in Table 3.1.

Table 3.1 Storage modulus model Parameters

$\dot{\varepsilon}^{ref}(1/\mathrm{s}), E_{m1}^{ref}, E_{m2}^{ref}, E_{m3}^{ref}(\mathrm{MPa})$	1, 5850, 5800, 1500
T_{β}^{ref} , T_{g}^{ref} , T_{f}^{ref} (°C)	90, 97, 100
c_1^g, c_2^g (°C)	32.58, 83.5
m_1, m_2, m_3, s	5,40,20,0.087
ξ, ζ	0.7, 0.5
2k, l, n, 2m, 2p (Hill's parameters of graphene) [25]	1700, 6.8, 10200, 738, 204000

Storage modulus versus temperature curves for neat epoxy, 0.1wt% and 0.5wt% graphene-epoxy nanocomposite are depicted in Figures 3.9-3.11.

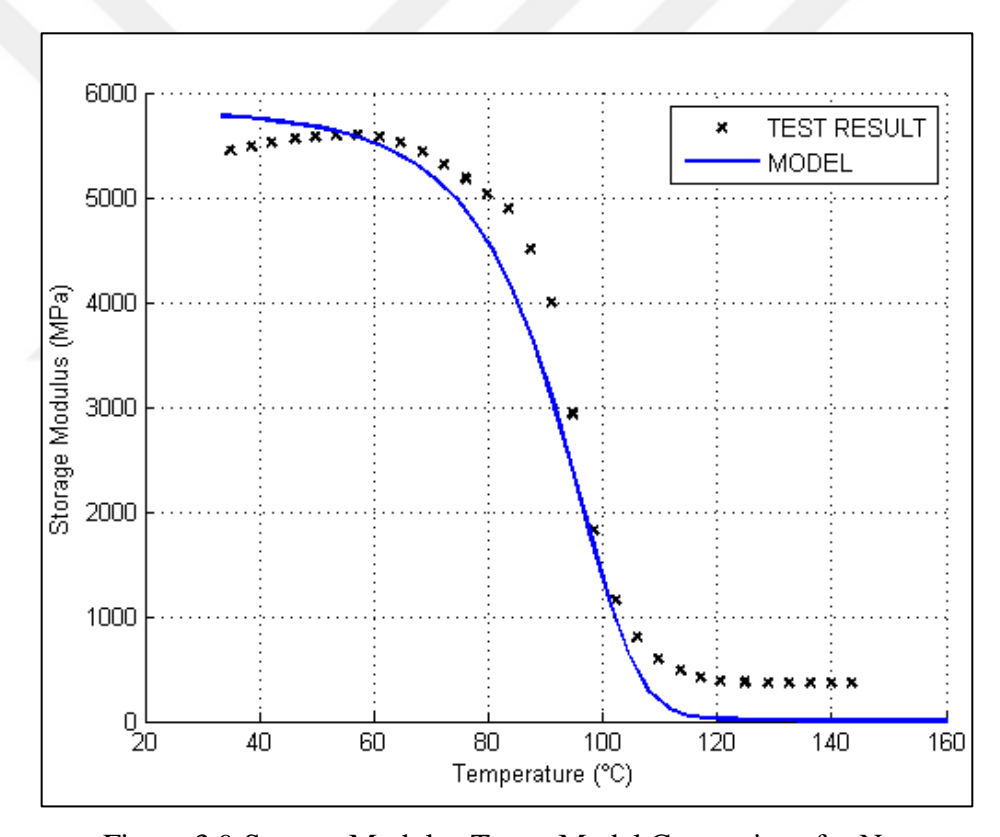


Figure 3.9 Storage Modulus Test – Model Comparison for Neat epoxy

For neat epoxy, effective elasticity modulus is compared to DMA test results given in Chapter 2. Due to Mahieux – Reifsdner equation given in eq. 3.36, storage modulus values are successfully modeled for above, transition region and below the glass transition. This elasticity modulus definition enables the model for suitable for thermomechanical analysis.

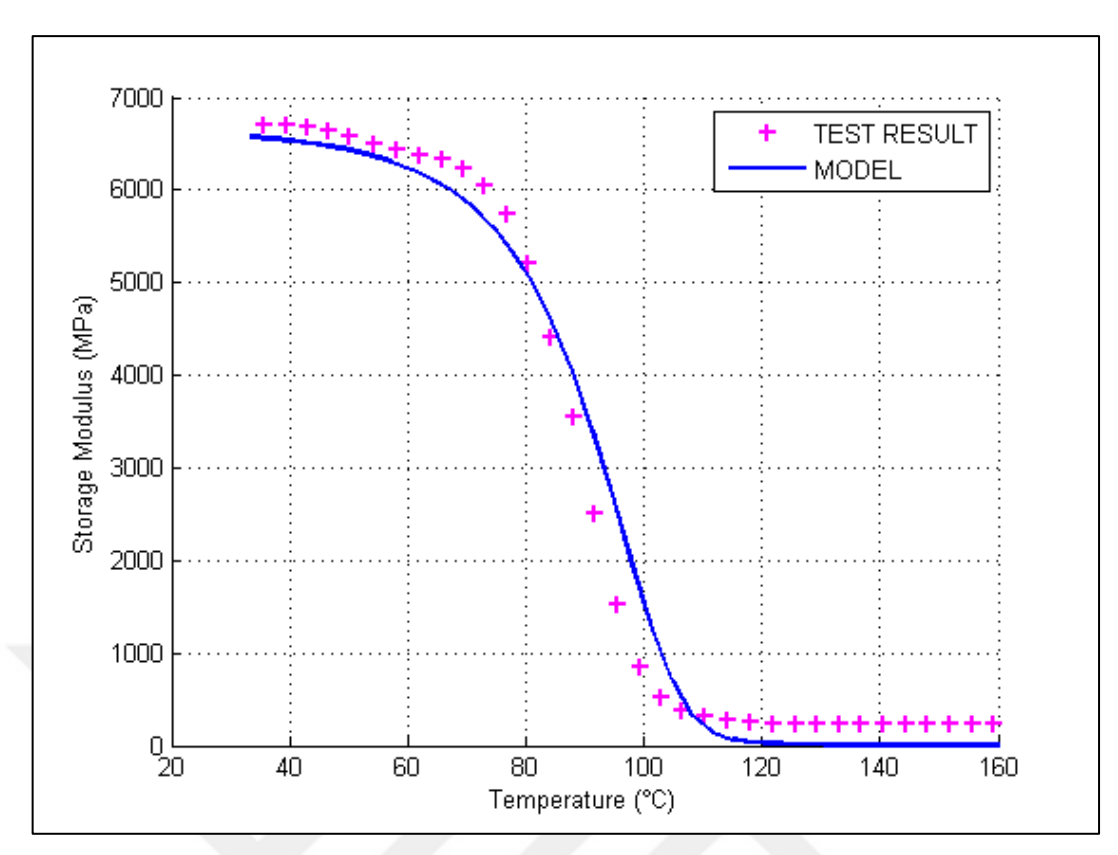


Figure 3.10 Storage Modulus Test – Model Comparison for) 0.1wt% Grapheneepoxy nanocomposite

Figure 3.10 shows the storage modulus test versus model response. Thanks to the Mori-Tanaka scheme explained above, the modified model is accomplished to give the Storage / Elasticity modulus values for different graphene fractions. The capability of modeling the glass transition for storage modulus is still present as seen in figures.

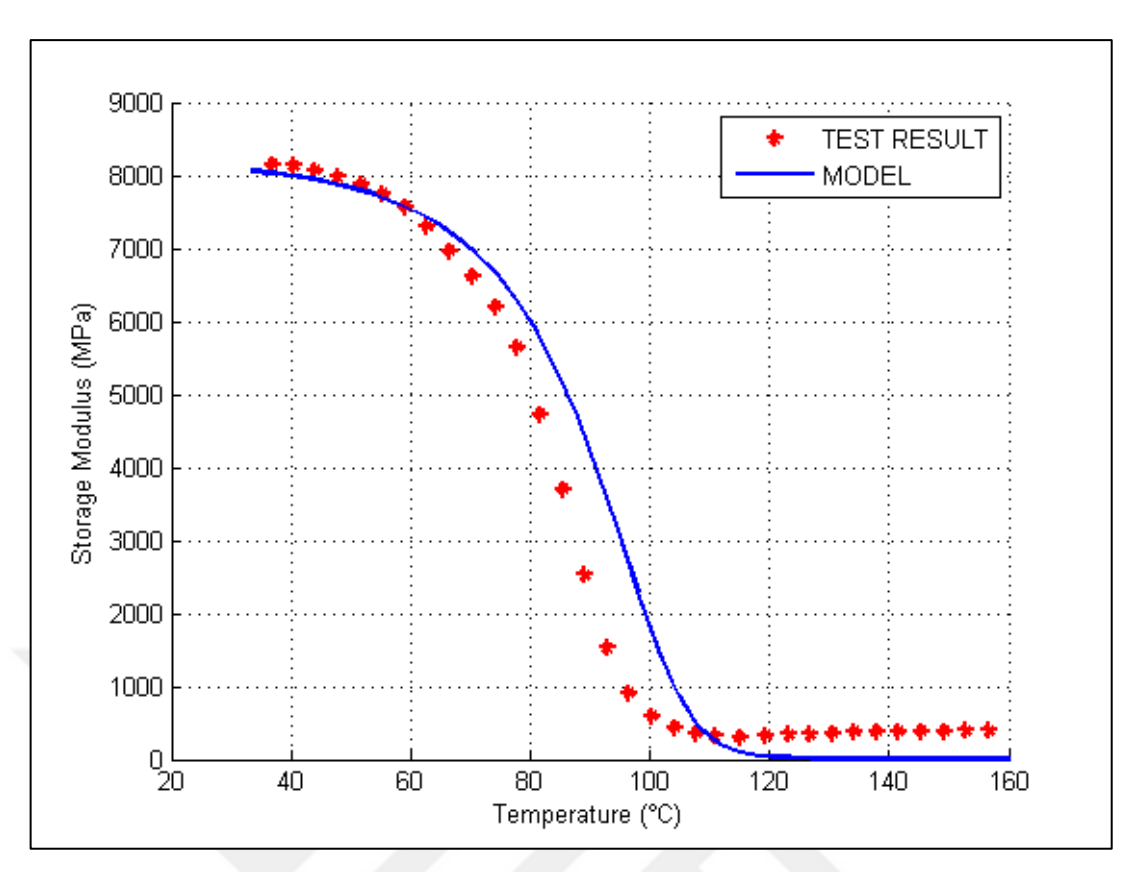


Figure 3.11 Storage Modulus Test – Model Comparison for) 0.5wt% Grapheneepoxy nanocomposite

As seen from the figures above, the modified Mahieux model, with the addition of graphene composition using Ji's theory, is capable of modeling the storage (as well as elasticity) modulus of graphene-epoxy nanocomposite materials with a good accuracy for temperatures above and below glass transition.

3.4 Modifications on visco-plastic part of Cooperative-VBO theory to model stiffening effect of graphene

On the viscoplastic part of the Cooperative-VBO theory, two scalar valued material parameters of plastic strain rate function γ^p is redefined as functions of graphene fraction using Tagayanagi averaging approach. This approach is also used successfully in their work by Matadi et al. [47] for organo-clay nano-composites. Redefined parameters successfully model the yield point of composite materials.

As seen from the test results, inhesion of graphene in the composite structure not only affects the start of the yield but also affects the post – yield behavior. In this manner, Two parameters of the former tangent modulus equation [33,37] is redefined as functions of graphene content. The proposed model successfully models the

compression behavior of composite materials for different graphene fractions at different strain rates.

As seen from figures 2-5 the proposed visco-plasticity model is capable of modeling the effect of graphene composition successfully. The model is also capable to model the mechanical behavior for temperatures above and below glass transition, but the set of tests we used [17] does not involves such data. Therefore this ability of the proposed model could not be compared to test data but model responses are shown at figure 6.

Cooperative-VBO approach for finite deformation theory proposes an additive form of the rate of deformation tensor which is given by Eq. 3.37,

$$\boldsymbol{d} = \boldsymbol{d}^e + \boldsymbol{d}^{vp} = \frac{1+v}{CE} \dot{\boldsymbol{s}} + \frac{3}{2} \dot{\gamma}_p \frac{s-g}{\Gamma}$$
(3.37)

In the plastic strain rate expression given in Eq 3.11, two parameters, activation energy ΔH_{β} and activation volume V relates to particular material properties and controls the beginning state of plastic strain. Therefore it is considered that defining these two parameters as functions of graphene content, defines the composite material's yield behavior. These definitions are done using the Tagayanagi averaging approach. The expressions are given below (Eq 3.36-3.37);

$$\Delta H_{\beta}^{eff} = \frac{\varphi \,\Delta H_r \,\Delta H_m}{\Omega \,\Delta H_m + (1 - \Omega)\Delta H_r} + (1 - \varphi)\Delta H_m \tag{3.38}$$

$$V^{eff} = \frac{\varphi \, V_r \, V_m}{\Omega \, V_m + (1 - \Omega) V_r} + (1 - \varphi) V_m \tag{3.39}$$

Here, like effective elasticity modulus definition, subscript r stands for the reinforcement and subscript m stands for the polymer matrix phases. The volume fractions of graphene and polymer matrix represented as f_c and f_m . Parameters φ and Ω are related to fractions of graphene and polymer matrix which are defined as;

$$f_c = \varphi \cdot \Omega \tag{3.40}$$

$$f_m = 1 - \varphi \cdot \Omega \tag{3.41}$$

A basic understanding of the Tagayanagi method shows that the parameters φ and Ω , represents the state of stress transfer (in parallel or series), in other words they define the model shows more or less series or parallel character. As seen on Eq. (3.38-3.39), only one of them is independent.

Therefore, the plastic shear strain rate (flow) function $\dot{\gamma}_p$ is re-defined for graphene nanocomposites as given in Eq. 3.41;

$$\dot{\gamma}_p = \dot{\gamma}_0 \exp(-\frac{\Delta H_{\beta}^{eff}}{RT}) sinh^n \left(\frac{(\Gamma - t_i)V^{eff}}{2kT}\right)$$
(3.42)

As seen from the test results, inhesion of graphene in the composite structure not only affects the start of the yield but also affects the post – yield behavior. In this manner, Two parameters of the former tangent modulus equation given in Eq. 3.42 [33,37] is redefined as functions of graphene content.

$$E_{T} = \frac{E_{T0} \left[1 + e^{\alpha \left| \varepsilon^{\gamma p} \right|} \right]^{\beta}}{2} \tag{3.43}$$

In this equation, two scalar parameters, E_{T0} and α are defined as functions of graphene weight fraction, c_m using curve fitting methods. These equations are also given below;

$$E_{t0} = aexp^{bc_m} + cexp^{dc_m} (3.44)$$

$$\alpha = f c_m^3 + g c_m^2 + h c_m + j \tag{3.45}$$

VBO model uses a scalar isotropic stress to model hardening and softening behavior of the materials. In this work isotropic stress, A is used as a constant.

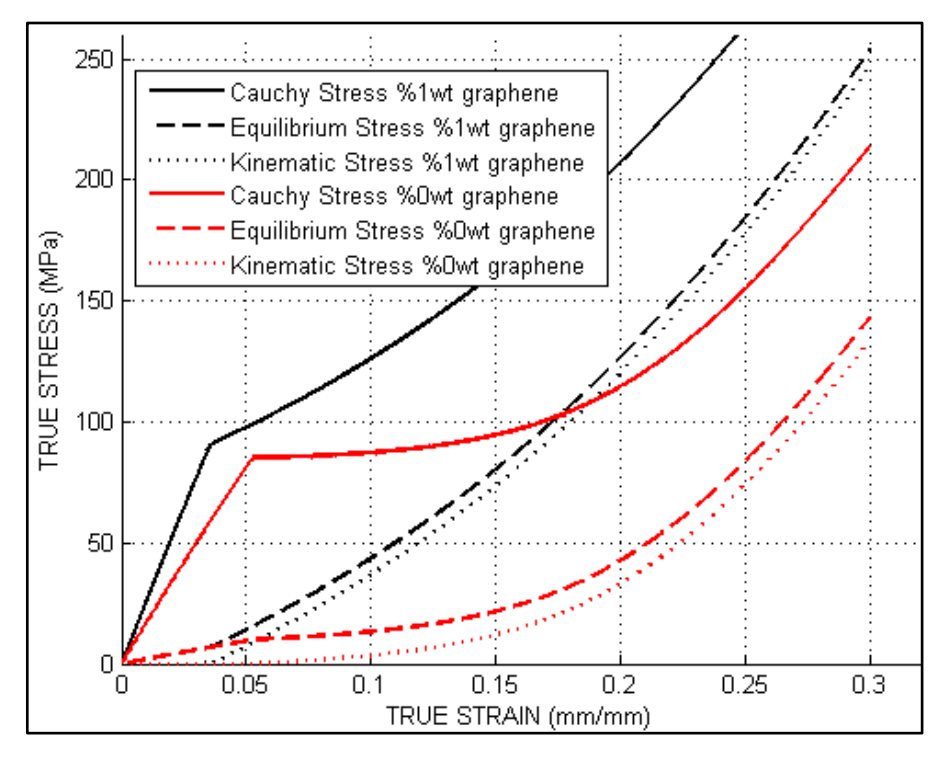


Figure 3.12 Evolution of the three stress-like State Variables of Cooperative-VBO model for Nanocomposites for different graphene fractions

As seen from figure 3.12, with the effective elasticity modulus definition and variable ΔH_{β}^{eff} and V^{eff} definitions, the model response varies with changing graphene content. Yield stress and elasticity modulus is increased with increasing graphene content. And thanks to the variable tangent modulus definition, post yield behavior is also changing with changing graphene fraction.

3.5 Simulation Results

The validity of the newly introduced nanocomposite model is demonstrated by modeling uniaxial compression and tensile behavior of graphene-epoxy nanocomposites. Test data is obtained from the work of Shadlou et al. [17]. The parameters used in the simulations are as given in Table 3.2-3.4. The density of graphene is taken as 2 g/cm³ and the density of matrix material is taken as 0,95 g/cm³ for converting mass fraction to volume fraction.

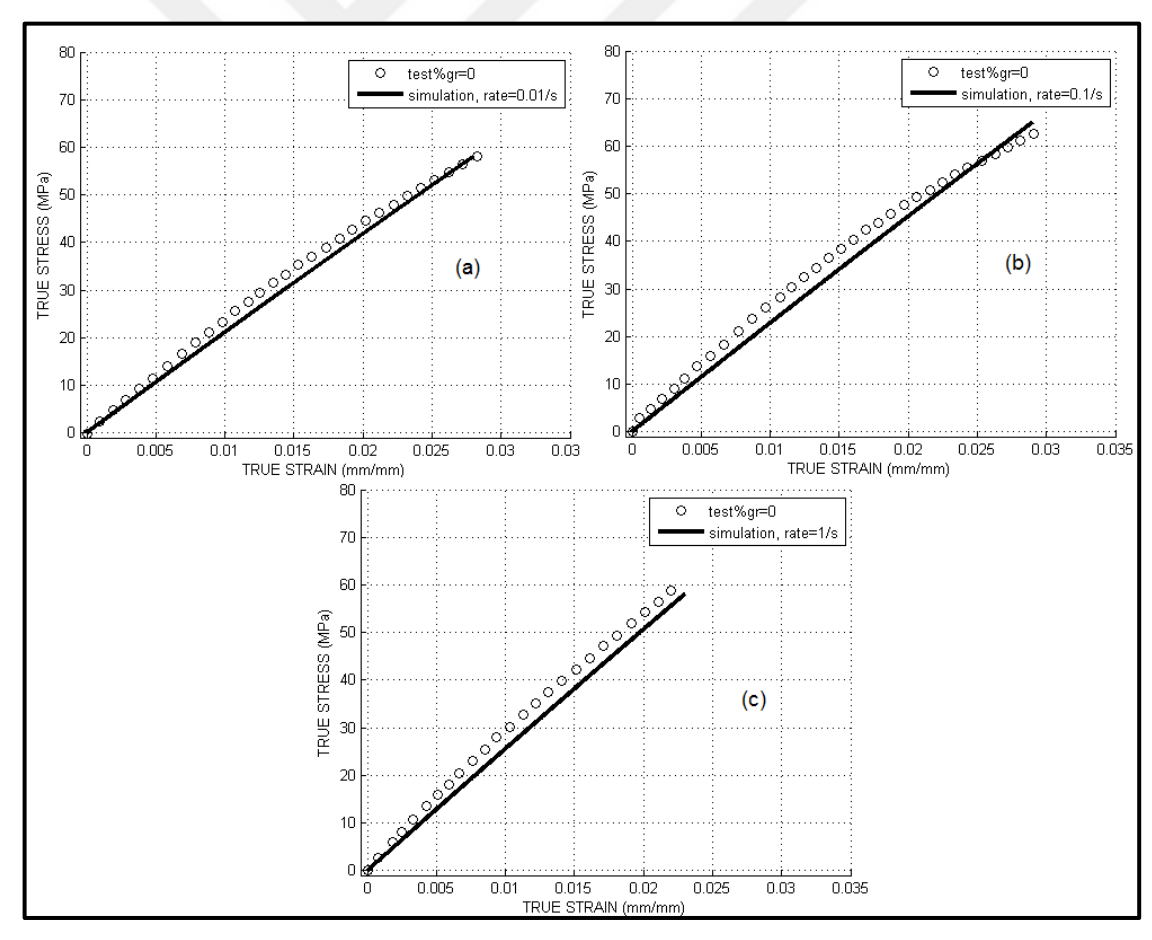


Figure 3.13 Comparison of model responses to compression test data [17] (graphene %wt.=0) a) strain rate=0.01 /s b) strain rate=0.1 /s c) strain rate=1/s

Figure 3.13 shows the tensile test results of neat epoxy material for three different strain rates. As seen from the figure, the new proposed model is still capable of modeling the varying tensile behavior for different strain rates.

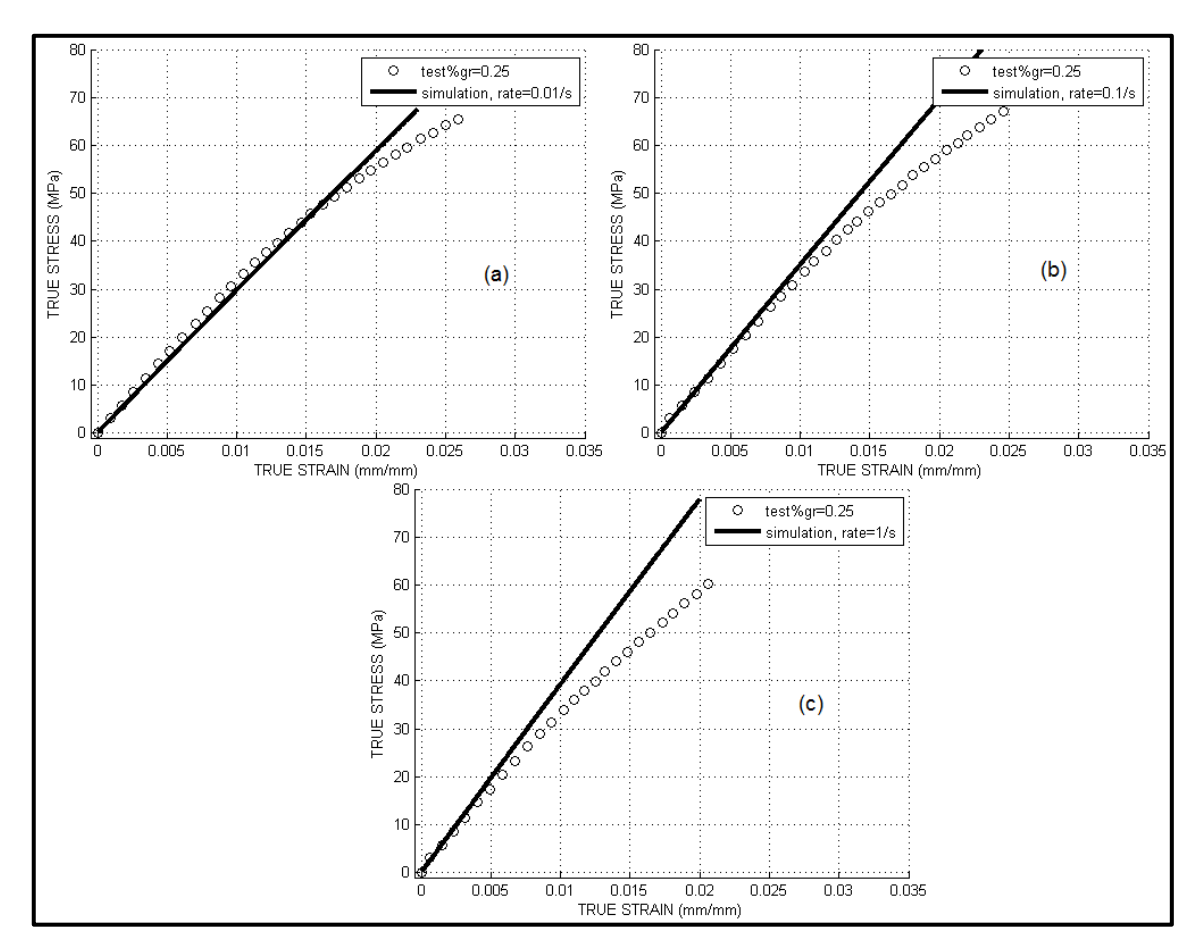


Figure 3.14 Comparison of model responses to compression test data [17] (graphene %wt.=0.25) a) strain rate=0.01 /s b) strain rate=0.1 /s c) strain rate=1/s

As seen from figures 3.13 - 3.16, new proposed model is capable of modeling tensile test results for three different strain rates. But tensile behavior of the composite material is shows brittle behavior; therefore the model capabilities for the nonlinear post yield behavior could not be confirmed with tensile test results. Therefore, compression behavior is also modeled in the following sections.

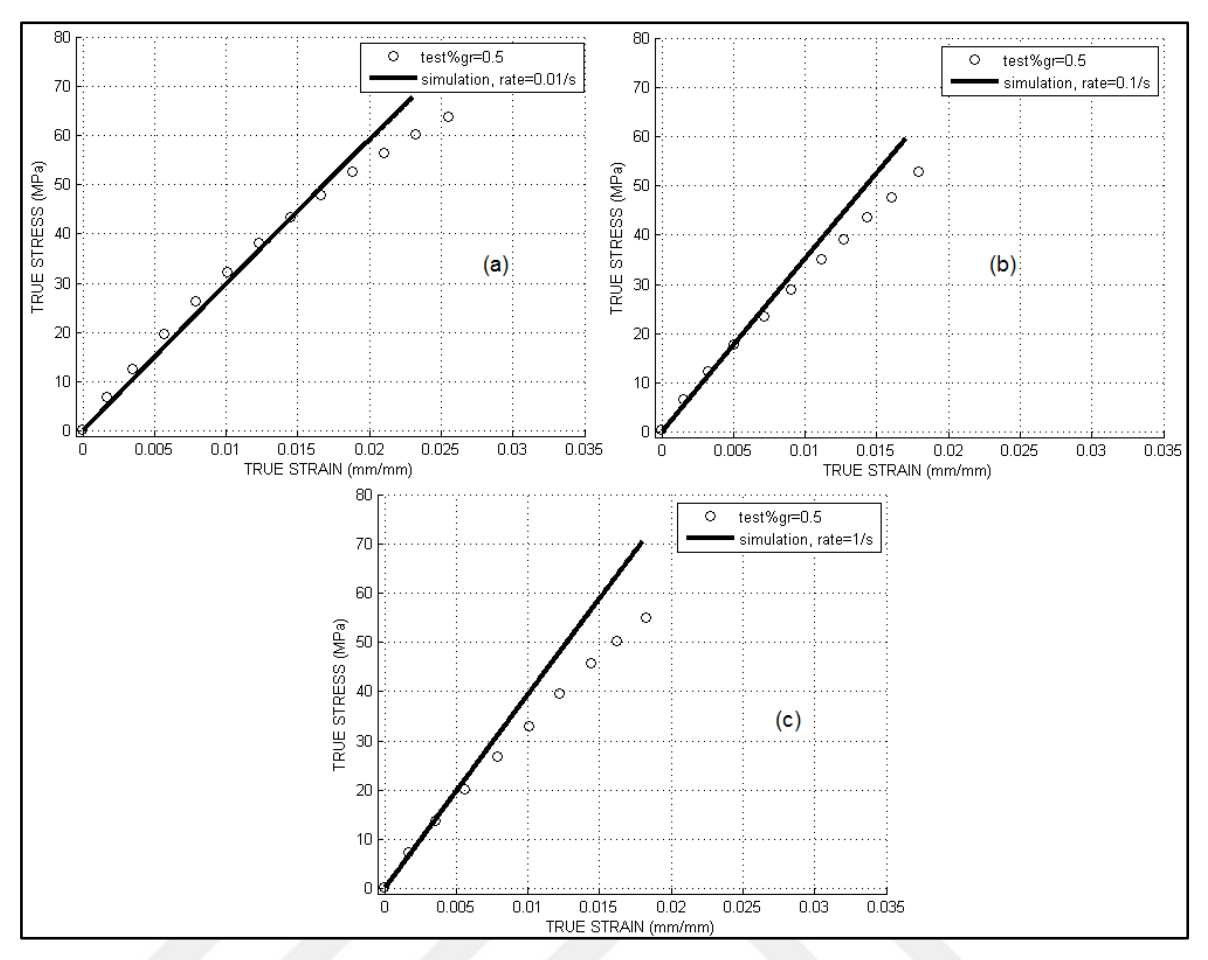


Figure 3.15 Comparison of model responses to compression test data [17] (graphene % wt.=0.5) a) strain rate=0.01 /s b) strain rate=0.1 /s c) strain rate=1/s

As mentioned above, Figures 3.14-3.16 is not capable of giving model capabilities for post yield behavior. But thanks to the new proposed effective elastic modulus definition, the viscoelastic part is successfully confirmed for three different graphene fractions.

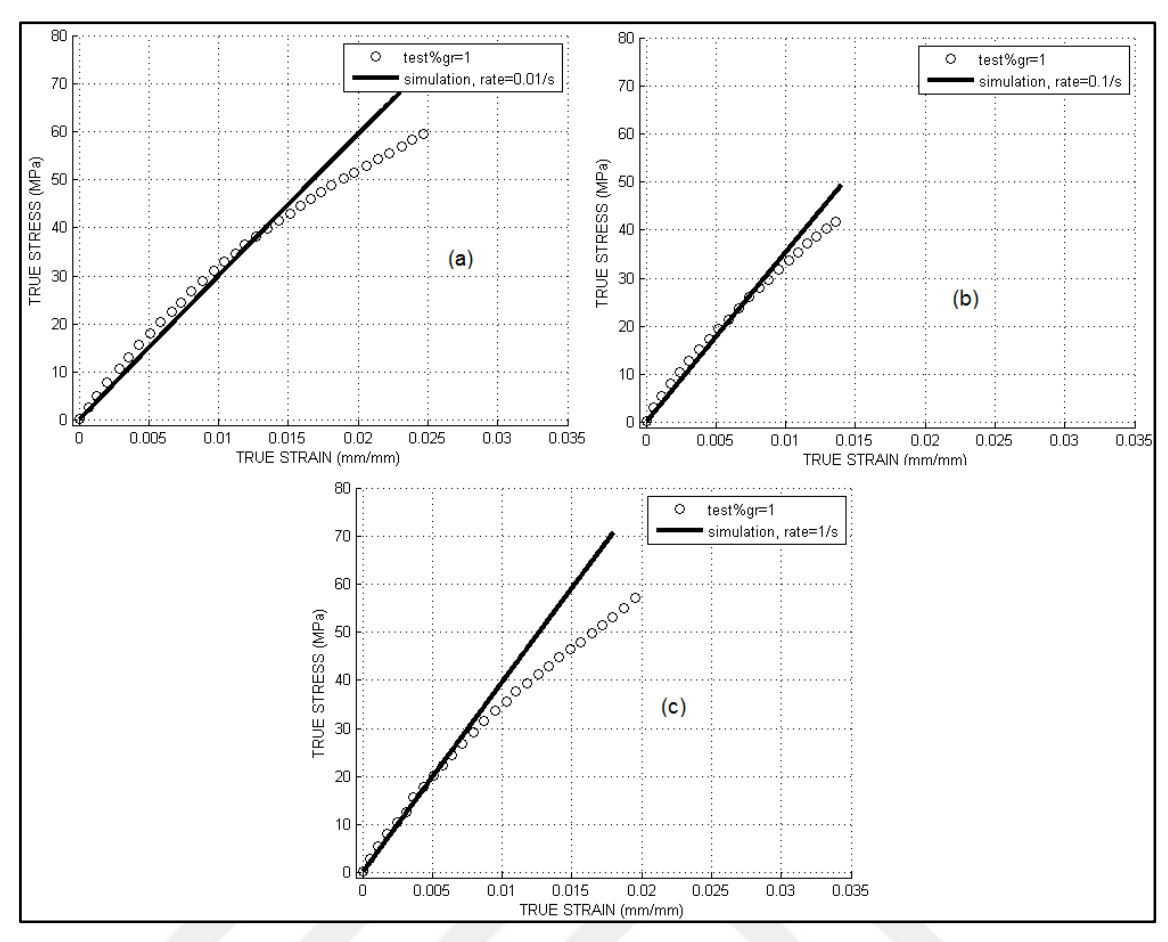


Figure 3.16 Comparison of model responses to compression test data [17] (graphene %wt.=1) a) strain rate=0.01 /s b) strain rate=0.1 /s c) strain rate=1/s

Table 3.2 Parameters for the flow rule, strain softening, calculation of $\Delta H_{\beta}^{eff},\,V^{eff}$, and Tangent modulus E_t

$\dot{\gamma}_0$ (s-1)	8e23
N, R (J/mol.K), k (m ² kgs ⁻² K ⁻¹)	5, 83e-4, 1.38e-23
Vm, Vr (m ³)	12e-29, 1.71e-29
ΔHβm , ΔHβr (kJ mol-1)	85, 3071.93
$h(MPa.K-1), \tau_{ps}(MPa)$	19 ,0.26
a, b, c, d	500, -3.4, -450, -6877
f, g, h, j	-1.79e8, 3.1e6, -1.46e4, 25

Table 3.3 Parameters for the shape function (Ψ) , C function, isotropic stress (A) and tangent modulus (E_t)

C1 (MPa), C2(MPa), C3, C4, ξ, ζ	3, 200, 3, 0.3, 1, 2
. λ and α	1.5, 1.4
A (MPa)	9060
β	1

Table 3.4 Parameters for Effective Elastic Moduli

$\dot{\varepsilon}^{ref}(1/\mathrm{s})$	1
E_{m1}^{ref} , E_{m2}^{ref} , E_{m3}^{ref} (MPa)	2500, 2000, 1000
T_{β}^{ref} , T_{g}^{ref} , T_{f}^{ref} (K)	290, 387, 466
c_1^g, c_2^g	32.58, 83.5
m ₁ , m ₂ , m ₃ , s	5, 40, 20,0.087
ξ, ζ	0.99, 0.01
2k, l, n, 2m, 2p (Hill's parameters of graphene) [25]	1700, 6.8, 10200, 738, 204000

Figure 3.17 reveals the compression stress-strain behavior of pure epoxy and graphene-epoxy nanocomposite with different weight fractions: 0%, 0.25%, 0.5%, 1% at the strain rate of 0.01/s. As seen from the figure, the proposed model is capable of giving the material response for different graphene fractions.

The material parameters are determined using the compression test seen on Figure 3.17 - (a). Therefore all of the other curves are predictions of the model. In other words only strain rate and/or graphene fraction parameters are changed to obtain all other curves.

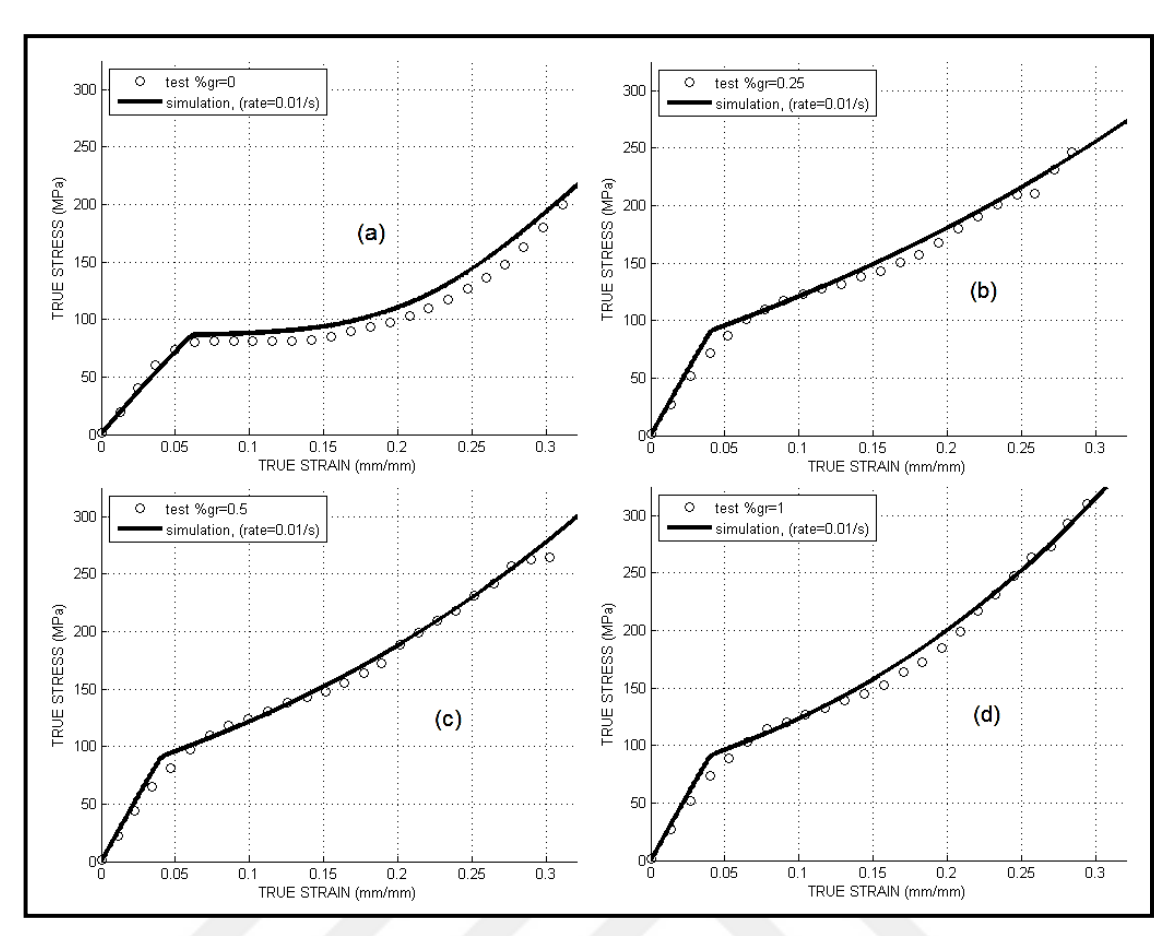


Figure 3.17 Comparison of model responses to compression test data [17] (strain rate = 0.01/s) a) wt%0 graphene b) wt%0.25 graphene c) wt%0.5 graphene d) wt%1 graphene

In Fig. 3.18 below, comparison of compression tests with model responses for 25wt% nanocomposite materials on four different strain rates: 0.01/s, 0.1/s, 1/s and 10/s is given. The model responses have shown good agreement for different strain rates.

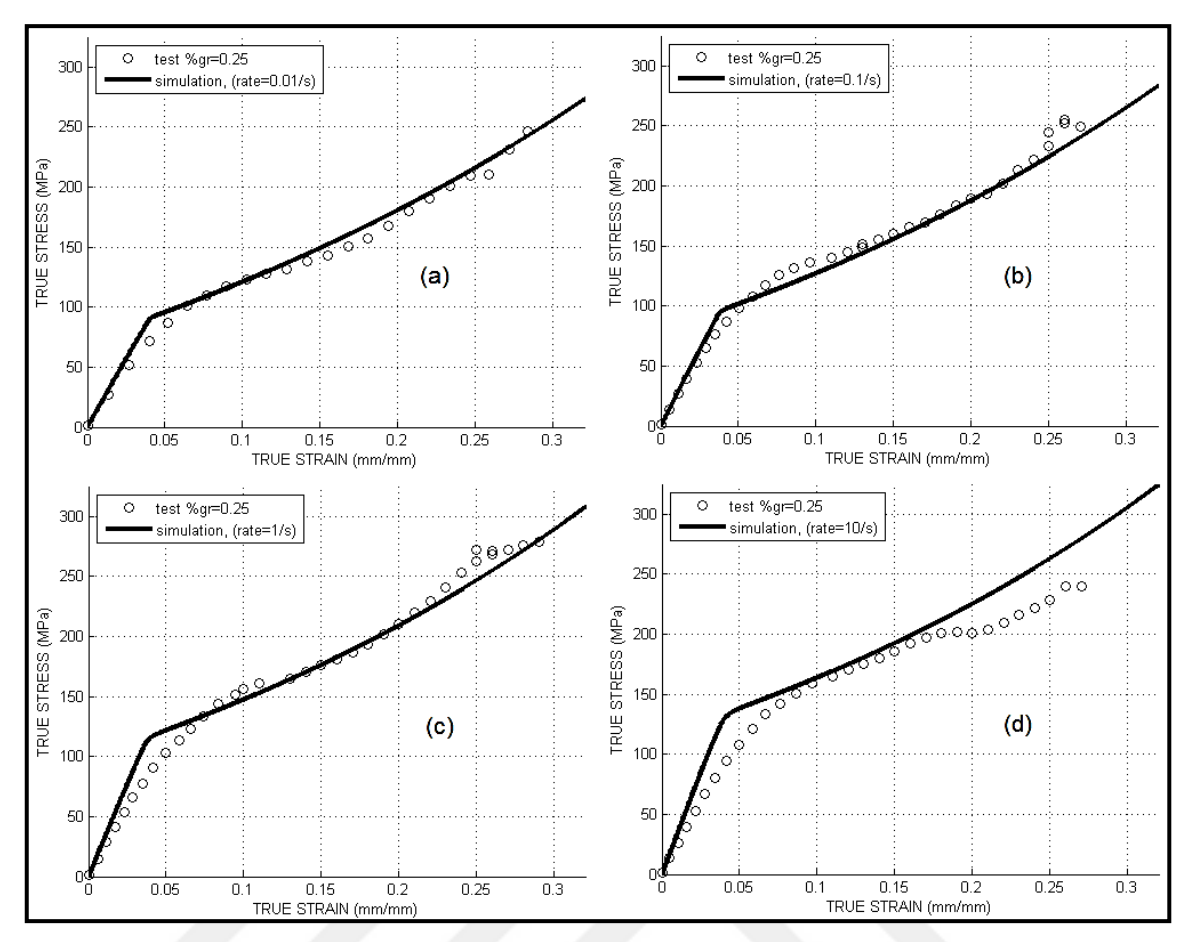


Figure 3.18 Comparison of model responses to compression test data [17] (graphene %wt.=0.25) a) strain rate=0.01 /s b) strain rate=0.1 /s c) strain rate=1 /s d) strain rate=10/s

In figure 3.19 and 3.20 model responses are compared to test results for %wt0.5 and %wt1 at different strain rates. Model responses have also shown good agreement with those test results.

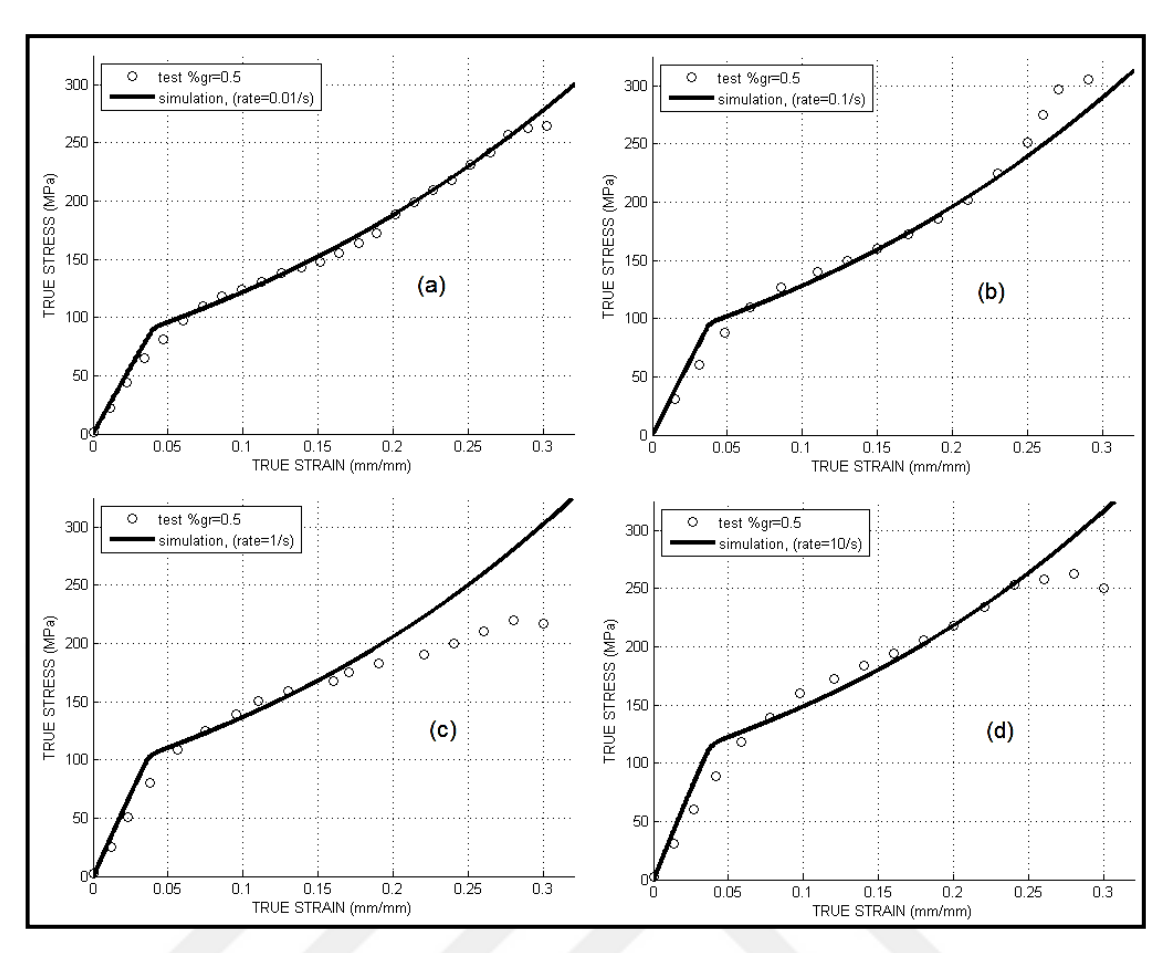


Figure 3.19 Comparison of model responses to compression test data [17] (graphene % wt. = 0.5) a) strain rate=0.01 /s b) strain rate=0.1 /s c) strain rate=1 /s d) strain rate=10/s

As mentioned before, the nonlinear post yield behavior of the proposed model is confirmed by compression tests. ΔH_{β}^{eff} and V^{eff} definions for graphene content and the variable tangent modulus parameter definitions has shown good agreement with the test results.

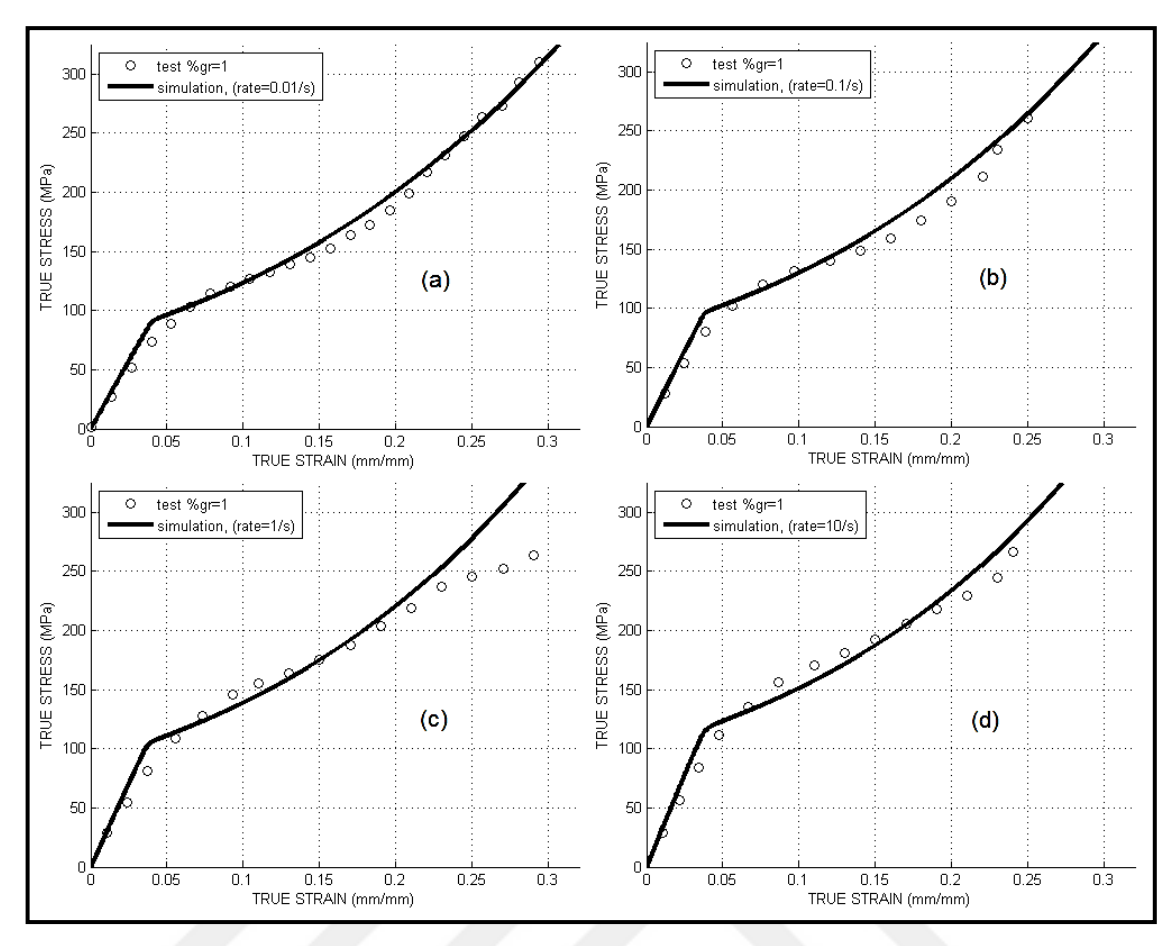


Figure 3.20 Comparison of model responses to compression test data [17] (graphene %wt.=1) a) strain rate=0.01 /s b) strain rate=0.1 /s c) strain rate=1 /s d) strain rate=10 /s

The model is also capable to model the mechanical behavior for temperatures above and below glass transition, but the set of tests we used [17] does not involve such data. Therefore this ability of the proposed model could not be compared to test data but model responses are shown at Figure 3.21.

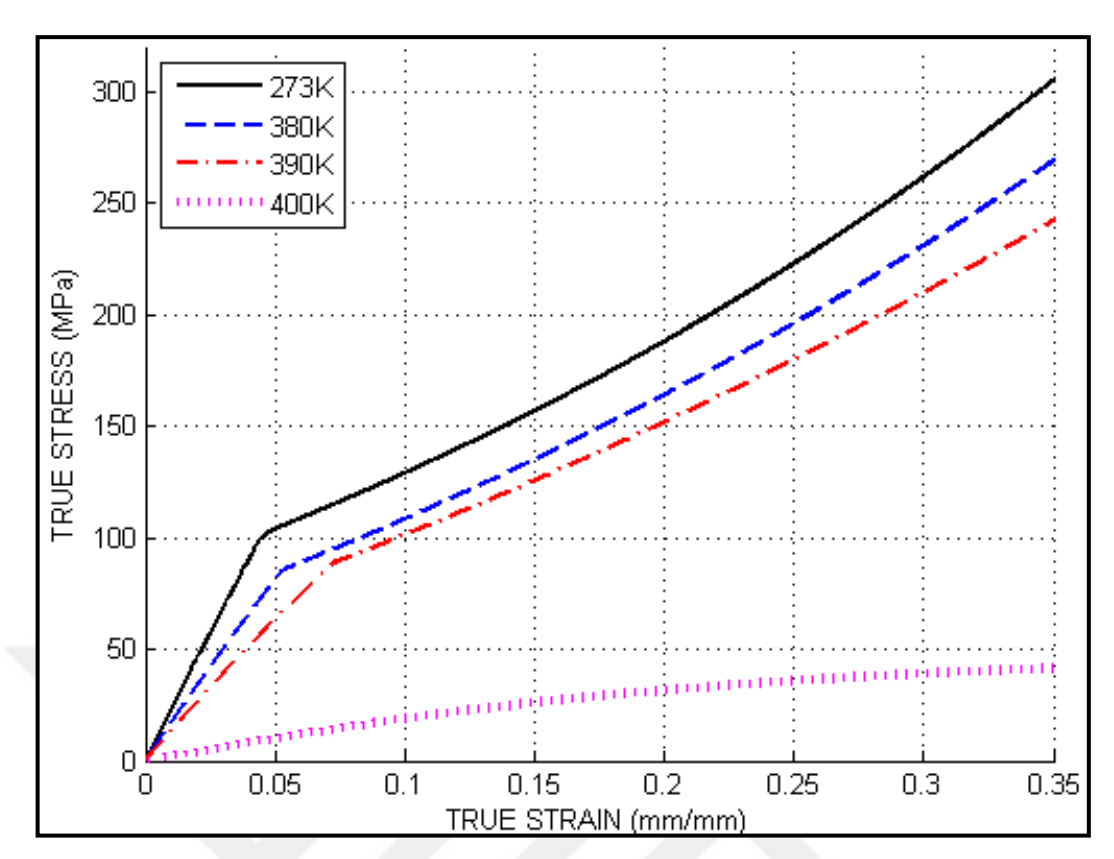


Figure 3.21 Model responses varying with temperature

In conclusion, with the modified parameters and the effective elasticity modulus equations explained above, the model is now capable of modeling the nonlinear viscoelastic-viscoplastic behavior of graphene nanocomposite material for varying strain rates, varying graphene content, also for different dissolution levels, and for varying temperature.

This capability of the proposed model is confirmed through tensile and compression test results.

FINITE ELEMENT METHOD PROCEDURE FOR COOPERATIVE VBO MODEL

4.1 Integration of Constitutive Equations with the Forward Gradient Method

In this part, the Cooperative VBO theory of Çolak et al. [33] is implemented to a commercial FEM solver, ABAQUS®, via user material subroutine, UMAT.

The problem can be explained as; denoting the time at the beginning of the increment by t_n and the time at the end of the increment by t_{n+1} , Given the value of σ , g, γ^p , d^{in} at the time t_n , and d at time t_{n+1} , determine the values of σ , g, $\gamma^p f$, d^{in} at the time t_{n+1} .

As mentioned before, Cooperative VBO model uses an additive form of total strain tensor as;

$$\boldsymbol{d} = \boldsymbol{d}^e + \boldsymbol{d}^{vp} \tag{4.1}$$

With;

$$\boldsymbol{d}^{e} = \frac{1+\nu}{C \cdot E} \dot{\boldsymbol{s}} \tag{4.2}$$

And

$$\boldsymbol{d}^{vp} = \frac{3}{2}\dot{\gamma}^p \frac{\dot{s} - \dot{g}}{\Gamma} \tag{4.3}$$

Here the bold lowercase letters define a second order tensor and a bold uppercase letters define a fourth order tensor.

In a UMAT subroutine, the Cauchy stress tensor *s* and the Jacobian matrix [J] should be updated at each increment.

In Cooperative-VBO model of Colak et al.[33], the Cauchy stress tensor evolves with,

$$\dot{\mathbf{s}} = \frac{1+\nu}{CE} (\mathbf{d} - \mathbf{d}^{vp}) \tag{4.4}$$

And the deviator of plastic strain rate tensor is defined as;

$$\boldsymbol{d}^{vp} = \frac{3}{2}\dot{\gamma}^p \frac{\dot{\boldsymbol{o}}}{\Gamma} \tag{4.5}$$

With overstress tensor defined as;

$$\dot{\boldsymbol{o}} = \dot{\boldsymbol{s}} - \dot{\boldsymbol{g}} \tag{4.6}$$

So the evolution law of *s* becomes;

$$\dot{\mathbf{s}} = \frac{C \cdot E}{1 + \nu} \left(\mathbf{d} - \frac{3}{2} \dot{\gamma}^p \frac{\dot{\mathbf{o}}}{\Gamma} \right) \tag{4.7}$$

Then, it is assumed that deviator of Cauchy stress, s can be updated as;

$${}^{(n+1)}\mathbf{s} = {}^{(n)}\mathbf{s} + \Delta t \cdot {}^{(n+1)} \cdot {}^{\cdot} \mathbf{s} = {}^{(n)}\mathbf{s} + {}^{(n+1)}\Delta \mathbf{s}$$

$$(4.8)$$

With:

$$\Delta \mathbf{s} = \Delta t \cdot \left[\frac{C \cdot E}{1 + \upsilon} (\mathbf{d} - \frac{3}{2} \gamma^{p} \frac{\mathbf{o}}{\Gamma}) \right] = \left[\frac{C \cdot E}{1 + \upsilon} \left(\Delta \mathbf{d} - \frac{3}{2} \Delta \gamma^{p} \frac{\mathbf{o}}{\Gamma} \right) \right]$$
(4.9)

However, in the present model, ${}^{(n+1)}C$, ${}^{(n+1)}\mathbf{0}$, ${}^{(n+1)}\Gamma$, γ^p are not known for the next step.

Therefore, in order to simplify the update algorithm, one can assume that,

$$\Delta \mathbf{s} = \left[\frac{{}^{(n)}C \cdot E}{1 + \upsilon} \cdot {}^{(n+1)}\Delta \mathbf{d} - \frac{3}{2} \cdot \frac{{}^{(n)}C \cdot E}{1 + \upsilon} \cdot {}^{(n+1)}\Delta \gamma^{p} \frac{{}^{(n)}\mathbf{o}}{{}^{(n)}\Gamma} \right]$$
(4.10)

Where ${}^{(n+1)}\Delta \mathbf{e}$ is the deviator of total strain increment tensor at time increment (n+1) provided by ABAQUS implicit solver and ${}^{(n+1)}\Delta \gamma^p$ is the effective inelastic strain increment at increment (n+1).

Following the forward gradient scheme given by Gomaa [28] for VBO model [33] one can write,

$$\gamma^{p} \cong \frac{\Delta \gamma^{p}}{\Delta t}$$
(4.11)

$$^{(n+1)}\Delta\gamma^{p} = \Delta t \cdot \left((1-\eta) \cdot {}^{(n)}\gamma^{p} + \eta \cdot {}^{(n+1)}\gamma^{p} \right)$$

$$\tag{4.12}$$

And using Taylor series expansion for derivative of $\stackrel{\cdot}{\gamma}^p$ as,

$$\gamma = \gamma + \eta \cdot \frac{d}{dt} \cdot \gamma \cdot \Delta t + \dots$$

$$(4.13)$$

The second order terms are neglected in Taylor series.

Then,

$$^{(n+1)}\Delta\gamma^{p} = \Delta t \cdot \begin{pmatrix} ^{(n)} \cdot ^{p} \\ \gamma + \eta \cdot \frac{d}{dt} \cdot ^{(n)} \cdot ^{p} \\ \gamma \cdot \Delta t \end{pmatrix}$$

$$\tag{4.14}$$

Here, η is forward gradient method parameter, which is $0 \le \eta \le 1$. 0.5 is used in this work for best accuracy.

Following the framework proposed by Gomaa, some algebraic arrangements can be made. And then the plastic strain rate γ at increment (n+1) can be expressed as;

$$\gamma^{p} \cong \frac{\Delta \gamma^{p}}{\Delta t} = \alpha \left(\mathbf{o} : \mathbf{d} \right) + \xi \tag{4.15}$$

With

$$\xi = \frac{\gamma}{\zeta} \tag{4.16}$$

$$\alpha = \Delta t \cdot P \cdot \frac{\eta}{\zeta} \tag{4.17}$$

And

$$\zeta = 1 - \eta \cdot \Delta t \left[Q \frac{\delta \dot{\gamma}}{\delta \Gamma} + h(1 - ti / \tau_{ps}) \cdot \frac{\delta \dot{\gamma}}{\delta ti} \right]$$
(4.18)

Q and P are intervening variables defined in the algorithm for legibility purposes as;

$$Q = -\frac{3}{2} \left[\left(\frac{C \cdot E}{1 + \nu} - \frac{2}{3} \overline{E}_{t} \right) \cdot (1 - \psi) + \frac{2}{3} \overline{\psi} \cdot \left(1 - \frac{3}{2} \cdot \frac{\mathbf{o} \cdot (\mathbf{g} - \mathbf{k})}{\Gamma \cdot A} \right) \right]$$
(4.19)

And

$$P = \frac{3 \cdot (1 - \psi)}{2 \cdot \Gamma} \cdot \frac{C \cdot E}{1 + \nu} \tag{4.20}$$

Therefore \mathbf{d}^{vp} is defined as;

$$\mathbf{d}^{vp} = \frac{3 \cdot \alpha}{2 \cdot \Gamma} \cdot (\mathbf{o} \otimes \mathbf{o}) : \mathbf{d} + \frac{3}{2 \cdot \Gamma} \cdot \xi \cdot \mathbf{o}$$
(4.21)

In agreement with the work of Gomaa, a fourth order tensor Ω is defined as;

$$\mathbf{\Omega} = \frac{3 \cdot \alpha}{2 \cdot \Gamma} \cdot (\mathbf{o} \otimes \mathbf{o}) \tag{4.22}$$

Where $\mathbf{o} \otimes \mathbf{o}$ represents the dyadic product of overstress tensor, \mathbf{o} . It should be noted that the fourth order tensor Ω is symmetric.

Then \mathbf{d}^{vp} can be rewritten as;

$$\mathbf{d}^{vp} = \mathbf{\Omega} : \mathbf{d} + \frac{3}{2 \cdot \Gamma} \cdot \boldsymbol{\xi} \cdot \mathbf{o}$$

(4.23)

Now the necessary equations to update the Cauchy stress tensor \mathbf{s} and solution dependent state variables, equilibrium stress \mathbf{g} and kinematic stress \mathbf{k} at increment (n+1) can be defined as;

$$\Delta \mathbf{s} = \frac{C \cdot E}{1 + \nu} \left[\mathbf{\Omega}_{s}^{\text{tan}} : \Delta \mathbf{d} - \frac{3}{2 \cdot \Gamma} \cdot \boldsymbol{\xi} \cdot \Delta t \cdot \mathbf{o} \right] + \frac{E}{1 - 2 \cdot \nu} \cdot tr(\Delta \mathbf{d}).\mathbf{I}$$
(4.24)

Where

$$\mathbf{\Omega}_{s}^{\tan} = \mathbf{I} - \mathbf{\Omega} \tag{4.25}$$

I is the fourth order identity tensor. And **g**, equilibrium stress, is calculated as;

$$\Delta \mathbf{g} = \mathbf{\Omega}_{g}^{\text{tan}} : \Delta \mathbf{d} - \frac{3}{2 \cdot \Gamma} \left[\frac{C \cdot \psi}{1 + \nu} - \frac{2}{3} \cdot \left(\frac{-\psi}{\psi} + \left(1 - \frac{\psi}{E} \right) \cdot \overline{E}_{t} \right) \right] \cdot \Delta t \cdot \xi \cdot \mathbf{o} - \frac{-\psi}{A} \cdot \gamma^{p} \cdot \Delta t \cdot \left(\mathbf{g} - \mathbf{k} \right)$$
(4.26)

Where:

$$\mathbf{\Omega}_{g}^{tan} = \frac{C \cdot \psi}{1 + \nu} \cdot \mathbf{I} - \left[\frac{C \cdot \psi}{1 + \nu} - \frac{2}{3} \left(\psi + \left(1 - \frac{\psi}{E} \right) \cdot \overline{E}_{t} \right) \right]$$
(4.27)

And k is calculated as

$$\Delta \mathbf{k} = \frac{2}{3} \cdot \overline{E}_{t} \cdot \left(\mathbf{\Omega} : \Delta \mathbf{d} + \frac{3}{2 \cdot \Gamma} \cdot \boldsymbol{\xi} \cdot \Delta t \cdot \mathbf{o} \right)$$
(4.28)

4.2 Definition of the Jacobian Matrix

Definition of the Jacobian matrix which is needed by the procedure is given below; In the case of isotropic elasticity, Jacobean matrix is the fourth order elasticity tensor. Using Lamé constants Jacobean matrix is given by;

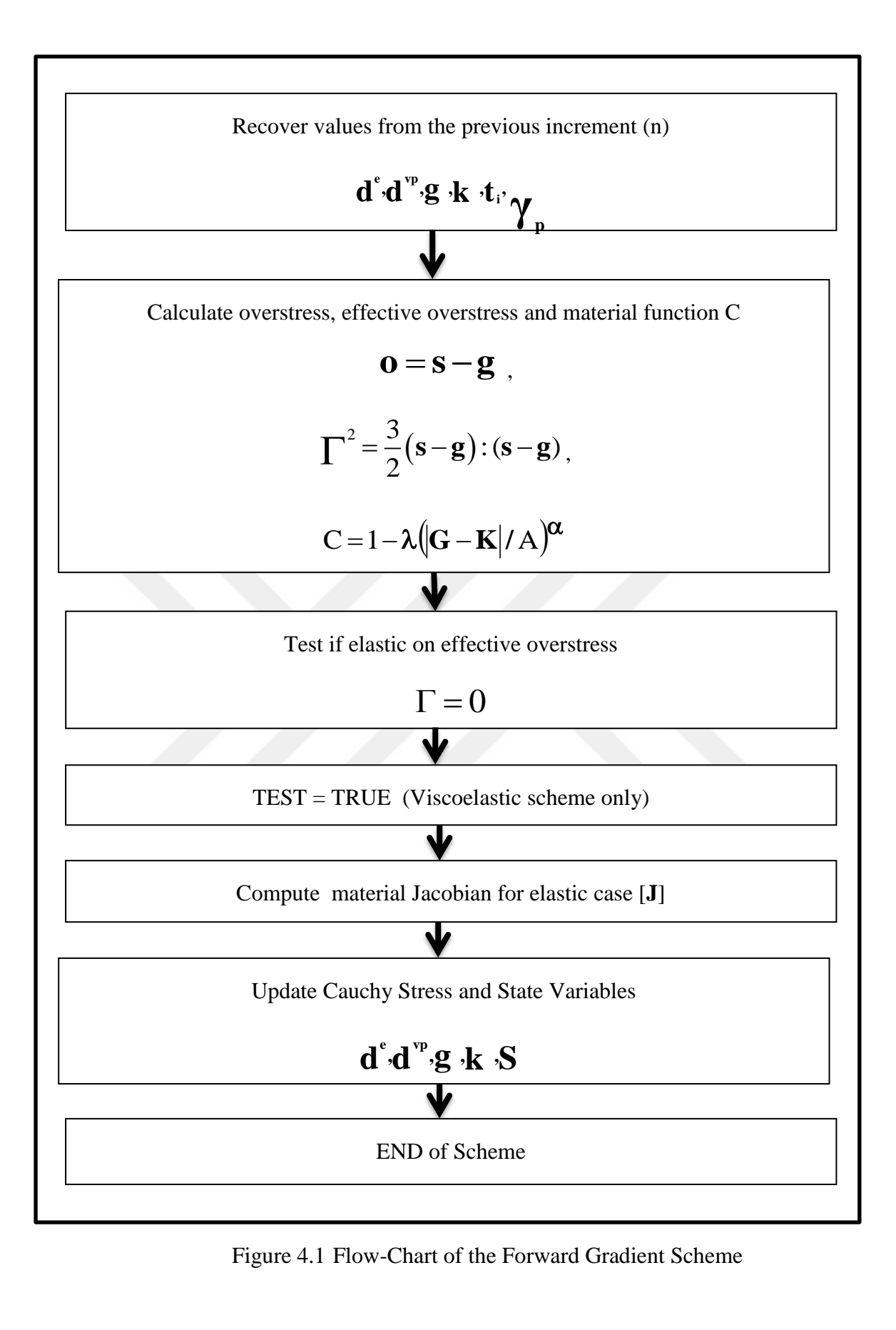
$$\begin{bmatrix}
\sigma_{11} \\
\sigma_{22} \\
\sigma_{33} \\
\sigma_{13} \\
\sigma_{12}
\end{bmatrix} = \begin{bmatrix}
2\mu + \lambda & \lambda & \lambda & 0 & 0 & 0 \\
\lambda & 2\mu + \lambda & \lambda & 0 & 0 & 0 \\
\lambda & \lambda & 2\mu + \lambda & 0 & 0 & 0 \\
0 & 0 & 0 & \mu & 0 & 0 \\
0 & 0 & 0 & 0 & \mu & 0 \\
0 & 0 & 0 & 0 & \mu & 0 \\
0 & 0 & 0 & 0 & 0 & \mu
\end{bmatrix} \cdot \begin{bmatrix}
\varepsilon_{11} \\
\varepsilon_{22} \\
\varepsilon_{33} \\
\varepsilon_{23} \\
\varepsilon_{13} \\
\varepsilon_{12}
\end{bmatrix}$$
(4.29)

For inelastic part, taking the partial derivative of Eq 4.23 with respect to $\Delta \mathbf{d}$, result in

$$[J] = \frac{\partial \Delta \mathbf{\sigma}}{\partial \Delta \mathbf{d}} = 2 \cdot \mu \cdot \mathbf{\Omega}_{s}^{\text{tan}} + \left(K - \frac{2 \cdot \mu}{3}\right) \cdot \mathbf{I} \otimes \mathbf{I}$$
(4.30)

In agreement with the scheme given by Gomaa et al. [28]

The workflow of the proposed scheme is given below;



 $(\Gamma=0)$ TEST=FALSE (Inelastic Scheme Starts)



Compute shape function Ψ and intervening variables P, Q, ζ , ξ , α (using values from increment (n))

$$\psi = \psi_1 + \left(\frac{C_2 - \psi_1}{\exp(C_3 \left| \epsilon^{in} \right|)}\right) \quad \psi_1 = C_1 \left(1 + C_4 \left(\frac{|G|}{A + |K| + \xi \Gamma^{\zeta}}\right)\right)$$

$$P = \frac{3 \cdot (1 - \psi)}{2 \cdot \Gamma} \cdot \frac{C \cdot E}{1 + \nu}$$

$$Q = -\frac{3}{2} \left[\left(\frac{C \cdot E}{1 + \nu} - \frac{2}{3} \overline{E}_{t} \right) \cdot (1 - \psi) + \frac{2}{3} \overline{\psi} \cdot \left(1 - \frac{3}{2} \cdot \frac{\mathbf{o} : (\mathbf{g} - \mathbf{k})}{\Gamma \cdot A} \right) \right]$$

$$\zeta = 1 - \eta \cdot \Delta t \left[Q \frac{\delta \gamma}{\delta \Gamma} + h(1 - ti / \tau_{ps}) \cdot \frac{\delta \gamma}{\delta ti} \right], \quad \xi = \frac{\gamma}{\zeta}, \quad \alpha = \Delta t \cdot P \cdot \frac{\eta}{\zeta}$$



Compute plastic strain rate γ and internal shear stress t_i and fourth order tensor Ω (using values from previous increment (n))

$$\gamma^{p} \cong \frac{\Delta \gamma^{p}}{\Delta t} = \alpha \left(\mathbf{o} : \mathbf{d} \right) + \xi, \ t_{i} = h \left(1 - \frac{t_{i}}{\tau_{ps}} \right) \gamma^{p}, \ \Omega = \frac{3 \cdot \alpha}{2 \cdot \Gamma} \cdot \left(\mathbf{o} \otimes \mathbf{o} \right)$$



Update inelastic Strain for increment (n+1)

$$\mathbf{d}^{vp} = \mathbf{\Omega} : \mathbf{d} + \frac{3}{2 \cdot \Gamma} \cdot \boldsymbol{\xi} \cdot \mathbf{o}$$

Figure 4.1 Flow-Chart of the Forward Gradient Scheme (cont'd)

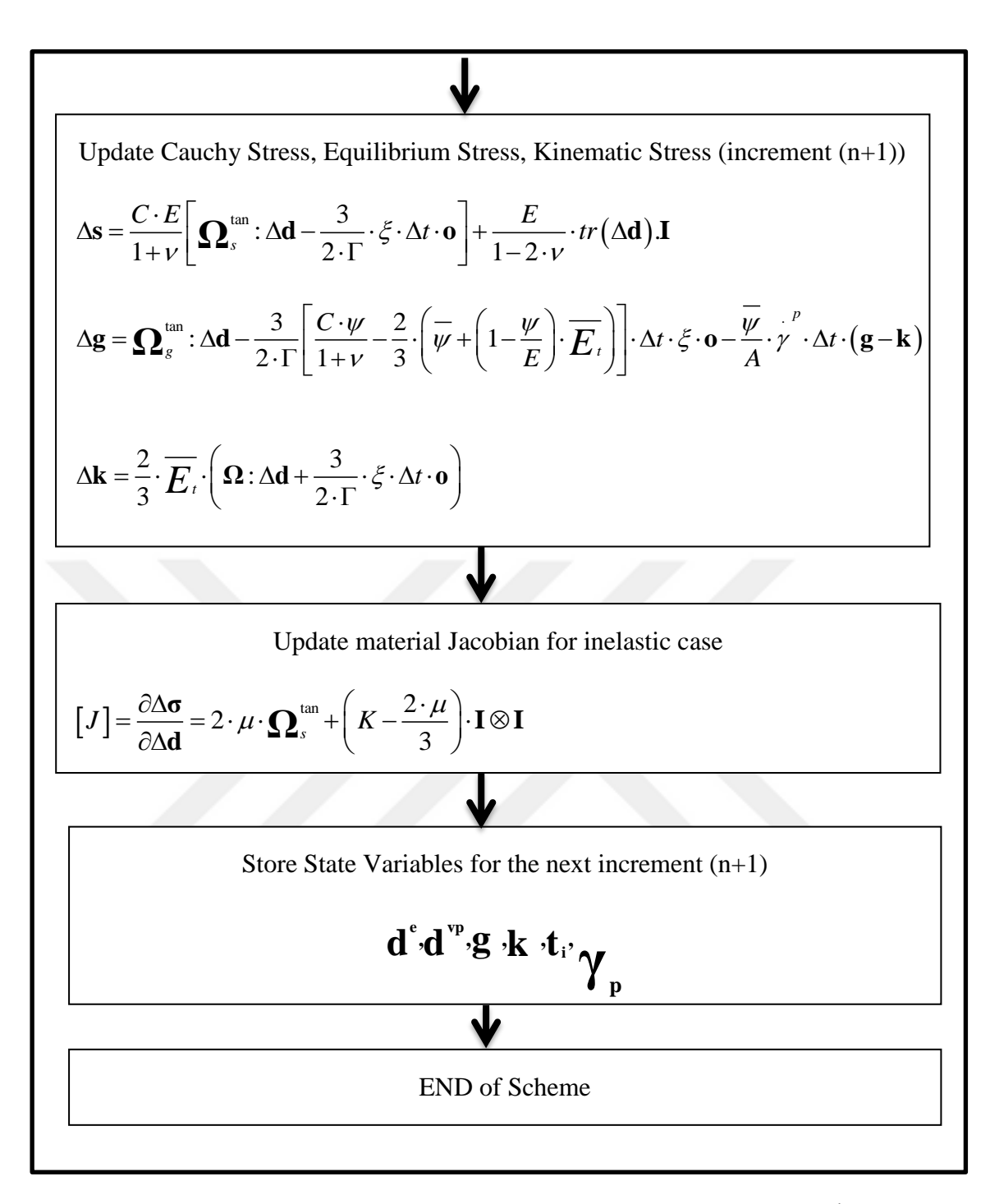


Figure 4.1 Flow-Chart of the Forward Gradient Scheme (cont'd)

4.3 FEM Integration Scheme Results

In this part, the new proposed integration scheme for the new proposed model results are compared to the model results obtained at Section 3. Except the ones explained in figure captions, all parameters are the same as the parameters given in tables 3.2 - 3.4. All results are taken using ABAQUS ® 6.13-1 and Parallel Studio XE 2013 as required by ABAQUS. The finite element model is defined with one cubic C3D8R. Time step

required by the solver is 1e-5 s for all simulations except fig. 4.3 (strain rate=1/s, time step = 1e-7).

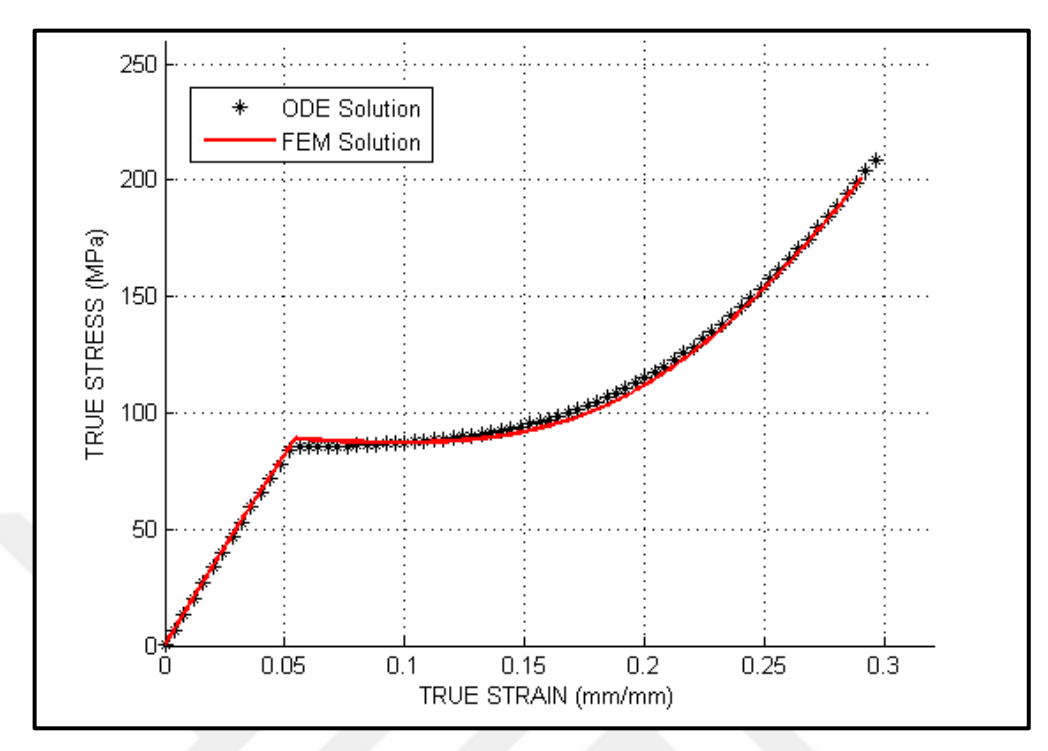


Figure 4.2 ODE solution – FEM solution comparison for %wt=0, Strain rate = 0.01/s Temperature = 296 K

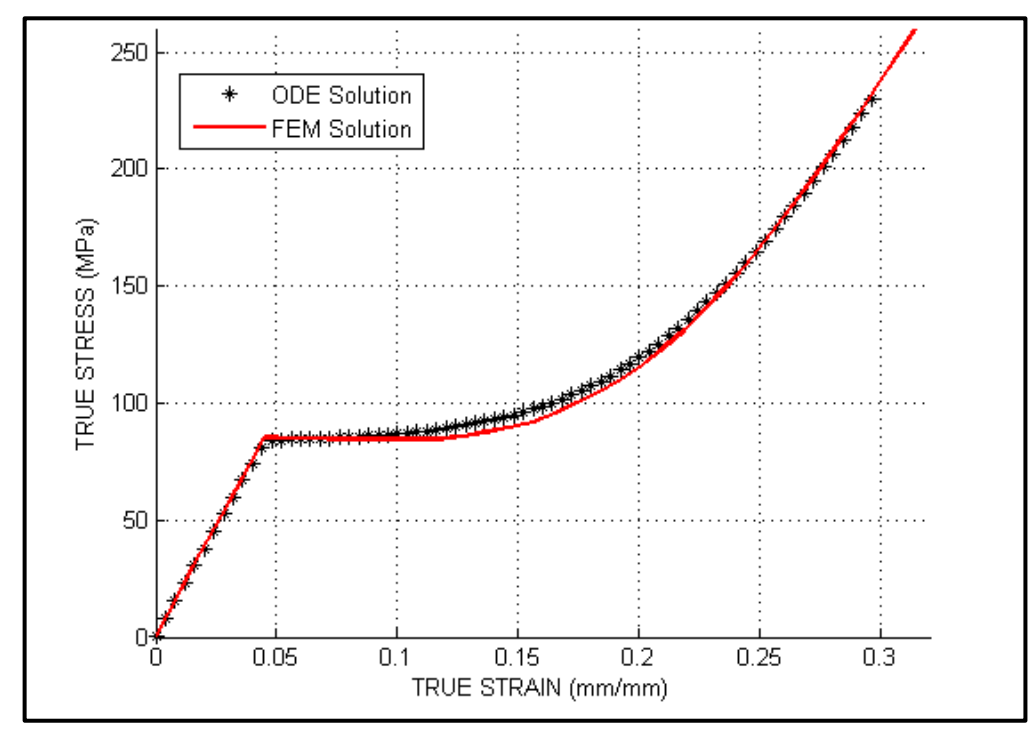


Figure 4.3 ODE solution – FEM solution comparison for % wt=0, Strain rate = 0.1/s Temperature = 296 K

Figures 4.2-4.4 shows that, with the integration scheme, new proposed model is still capable of modeling mechanical behavior for three different strain rates. This seems important for potential structural analysis using the proposed integration scheme and FEM method.

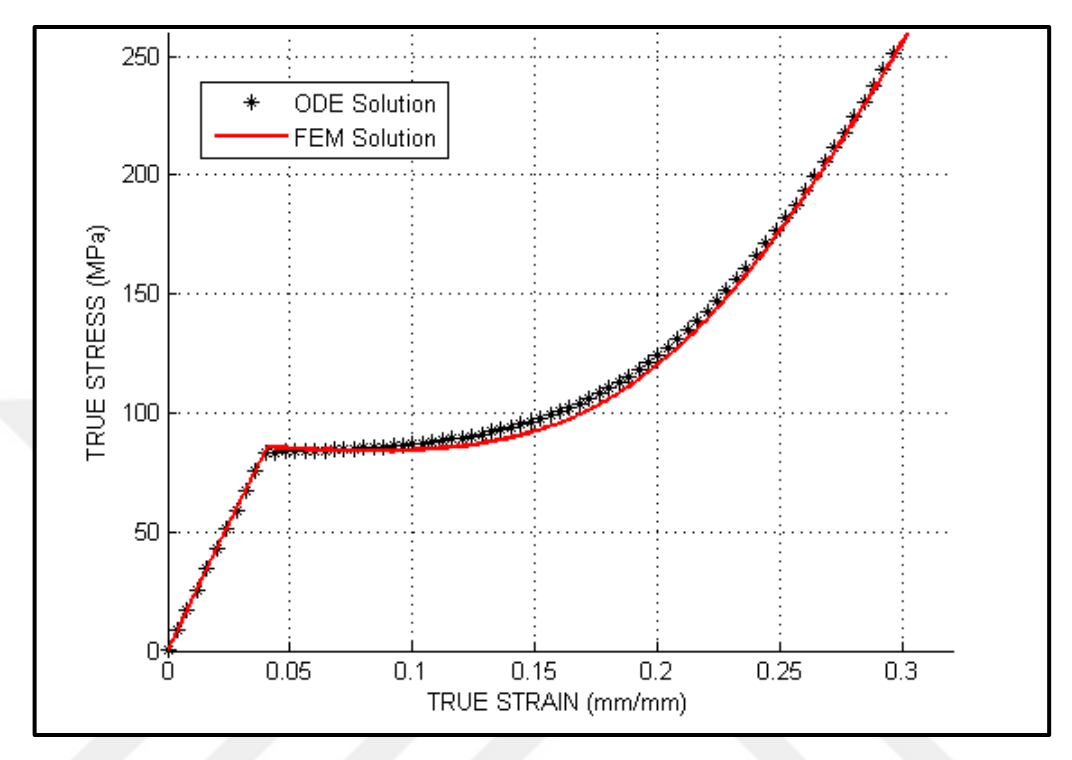


Figure 4.4 ODE solution – FEM solution comparison for %wt=0, Strain rate = 1/s Temperature = 296 K (Step time (DTIME) = 1e-7)

For higher strain rates, time step required by the FEM solver should be decreased as seen in figure 4.3 in order to catch the flow and nonlinear behavior of the material.

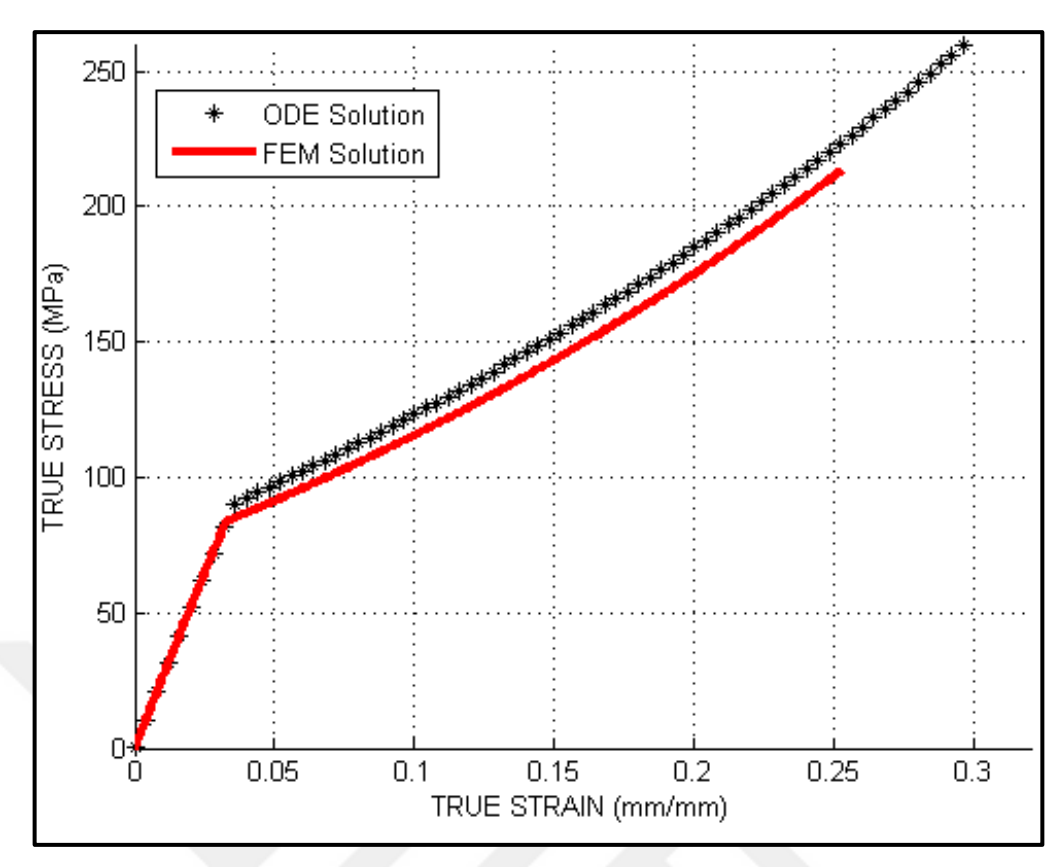


Figure 4.5 ODE solution – FEM solution comparison for %wt=0.25, Strain rate = 1e-2/s Temperature = 296 K

As seen from figures 4.5 to 4.7, the explicit integration scheme is giving consistent results with the ODE solution obtained and verified at Section 3.

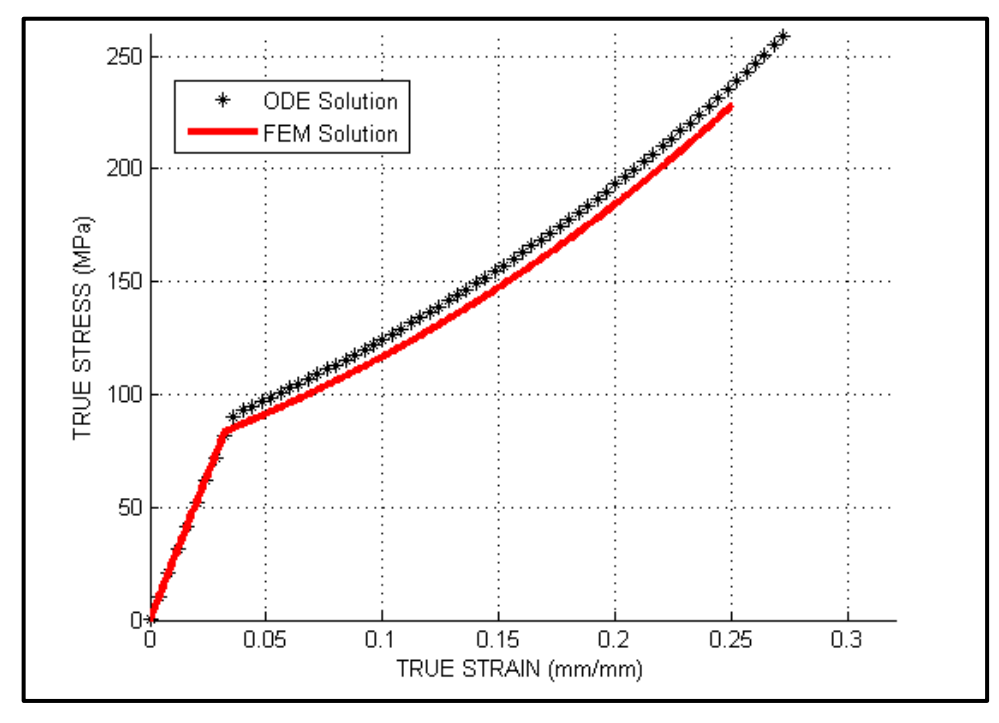


Figure 4.6 ODE solution – FEM solution comparison for %wt=0.5, Strain rate = 1e-2/s Temperature = 296 K

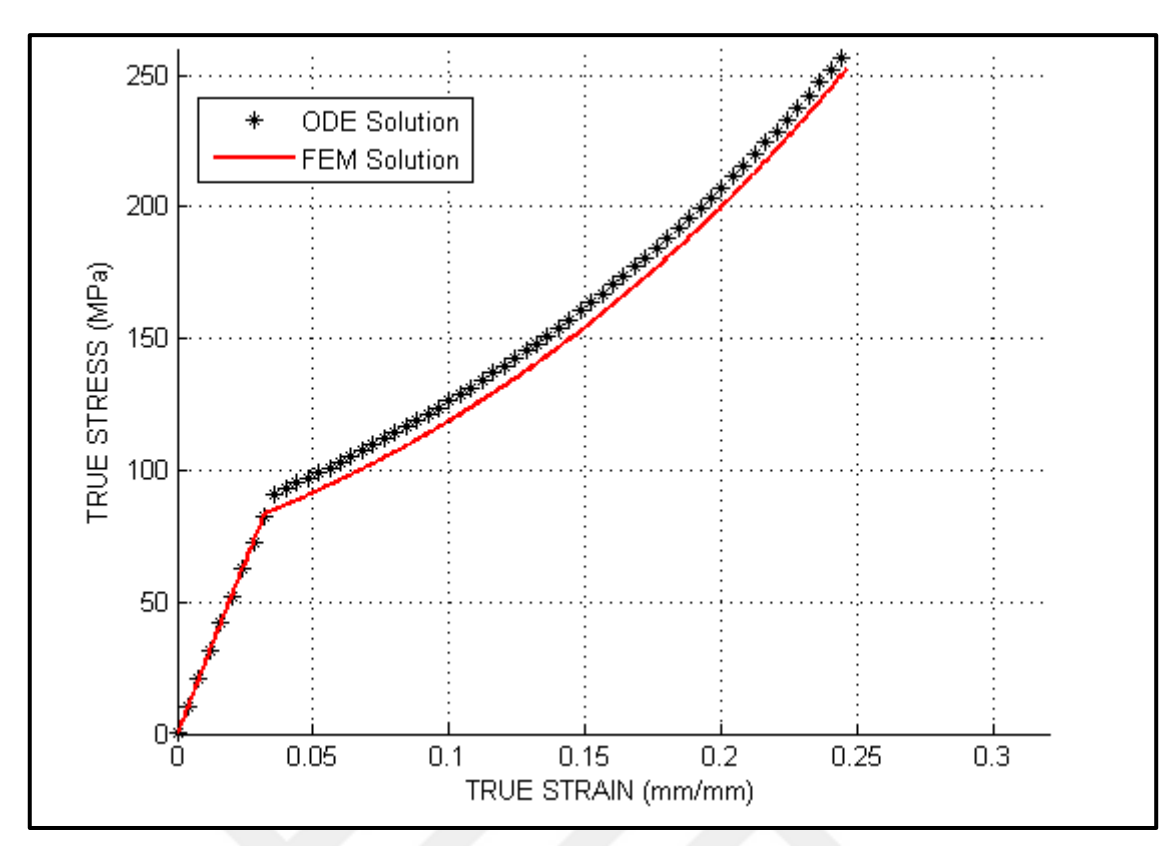


Figure 4.7 ODE solution – FEM solution comparison for %wt=1, Strain rate = 1e-2/s Temperature = 296 K

To test the convergence behavior of the scheme, the simulations are made for different time steps (Figure 4.7). As seen from the figure, for time steps smaller than 1e-3, the results are oscillated and not converged. But for smaller time steps, the results are converged and stayed stable. The oscillatory behavior is a result of the explicit integration scheme.

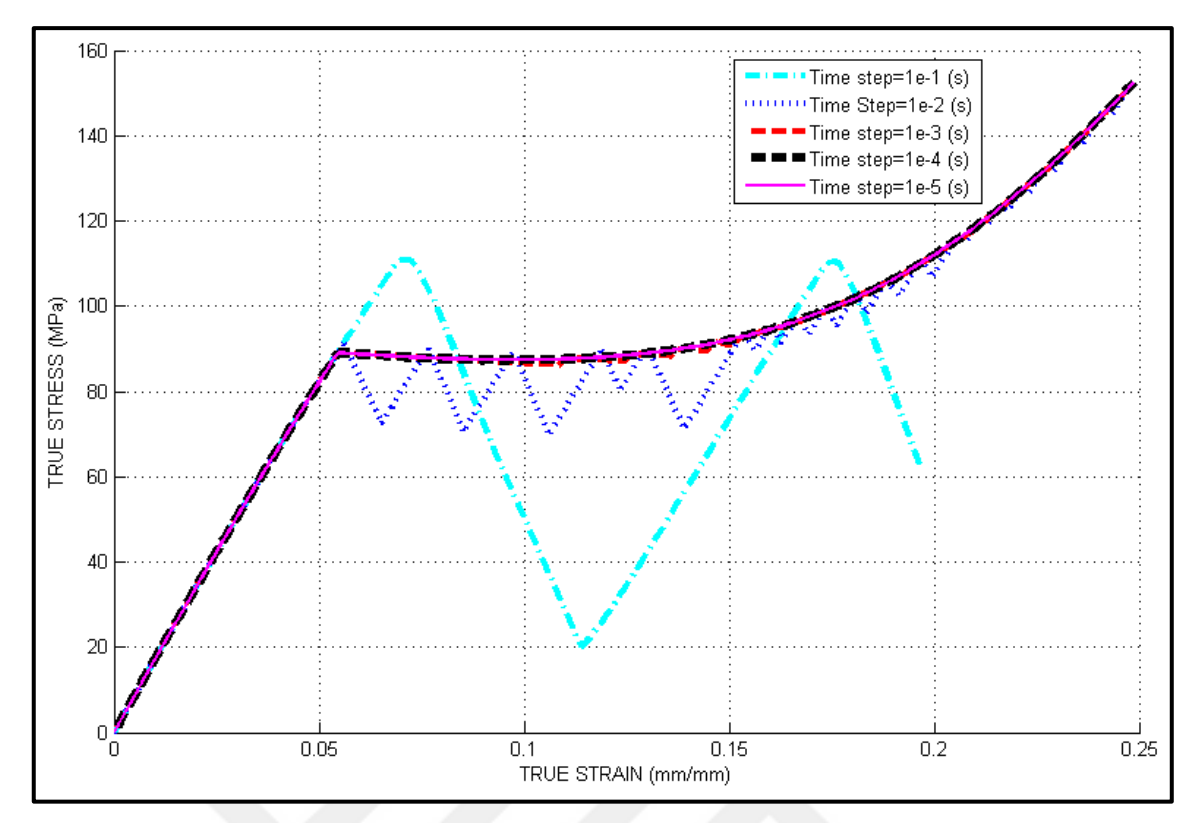


Figure 4.8 FEM Scheme results for different step times.

The simulations are made also for 1-4096 elements. Those results are also shown an almost identical result. After 64 elements, the results did not change at all.

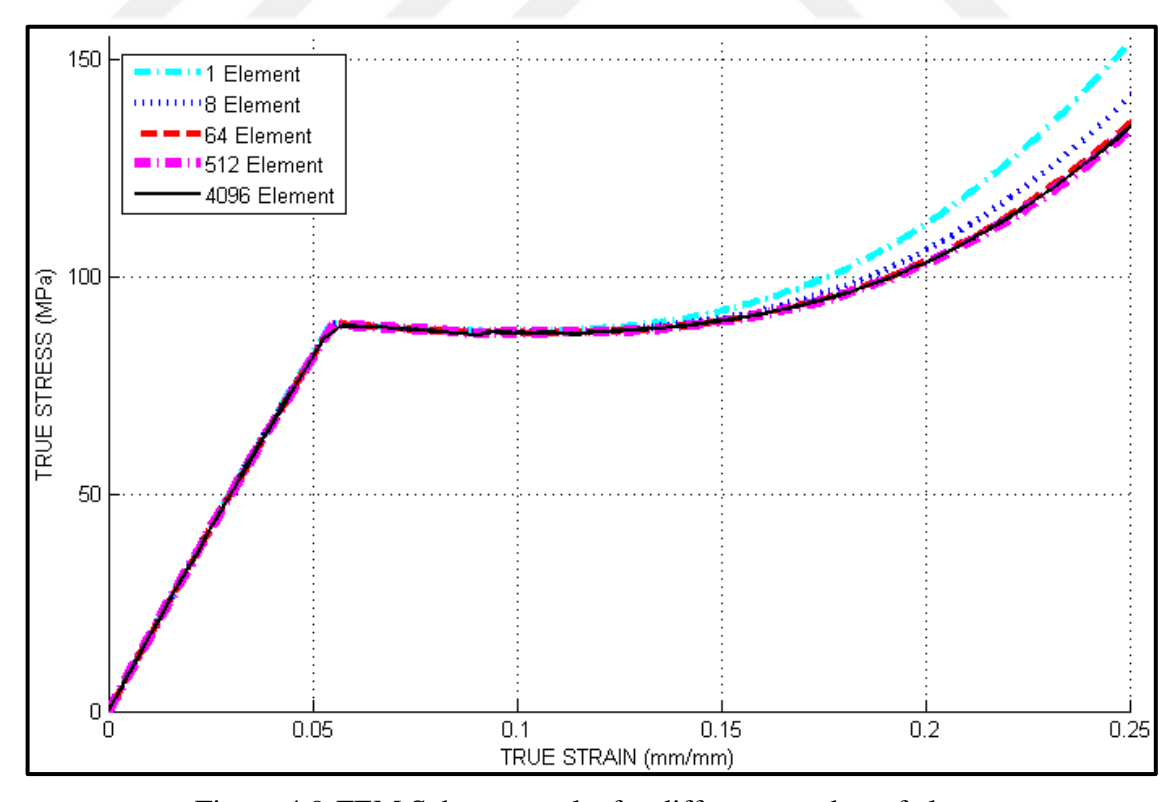


Figure 4.9 FEM Scheme results for different number of elements.

In brief, a forward gradient scheme for the new proposed viscoplasticity model for nanocomposites is developed. This scheme gives consistent results when compared to the ODE solution results obtained and verified through tensile and compression tests in Chapter 3. This part seemed important by the author of this work to show that the new Nanocomposite model has a great potential in possible structural FEM analysis which hopefully needed for the industrial applications of such materials.

RESULTS AND DISCUSSION

In this work, total viscoelastic – viscoplastic mechanical behavior of epoxy matrix graphene nanocomposites is investigated. Materials are prepared for two different weight fractions, 0.1%wt, and 0.5% wt. Two different types of solvents, acetone and NMP, are used to see the effect of solvents on dispersion state of graphene. It is found that NMP as a solvent is not suitable due to its evaporation problems. The residual of the solvent leads to a decrease on mechanical properties. And it is stated that the dispersion of graphene is still an important issue on nanocomposite production.

The produced samples are subjected to tensile tests and DMA tests for characterization. Graphene flakes, acted as reinforcement agents and the elasticity modulus and strength are enhanced for both weight fractions. Due to agglomeration effects, 0.1% wt specimens are showed a slightly more better results compared to 0.5% wt specimens. On DMA tests, Tg is stayed almost constant. A slight decrease on Tg was expected. But non-functionalization of the GPL used has led to a weak interface, which is interpreted the constancy on Tg values.

In order to model the mechanical behavior of the material, Cooperative – VBO theory of Çolak et al. is extended. In this manner, the effective modulus definition developed by Ji et al. is coupled with temperature and rate dependent Mahieux – Reifsnider equation used successfully in previous works of researchers. Therefore an effective elasticity modulus definition is obtained which is capable of modeling the visco-elastic response of graphene nano-composites for different temperatures and strain rates. The accuracy of the proposed model is investigated by comparing the model responses to storage modulus tests reported by Acar et al. The results showed that the proposed

model is capable of modeling storage modulus for different graphene fractions with changing temperature successfully.

On the viscoplastic part, two scalar valued material parameters of plastic strain rate function is redefined as functions of graphene fraction using Tagayanagi averaging approach. Redefined parameters successfully model the yield stress of composite materials. But, as seen from the test results, inhesion of graphene in the composite structure not only affects the start of the yield but also affects the post – yield behavior. In this manner, Two parameters of the former tangent modulus equation[33], [37] is redefined as functions of graphene content. The proposed model successfully models the compression behavior of composite materials for different graphene fractions at different strain rates. As seen from the results, the proposed visco-plasticity model is capable of modeling the effect of graphene composition successfully. The model is also capable to model the mechanical behavior for temperatures above and below glass transition, but the set of tests used [17] does not involves such data. Therefore this ability of the proposed model could not be compared to test data but model responses are shown. In brief, it is shown that the proposed version of Cooperative-VBO approach is capable of modeling the total viscoelastic-viscoplastic behavior of graphene – epoxy Nanocomposites successfully.

In continuation of the work a finite element method framework is developed, for the use of the model on computational analysis. This framework uses the forward gradient method for numerical integration of the differential values used in the model. It should also be noted that for different matrix materials or different nano fillers the model and the FEM implementation scheme will still be valid and consistent after a careful parameter determination procedure.

- [1] Lee, C., Wei, X., Kysar, J.W., and Hone, J., (2008). "Measurement of the Elastic Properties and Intrinsic Strength of Monolayer Graphene", Science, 321 (5887): 385-388.
- [2] Zhang, B.-T., Zheng, X., Li, H.-F., and Lin, J.-M., (2013). "Application of Carbon-Based Nanomaterials In Sample Preparation: A Review", Analytica Chimica Acta, 784 1–17.
- [3] Bonaccorso, F., Lombarda, A., Hasan, T., Sun, Z., Colombo, L., and Ferrari, A.C., (2012). "Production And Processing Of Graphene And 2d Crystals", Materials Today, 15(12): 584–588.
- [4] Verdejo, R., Bernal, M.M., Romasanta, L.J., and Lopez-Manchado, M.A., (2011). "Graphene Filled Polymer Nanocomposites", Journal of Materials Chemistry, 21(10): 3301.
- [5] Ramanathan, T., Abdala, A.A., Stankovich, S., Dikin, D.A., Herrera-Alonso, M., Piner, R.D., Adamson D. H., Schniepp H. C., Chen X., Ruoff R. S., Nguyen S. T., Aksay I. A., Prud'Homme R. K. and Brinson L. C., (2008). "Functionalized Graphene Sheets For Polymer Nanocomposites", Nature Nanotechnology. 3 (6): 327–331.
- [6] Prasad, K.E., Das, B., Maitra, U., Ramamurty, U., and Rao, C.N.R., (2009). "Extraordinary Synergy In The Mechanical Properties Of Polymer Matrix Composites Reinforced With 2 Nanocarbons", Proceedings of the National Academy of Sciences, 106(32):13186–13189.
- [7] Rafiee, M.A., Rafiee, J., Wang, Z., Song, H., Yu, Z.-Z., and Koratkar, N., (2009). "Enhanced Mechanical Properties of Nanocomposites at Low Graphene Content", ACS Nano, 3 (12): 3884–3890.
- [8] Barroso-Bujans, F., Cerveny, S., Verdejo, R., del Val, J.J., Alberdi, J.M., Alegría, A. and Colmenero J., (2010). "Permanent Adsorption Of Organic Solvents In Graphite Oxide And Its Effect On The Thermal Exfoliation", Carbon, 48 (4): 1079–1087.
- [9] Prolongo, S.G., Jimenez-Suarez, A., Moriche, R., and Ureña, A., (2013). "In Situ Processing Of Epoxy Composites Reinforced With Graphene Nanoplatelets", Composites Science and Technology, 86 185–191.
- [10] Wang, J., Shi, Z., Ge, Y., Wang, Y., Fan, J., and Yin, J., (2012). "Solvent Exfoliated Graphene For Reinforcement Of PMMA Composites Prepared By In Situ Polymerization", Materials Chemistry and Physics, 136 (1): 43–50.

- [11] Kuila, T., Bose, S., Khanra, P., Kim, N.H., Rhee, K.Y., and Lee, J.H., (2011). "Characterization And Properties Of In Situ Emulsion Polymerized Poly(Methyl Methacrylate)/Graphene Nanocomposites", Composites Part A: Applied Science and Manufacturing, 42 (11): 1856–1861.
- [12] Layek, R.K., Samanta, S., Chatterjee, D.P., and Nandi, A.K., (2010). "Physical And Mechanical Properties Of Poly(Methyl Methacrylate) -Functionalized Graphene/Poly(Vinylidine Fluoride) Nanocomposites: Piezoelectric B Polymorph Formation", Polymer, 51 (24): 5846–5856.
- [13] Potts, J.R., Lee, S.H., Alam, T.M., An, J., Stoller, M.D., Piner, R.D. and Ruoff R. S., (2011). "Thermomechanical Properties Of Chemically Modified Graphene/Poly(Methyl Methacrylate) Composites Made By In Situ Polymerization", Carbon, 49 (8): 2615–2623.
- [14] Vallés, C., Kinloch, I.A., Young, R.J., Wilson, N.R., and Rourke, J.P., (2013). "Graphene Oxide And Base-Washed Graphene Oxide As Reinforcements In PMMA Nanocomposites", Composites Science and Technology, 88: 158–164.
- [15] Tang, L.-C., Wan, Y.-J., Yan, D., Pei, Y.-B., Zhao, L., Li, Y.-B., Wu L. B., Jiang J.X. Lai G.Q., (2013). "The Effect Of Graphene Dispersion On The Mechanical Properties Of Graphene/Epoxy Composites", Carbon, 60: 16–27.
- [16] Ahmadi-Moghadam, B., Sharafimasooleh, M., Shadlou, S., and Taheri, F., (2015). "Effect Of Functionalization Of Graphene Nanoplatelets On The Mechanical Response Of Graphene/Epoxy Composites", Materials & Design, 66: 142–149.
- [17] Shadlou, S., Ahmadi-Moghadam, B., and Taheri, F., (2014). "The Effect Of Strain-Rate On The Tensile And Compressive Behavior Of Graphene Reinforced Epoxy/Nanocomposites", Materials & Design, 59: 439–447.
- [18] Yue, L., Pircheraghi, G., Monemian, S.A., and Manas-Zloczower, I., (2014). "Epoxy Composites With Carbon Nanotubes And Graphene Nanoplatelets Dispersion And Synergy Effects", Carbon, 78: 268–278.
- [19] Prolongo, S.G., Jiménez-Suárez, A., Moriche, R., and Ureña, A., (2014). "Graphene Nanoplatelets Thickness And Lateral Size Influence On The Morphology And Behavior Of Epoxy Composites", European Polymer Journal, 53: 292–301.
- [20] Rafiee, M.A., Rafiee, J., Wang, Z., Song, H., Yu, Z.-Z., and Koratkar, N., (2009). "Enhanced Mechanical Properties of Nanocomposites at Low Graphene Content", ACS Nano, 3 (12): 3884–3890.
- [21] Xu, M., Paci, J.T., Oswald, J., and Belytschko, T., (2012). "A Constitutive Equation For Graphene Based On Density Functional Theory", International Journal of Solids and Structures, 49 (18): 2582–2589.
- [22] Parashar, A. and Mertiny, P., (2012). "Multiscale Model To Investigate The Effect Of Graphene On The Fracture Characteristics Of Graphene/Polymer Nanocomposites", Nanoscale Research Letters, 7 (1): 1–8.
- [23] Spanos, P.D. and Kontsos, A., (2008). "A Multiscale Monte Carlo Finite Element Method For Determining Mechanical Properties Of Polymer Nanocomposites", Probabilistic Engineering Mechanics, 23 (4): 456–470.

- [24] Montazeri, A. and Rafii-Tabar, H., (2011). "Multiscale Modeling Of Graphene-And Nanotube-Based Reinforced Polymer Nanocomposites", Physics Letters A, 375 (45): 4034–4040.
- [25] Ji, X.-Y., Cao, Y.-P., and Feng, X.-Q., (2010). "Micromechanics Prediction Of The Effective Elastic Moduli Of Graphene Sheet-Reinforced Polymer Nanocomposites", Modelling and Simulation in Materials Science and Engineering, 18 (4): 45005.
- [26] Khani, N., Yildiz, M., and Koc, B., (2016). "Elastic Properties Of Coiled Carbon Nanotube Reinforced Nanocomposite: A Finite Element Study", Materials & Design, 109 123–132.
- [27] Flatscher, T. and Pettermann, H.E., (2011). "A Constitutive Model For Fiber-Reinforced Polymer Plies Accounting For Plasticity And Brittle Damage Including Softening Implementation For Implicit FEM", Composite Structures, 93 (9): 2241–2249.
- [28] Gomaa, S., Sham, T.-L., and Krempl, E., (2004). "Finite Element Formulation For Finite Deformation, Isotropic Viscoplasticity Theory Based On Overstress (FVBO)", International Journal of Solids and Structures, 41 (13): 3607–3624.
- [29] Gomaa, S., (2000). Computational Procedures For Finite Deformation Rate-Independent Plasticity And Visco-Plasticity Based On Overstress, PhD. Thesis, Faculty of Rensselaer Polytechnic Institute, New York
- [30] ASTM D638-10, (2010). Test Method for Tensile Properties of Plastics, ASTM International, Philadelphia.
- [31] Young, R.J., Kinloch, I.A., Gong, L., and Novoselov, K.S., (2012). "The Mechanics Of Graphene Nanocomposites: A Review", Composites Science and Technology, 72 (12): 1459–1476.
- [32] Naebe, M., Wang, J., Amini, A., Khayyam, H., Hameed, N., Li, L.H., Chen Y. and Fox B., (2014). "Mechanical Property and Structure of Covalent Functionalised Graphene/Epoxy Nanocomposites", Scientific Reports, 4: 4375.
- [33] Çolak, O.U., Ahzi, S., and Remond, Y., (2013). "Cooperative Viscoplasticity Theory Based On The Overstress Approach For Modeling Large Deformation Behavior Of Amorphous Polymers: Cooperative Viscoplasticity Theory", Polymer International, 62: 1560-1565
- [34] Richeton, J., Ahzi, S., Daridon, L., and Rémond, Y., (2005). "A Formulation Of The Cooperative Model For The Yield Stress Of Amorphous Polymers For A Wide Range Of Strain Rates And Temperatures", Polymer, 46 (16): 6035–6043.
- [35] Richeton, J., Ahzi, S., Vecchio, K.S., Jiang, F.C., and Makradi, A., (2007). "Modeling And Validation Of The Large Deformation Inelastic Response Of Amorphous Polymers Over A Wide Range Of Temperatures And Strain Rates", International Journal of Solids and Structures, 44 (24): 7938–7954.
- [36] Dusunceli, N. and Colak, O.U., (2008). "Modelling Effects Of Degree Of Crystallinity On Mechanical Behavior Of Semicrystalline Polymers", International Journal of Plasticity, 24 (7): 1224–1242.

- [37] Colak, O.U. and Acar, A., (2012). "Modeling Of Hygro-Thermo-Mechanical Behavior Of Nafion NRE212 For Polymer Electrolyte Membrane Fuel Cells Using The Finite Viscoplasticity Theory Based On Overstress For Polymers (FVBOP)", Mechanics of Time-Dependent Materials, 17 (3): 331–347.
- [38] Krempl, E., McMahon, J.J., and Yao, D., (1986). "Viscoplasticity Based On Overstress With A Differential Growth Law For The Equilibrium Stress", Mechanics of Materials, 5 (1): 35–48.
- [39] Bordonaro, C.M. and Krempl, E., (1992). "The Effect Of Strain Rate On The Deformation And Relaxation Behavior Of 6/6 Nylon At Room Temperature", Polymer Engineering and Science, 32 (16): 1066–1072.
- [40] Colak, O., (2005). "Modeling Deformation Behavior Of Polymers With Viscoplasticity Theory Based On Overstress", International Journal of Plasticity, 21 (1): 145–160.
- [41] Richeton, J., Schlatter, G., Vecchio, K.S., Rémond, Y., and Ahzi, S., (2005). "A Unified Model For Stiffness Modulus Of Amorphous Polymers Across Transition Temperatures And Strain Rates", Polymer, 46 (19): 8194–8201.
- [42] Ho, K. and Krempl, E., (2002). "Extension Of The Viscoplasticity Theory Based On Overstress (VBO) To Capture Non-Standard Rate Dependence In Solids", International Journal of Plasticity, 18 (7): 851–872.
- [43] Mahieux, C.A. and Reifsnider, K.L., (2002). "Property Modeling Across Transition Temperatures In Polymers: Application To Thermoplastic Systems", Journal of Materials Science, 37 (5): 911–920.
- [44] Mahieux, C.A. and Reifsnider, K.L., (2001). "Property Modeling Across Transition Temperatures In Polymers: A Robust Stiffness–Temperature Model", Polymer, 42 (7): 3281–3291.
- [45] Acar, A., Çolak, Ö.Ü., and Uzunsoy, D., (2015). "Synthesis And Characterization Of Graphene-Epoxy Nanocomposites", Materials Testing, 57 (11–12): 1001–1005.
- [46] Hill, R., (1964). "Theory Of Mechanical Properties Of Fibre-Strengthened Materials: I. Elastic Behaviour", J. Mech. Phys. Solids, 12 (12): 199–212.
- [47] Matadi R., Gueguen O, Ahzi S, Gracio J., Muller R., and Ruch D., (2010). "Investigation Of The Stiffness And Yield Behaviour Of Melt-Intercalated Poly(Methyl Methacrylate)/Organoclay Nanocomposites: Characterisation And Modelling", Journal of Nanoscience and Nanotechnology, (10): 2956–2961.

CURRICULUM VITAE

PERSONAL INFORMATION

Name Surname : Alperen ACAR

Date of birth and place :02/02/1986 BALIKESİR / TURKEY

Foreign Languages :English

E-mail :alpacar@yildiz.edu.tr

EDUCATION

Degree	Department	University	Date of
			Graduation
Ph. D.	Mechanical Eng.	YTU	2016
Master	Mechanical Eng.	ITU	2011
Undergraduate	Mechanical Eng.	YTU	2008
High School	Applied Sciences	Rahmi Kula And. Lis /Balıkesir	2004

WORK EXPERIENCE

Year	Corporation/Institute	Enrollment
2009 - Present	YTU / College of Mech. Eng.	Res. Asst.

PUBLISHMENTS

Papers

- 1- Acar, A., Çakir, Ö. Ü. Ç., and Uzunsoy, D., (2015). "Synthesis And Characterization Of Graphene-Epoxy Nanocomposites", Materials Testing, 57(11-12): 1001-1005.
- 2- Colak, O. Ü., Acar, A., and Ergenekon, E., (2014). "Investigation of Hygro-Thermal Cycle Effects on the Membranes of Proton Exchange Membrane Fuel Cells", Journal Of Testing And Evaluation, 42(2): 1-6.
- 3- Colak, O. U., and Acar, A., (2013). "Modeling Of Hydro-Thermo-Mechanical Behavior Of Nafion NRE212 For Polymer Electrolyte Membrane Fuel Cells Using The Finite Viscoplasticity Theory Based On Overstress For Polymers (FVBOP)", Mechanics Of Time-Dependent Materials, 17(3): 331-347.

Conference Papers

- 1- Acar, A., Çolak, Ö., and Uzunsoy, D., (2016). "Modeling of Storage Modulus of Graphene-Epoxy Nanocomposite" ACSM (4th International Conference on Advances In Civil, Structural and Mechanical Engineering), 07-08 May 2016, Bangkok, Thailand
- 2- Acar, A., Çolak, Ö., and Uzunsoy, D., (2014). "Fabrication and Mechanical Characterization of Graphene–Epoxy Nano Composites", ICPB (International Conference on Polymeric Behavior), 22-26 September 2014, Vienna, Austria
- 3- Acar, A., and Çolak, Ö., (2012). "Determination Of Temperature Dependent Elasticity Modulus Of Pfsa Membranes Using Dynamic Mechanical Analysis (Dma) Technique", IMSP (International Materials Symposium), 10-12 October 2012, Denizli, Turkey.
- 4- Acar, A., Çolak, Ö., and Ergenekon, E., (2011). "Investigation of Hygro-Thermal Cycle Effects on PEM Fuel Cell Membranes", AMPT 2012 (14th International Conference on Advances in Materials and Processing Technologies).13-16 -July 2011, Istanbul, Turkey.
- 5- Acar, A., and Çolak, Ö., (2010). "Modeling of Humidity and Temperature Effects on Uniaxial Tension Behavior of Perfluoro-sulfonic Acid (PFSA) Membrane Nafion 112", 4th International Conference on Polymeric Behavior IUPAC, 19-23 September 2010, Lodz, Poland

Projects

- 1- Elektrik Ark Oluşturma Yöntemi ile Grafen Sentezi, Grafen Takviyeli Epoksi Nano Kompozit Üretimi ve Karakterizasyonları Role on the Project: Researcher, Institution: BAP (2012-2015)
- 2- Graphene-PMMA nanocomposite; Processing, Experimental Characterization and Modeling Role on the Project: Researcher, Institution: TÜBİTAK (2013-2015)
- 3- Hidro-Termal Çevrime Maruz Kalan Proton Değişim Membranli Yakit Hücrelerinde Membranin Modellenmesi Role on the Project: Researcher, Institution: TÜBİTAK (2009-2012)

AWARDS

1. ACSM 2016 Best Paper Award